ICHF
Institute of Physical Chemistry PAS

High-throughput and precise methods for bacteria counting, identification and antibiotic susceptibility testing

Natalia Pacocha

Supervisor: Prof. dr hab. Piotr Garstecki

Auxiliary supervisor: dr Ott Scheler

The dissertation was prepared within the International PhD Studies at the

Institute of Physical Chemistry of the Polish Academy of Sciences

Kasprzaka 44/52, 01-224 Warsaw

Warsaw, August 2021

Acknowledgment

I have received a great deal of support and assistance throughout working in the laboratory and writing this dissertation.

I want to thank my supervisor, Professor Piotr Garstecki, for his invaluable expertise in defining research questions and methodology. Your inquiring comments and percipient feedback sharpened my thinking and pushed my work to a higher level.

I want to acknowledge my auxiliary supervisor, Professor Ott Scheler, for introducing me to the world of microfluidics and valuable guidance during my research projects. Thank you for your patient support.

Many thanks to the current and former members of the Group of Microfluidics and Complex Fluids and the Department of Soft Condensed Matter for their help with my research and administrative duties, fruitful collaborations, interesting scientific discussions and comments, designing and milling microfluidic chips. Especially many thanks to Ladislav Derzsi, Karol Makuch, Artur Ruszczak, Marta Zapotoczna, Justyna Gruszka, Michał Horka, Patryk Adamczuk and Karol Patyrak. I would also acknowledge the wonderful and resultful collaboration of the Physical Optics and Biophotonics Group members Jakub Bogusławski and Professor Maciej Wojtkowski.

Thank you, Robert, for having my back and motivating me towards my goals.

Serdecznie dziękuję moim Rodzicom, Babciom oraz Braciom za wsparcie okazane podczas studiów doktoranckich.

Acknowledgment for funding

The research presented in this dissertation was supported by the following projects:

1. Research was co-funded by Symfonia 2014/12/W/NZ6/00454 project *The role of antimicrobial protein-chemerin in skin pathophysiology* within Symfonia 2 Programme of National Science Centre

2. Research was co-funded by Maestro 10 2018/30/A/ST4/00036 project *Microfluidic methods for quantitative antibiotic susceptibility assays with single cell resolution* within Maestro 10 Programme of National Science Centre

List of publications

Publications related to the topic of the dissertation:

1. O. Scheler, **N. Pacocha**, P.R. Debski, A. Ruszczak, T.S. Kaminski, P. Garstecki, *Optimized droplet digital CFU assay (ddCFU) provides precise quantification of bacteria over a dynamic range of 6 logs and beyond*, Lab on a chip, 2017, 17, 1980-1987

2. **N. Pacocha**, O. Scheler, M.M. Nowak, L. Derzsi, J. Cichy, P. Garstecki, *Direct droplet digital PCR (dddPCR) for species specific, accurate and precise quantification of bacteria in mixed samples*, Analytical Methods, 2019, 11, 5730-5735

3. **N. Pacocha‡**, J. Bogusławski‡, M. Horka, K. Makuch, K. Liżewski, M. Wojtkowski, P. Garstecki, *High-throughput monitoring of bacterial cell density in nanoliter droplets: label-free detection of unmodified Gram-positive and Gram-negative bacteria*, Analytical Chemistry, 2021, 93, 843-8503
   ‡equal contribution

4. **N. Pacocha‡**, M. Zapotoczna‡, K. Makuch, J. Bogusławski, P. Garstecki, *You will know by its tail: a method for quantitative characterization of heterogeneity of bacterial populations using single-cell MIC profiling*. In preparation.
   ‡equal contribution

Other publications:

1. O. Scheler, K. Makuch, P.R. Debski, M. Horka, A. Ruszczak, **N. Pacocha**, K. Sozanski, O. Smolander, W. Postek, P. Garstecki, *Droplet digital antibiotic susceptibility screen reveals single-cell clonal heteroresistance pattern in an isogenic bacteria population*, Scientific Reports, 2020, 10

List of symbols and abbreviations

c	Concentration
γ	Surface tension
μ	Dynamic viscosity of the fluid
µTASs	Miniaturized total analysis systems
ρ_{neg}	Percentage content of negative droplets
ρ_{pos}	Percentage content of positive droplets
$f_+(0)$	Fraction of non-empty droplets without antibiotic treatment
$f_+(c)$	Fraction of non-empty droplets at antibiotic concentration c
$F_R(c)$	Fraction of recovering bacteria
N_+	Number of non-empty droplets
N	Total number of droplets
U	Characteristic velocity
AMR	Antimicrobial resistance
APD	Avalanche photodiode
AST	Antimicrobial susceptibility testing
ATP	Adenosine triphosphate
BHI	Brain heart infusion
BP	Bandpass filter
Ca	Capillary number
CFU	Colony forming unit
CLSI	Clinical and Laboratory Standards Institute
Ct	Cycle threshold
ddPCR	Droplet digital polymerase chain reaction
dddPCR	Direct droplet digital polymerase chain reaction
DM	Dichroic mirror
DNA	Deoxyribonucleic acid
dNTPs	Deoxynucleoside triphosphates
EUCAST	European Committee on Antimicrobial Susceptibility Testing
FISH	Fluorescence In Situ Hybridization
GFP	Green fluorescent protein
hVISA	vancomycin-intermediate *Staphylococcus aureus*

IPTG	Isopropyl β-D-1-thiogalactopyranoside
kbp	Kilo base pairs
LAMP	Loop-mediated isothermal amplification
LB	Lysogeny broth
LoC	Lab-on-a-chip
LPS	Lipopolysaccharides
LTA	Lipoteichoic acid
MALDI-TOF MS	Matrix assisted laser desorption ionization-time of flight mass spectrometry
MEMS	Micro-electromechanical systems
MIC	Minimal inhibitory concentration
MO	Microscope objective
mRNA	Messenger RNA
NCPs	Normal colony phenotypes
NGS	Next-generation sequencing
OD	Optical density
OD_{600}	Optical density measured at wavelength of 600 nm
PACS	PCR-activated cell sorting
PAP	Population analysis profile
PC	Polycarbonate
PCR	Polymerase chain reaction
PDMS	Polidimethylsiloxane
PMT	Photomultiplier
qPCR	Quantitative polymerase chain reaction
Re	Reynolds number
RNA	Ribonucleic acid
rRNA	Ribosomal ribonucleic acid
RNA-Seq	RNA sequencing
scMIC	Single-cell minimum inhibitory concentration
SCVs	Small colony variants
TA	Teichoic acid
TSA	Tryptic Soy Agar
TSB	Tryptic Soy Broth
YFP	Yellow fluorescent protein

Streszczenie (Abstract in Polish)

Mikroprzepływy oparte na kroplach zrewolucjonizowały dziedzinę biologii między innymi poprzez wprowadzenie emulsyjnej reakcji łańcuchowej polimerazy (droplet digital PCR) oraz sekwencjonowania genomu pojedynczych komórek. Wysoka przepustowość oraz możliwość powtarzania równoległego generacji kropel, manipulacji kroplami oraz ich detekcji sprzyja wprowadzaniu ciekawych innowacji w analizie bakterii oraz tworzeniu nowych metod ich diagnostyki. Małe objętości kropli (pikolitry, nanolitry) sprzyjają szybszej detekcji bakterii w porównaniu do standardowych kultur bakteryjnych hodowanych w znacznie większych objętościach (mililitry) ze względu na szybkie zagęszczenie kropli nowymi komórkami, produktami metabolizmu lub wydzielanymi molekułami. Mikroprzepływy kroplowe biorą udział w usprawnieniu technik identyfikacji i precyzyjnego liczenia bakterii, badania wrażliwości na działanie substancji antybakteryjnych (antimibrobial susceptibility testing, AST) oraz analizy fenotypowej i genotypowej heterogeniczności odpowiedzi populacji bakterii na antybiotyki. Metody te pomagają w walce z opornością oraz heteroopornością bakterii oraz pozwalają na zgłębienie mechanizmów ich powstawania. Tradycyjne fenotypowe metody AST (detekcja wzrostu bakterii w obecności antybiotyku), na przykład metoda mikrorozcieńczeń oraz E-test oparte są na wyznaczeniu minimalnego stężenia inhibitującego (MIC) wzrost bakterii. Metody te są wygodne i łatwe w użyciu, ale również wymagające czasowo oraz nie informujące o obecności heteroopornych subpopulacji.

Projekty badawcze, których wyniki opisuje ta rozprawa doktorska skupione były na ulepszeniu lub stworzeniu nowych metod mikroprzepływowych do analizy bakterii, takich jak liczenie, identyfikacja, detekcja wzrostu oraz oznaczanie wrażliwości na substancje antybakteryjne włączając w to analizę populacji baterii na poziomie pojedynczych komórek w celu oznaczenia ilości heteroopornej subpopulacji.

Rozprawa składa się z czterech rozdziałów. Rozdział 1 przedstawia charakterystykę bakterii, wyjaśnia pojęcia oporności oraz heterooporności bakterii na antybiotyki, opisuje standardowe oraz mikroprzepływowe metody liczenia oraz identyfikacji bakterii, techniki badania wrażliwości na antybiotyki oraz metody detekcji heterooporności. Rozdział 2 przedstawia materiały i metody zastosowane w pracach badawczych, natomiast Rozdział 3 prezentuje otrzymane wyniki w poszczególnych projektach:

I. Precyzyjne liczenie bakterii w szerokim zakresie dynamicznym- opracowaliśmy metodę, której wyjątkową cechą jest bardzo szeroki zakres dynamiczny wyznaczania stężenia

bakterii przy wykorzystaniu stosunkowo niewielkiej ilości kropel w porównaniu do standardowo stosowanych metod kropelkowych opartych jedynie na statystyce Poissona. Wyniki otrzymane z zastosowaniem opracowanej technologii są bardzo porównywalne do wyników otrzymanych z użyciem tradycyjnej metody liczenia kolonii bakteryjnych na płytkach agarowych. Natomiast opracowana technika jest mniej pracochłonna i ma potencjał na znaczne skrócenie czasu analizy.

II. Precyzyjne liczenie oraz identyfikacja bakterii w mieszaninie- jednoczesne liczenie oraz identyfikacja bakterii w mieszaninie bez izolowania poszczególnych szczepów możliwa jest dzięki zastosowaniu ilościowej reakcji łańcuchowej polimerazy. Natomiast metoda ta wymaga czasochłonnej kalibracji oraz wcześniejszego wyizolowania i oczyszczenia materiału genetycznego bakterii w przeciwieństwie do stworzonej przez nas techniki direct droplet digital PCR.

III. Wysokoprzepustowy system do detekcji wzrostu bakterii w nanolitrowych kroplach bez fluorescencyjnego znakowania komórek- tradycyjnie detekcja wzrostu bakterii w kroplach odbywa się poprzez pomiar intensywności fluorescencji, co ogranicza analizę większości klinicznie interesujących szczepów oraz wszechstronne użycie technik kroplowych w mikrobiologii. W związku z tym stworzyliśmy systemy oparte na pomiarze światła rozproszonego oraz autofluorescencji, które umożliwiają detekcję nieznakowanych bakterii Gram-ujemnych oraz Gram-dodatnich z częstotliwością skanowania 1200 kropli/s.

IV. Ilościowa analiza próbek bakteryjnych mikrofluidyczną metodą opartą na kroplach- standardowe techniki badania wrażliwości bakterii na antybiotyki nie dostarczają informacji na poziomie pojedynczych komórek oraz niska rozdzielczość testu nie pozwala na ilościowe oznaczenie subpopulacji występującej w małej ilości i wykazującej zmniejszoną wrażliwość na działanie antybiotyku. Stworzyliśmy metodę opartą na wyznaczaniu minimalnego stężenia inhibitującego pojedynczą komórkę (scMIC) służącą do charakteryzowania heterogeniczności populacji bakterii oraz do wyznaczania stężenia heteroopornych subpopulacji. Pomiar wzrostu bakterii w kroplach został przeprowadzony z użyciem detektora światła rozproszonego oraz autofluorescencji.

Rozdział 4 podsumowuje wyniki uzyskane w każdym z projektów badawczych oraz wskazuje ograniczenia i ewentualne modyfikacje w celu zwiększenia funkcjonalności stworzonych metod oraz systemów.

Abstract

Droplet microfluidics disrupted analytical biology by introducing droplet digital polymerase chain reaction and droplet-assisted single-cell sequencing. The same highly parallel and high-throughput techniques for droplet generation, manipulation, and detection brought similar essential innovations in the analysis of bacteria and created new promising diagnostics approaches. The stochastic confinement of single cells into droplets allows for the faster accumulation and detection of metabolic products and secreted molecules compared to bulk cultures. Droplet microfluidics brings innovation, particularly in bacteria identification, precise quantification, antibiotic susceptibility testing (AST), and analysis of phenotypic and genotypic heterogeneity in the response of bacterial populations to antibiotics. These methods help to combat and more comprehensively understand antibiotic resistance and heteroresistance of bacterial populations. The conventional phenotypic AST methods (bacteria growth detection in the presence of antibiotic) like the broth microdilution method and E-test are based on a minimum inhibitory concentration (MIC) measurement. They are convenient and relatively easy approaches, but also time demanding and have a too low resolution to assess population heteroresistance.

The dissertation presents results of the improvement and development of microfluidic methods to analyze bacteria and their antibiotic susceptibility patterns, i.e., quantification, identification, growth detection, and susceptibility testing, including analysis of bacterial population towards heteroresistance and quantification of the subpopulation with reduced susceptibility to antibiotics.

The dissertation is composed of four Chapters. Chapter 1 describes the essential methods for the characterization of bacteria, introduces the concept of antibiotic resistance and heteroresistance of bacteria, reviews the standard and microfluidic methods for bacteria counting, identification, antimicrobial susceptibility testing, and detection of heteroresistance. Chapter 2 describes used materials and methods, while Chapter 3 presents results and discussion of the following research projects:

I. Droplet digital CFU (ddCFU) assay for precise quantification of bacteria over a broad dynamic range- standard droplet digital assay requires a large number of compartments for precise bacteria quantification over a broad dynamic range. We developed an optimized approach with a drastically reduced number of droplets. The technology is at par with gold standard plate count, has simplified experimental setup, and reduced manual workload.

II. Species-specific, accurate, and precise quantification and identification of bacteria in mixed samples- simultaneous differentiation and quantification of bacteria is commonly performed by real-time polymerase chain reaction, which requires laborious calibration, and the method is affected by errors associated with extraction and purification of DNA. We developed a direct droplet digital PCR assay (dddPCR) to identify and quantify bacteria in a bacterial mixture where purification of genetic material and calibration curves is eliminated.

III. High-throughput label-free readout of bacteria density in nanoliter droplets- the most general approach of bacteria growth detection in droplets is based on the measurement of fluorescence intensity. The lack of a high-throughput label-free method prohibits analysis of the most interesting strains and widespread use of droplet technologies in microbiology. To resolve that complication, we devised methods based on the measurement of scattered or native fluorescence light of unlabeled Gram-negative and Gram-positive species with a screening frequency of 1200 droplets/s.

IV. Droplet-based assay for quantitative characterization of bacterial populations- standard antibiotic susceptibility testing does not inform about the diversity of the bacterial population in response to antibiotics at the single-cell level. Besides, its low resolution constricts the quantification of low-abundant subpopulations with increased antibiotic susceptibility. We developed a method based on the determination of single-cell minimum inhibitory concentration (scMIC) to characterize and quantify complex bacterial populations, including heteroresistance subpopulations. The measurement of bacteria growth in droplets was conducted using our novel dual label-free detection of scattered and autofluorescence light.

Chapter 4 summarizes the results and provides limitations and an outlook for possible future modifications to improve demonstrated assays and systems.

Spis treści

1. Introduction and Literature Review

Chapter 1 describes bacteria morphology, cell structure, function, and pathogenicity. We introduce the concept of phenotypic heterogeneity of cells in the bacteria population, starting with the description of resistance and heteroresistance of bacteria to antibiotics. Then we review the standard methods for bacteria counting, identification, antimicrobial susceptibility testing, and detection of heteroresistance. In conclusion, we focus on droplet microfluidics as a precise and accurate tool for mentioned microbiological applications.

1.1. Bacteria

Bacteria are a large group of prokaryotic microorganisms with a sizes usually around 0.5-1.0 µm in diameter and 2.0-5.0 µm in length[1]. They vary in shapes, ranging from spheres to rods and spirals. Bacteria are present in many different habitats on Earth, soil, water, plants, animals, and humans. An adult human is colonized with hundreds of different bacteria strains, and there are as much of bacterial as human cells[2]. They occupy the skin, oral cavity, airways, gastrointestinal and urogenital tract, but most of them are located in the guts[3]. They are essential for keeping the organism in good health. Despite the commensal bacteria, there is a group of harmful pathogens, which cause a range of serious infections such as tuberculosis, cholera, tetanus, syphilis, various skin and urinary tract infections, pneumonia, and overwhelming sepsis, which can often lead to death[4].

1.1.1. Cellular structure

Bacterial cell structure has been well studied due to its simplicity compared to larger organisms. Figure 1a presents a typical bacterial cell consisting of the cell envelope, cytoplasm, flagella, pili, bacterial DNA and plasmids, ribosomes, and intracellular membranes.

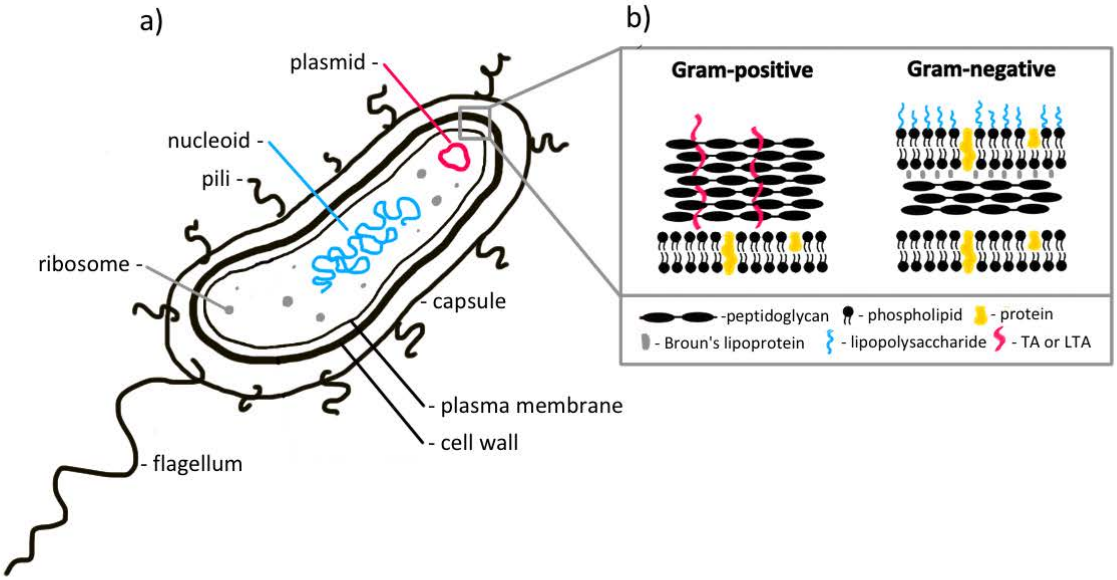

Figure 1. Schematic representation of a bacterial cell; a) section of the bacterial cell with the identification of its individual components; b) schematics of the cell walls of Gram-positive and Gram-negative bacteria.

The cell envelope is made up of two or three layers:

- **capsule**- produced by some species of bacteria, the outmost layer of the cell. It is composed of polysaccharides except for the capsule of *Bacillus anthracis*, which is

built of poly-γ-glutamate. Capsule plays several roles; it is mainly a protective covering conferring resistance to phagocytosis. Besides, it is an essential virulence factor for pathogen bacteria during the host infection[5].

- **cell wall**- most bacteria have one of two types of cell wall: gram-positive or gram-negative. They can be identified by developed in 1884 Gram's method, where gram-positive bacteria are stain purple, and gram-negative are stain pink. It is related to the difference in the cell wall structure (Figure 1b). The cell wall of gram-positive bacteria is consisted of 90% of peptidoglycan, providing high stiffness of the wall. The additional components contributing to the overall rigidity and maintenance of the cell shape are teichoic (TA) and lipoteichoic acids (LTA). They are also responsible for a net negative charge of the cell for the development of a proton motive force; they participate in cell division and take part in resistance to high salt concentration, high temperature, and even to β-lactam antibiotics. The cell wall of gram-negative bacteria contains much less peptidoglycan, around 5-10% of the total cell wall. It significantly composed of a lipid bilayer, integral proteins, and lipopolysaccharide (LPS). Additional structural integrity is guaranteed by Broun's lipoproteins covalently bonding to the peptidoglycan layer and the outer membrane.[6]

  Bacteria that do not color with gram-staining and remain colorless are atypical bacteria. These include the Chlamydiaceae, Legionella and the Mycoplasmataceae.

- **plasma membrane**- composed of two layers of phospholipids assembling in such a way to keep polar heads in contact with the water environment outside the cell and the cytoplasm inside. The non-polar fatty acid tails are secluded between hydrophilic regions. The bilayer contains the integral (embedded within the bilayer) and peripheral proteins (anchored outside the bilayer). They allow the plasma membrane to act as a semi-permeable barrier that permits an entrance of nutrients, does not let in toxins or antibiotics, and excretes waste molecules. Besides, the possibility of binding or absorbing small molecules empowers the cells to "communicate" with the surrounding environment. The plasma membrane also participates in the metabolic processes such as the transformation of light or chemical energy into an energy-carrying molecule, adenosine triphosphate (ATP).

The inner part of bacteria is filled with **cytoplasm**, gel-like fluid composed of water, nutrients, proteins, gases, wastes, and cell structures (devoid of bilipid membrane in contrast to eukaryotic cells):

- **nucleoid**- a region of the cytoplasm containing typically a single double-stranded DNA molecule (chromosome). It is a genetic material specifying bacterial abilities and characteristics. The set of nucleoid and plasmids represents a genome of the bacterial cell.
- **plasmids**- small extrachromosomal double-stranded and typically circular pieces of DNA that most bacteria have. They are not involved in bacteria reproduction. They replicate independently of the chromosome, and they are not essential to the cell but can have unique properties like conferring of antibiotic resistance. Plasmids became handy tools in genetic engineering due to the ability of inserting to them specific genes.
- **ribosomes**- protein-producing structures floating in the cytoplasm. They translate genetic information from nucleic acid to the information about the sequence of amino acids based on the proteins are produced.

Bacteria can also have additional structures outside the cell wall, which are not typical for every species of bacteria; they are often bound to the cell wall and/ or to the cell membrane:

- **pili**- thin filamentous appendages composed of pilin proteins. They are used by the cell to attach to other cells or surfaces. Pathogenic bacteria deprived of pili lose their ability to infect because they can not adhere to the host tissue. Pili appear to be responsible for twitching motility, and they are also involved in bacterial conjugation, which is an exchange of plasmids between two cells.[7]
- **flagella**- structures located at the polar end or ends or peritrichously arranged about the cell. They are composed of the filament, the hook, and the motor. Flagella mainly provide bacterial motility but can also help to fix surface colonization.[7]

1.1.2. Antibiotics

Antibiotics are antimicrobial substances that are used to treat bacterial infections. They may either kill or inhibit the growth of bacteria and are classified on the basis of mechanism of action[8]:

- antibiotics targeting cell wall synthesis: beta-lactam antibiotics, glycopeptides;
- breakdown of cell membrane structure or function: beta-lactam antibiotics, glycopeptides, polymyxins, ionophore antibiotics;
- inhibitors of protein biosynthesis: aminoglycosides, tetracyclines, chloramphenicol, macrolides, oxazolidinones;

- inhibitors of DNA replication: quinolones;
- blockage of key metabolic pathways: sulfonamides, trimethoprim.

The consequence of using antibiotics, especially their misuse and overuse, is the increasing number of antimicrobial-resistant bacteria causing hard-to-treat infections with increased risk of disease spread, severe illness, and death. Determination of bacterial resistance to antibiotics of all classes (phenotypic and genotypic) is crucial to develop new treatments to counter antimicrobial resistance.

1.1.3. Antibiotic resistance of bacteria

Antibiotic resistance of bacteria is one of the major concerns in the field of public health, and the issue is dangerously rising in all parts of the world. It leads to increased mortality and higher medical costs[9]. Infections like tuberculosis, pneumonia, gonorrhea, or salmonellosis are becoming more challenging to treat as the antibiotics are less effective. The resistance of bacteria occurs naturally but overusing antibiotics in humans and animals accelerates the process. Antimicrobial resistance (AMR) is encoded by several genes that can be transferred between cells by plasmid sharing.

There are a few mechanisms that bacteria developed to resist the effect of antibiotics[10–12].

- Reduced permeability of the cell. Gram-negative bacteria are less permeable than Gram-positive species due to the outer membrane forming a permeability barrier. Besides, bacteria can down regulate porin expression providing limited entry of antibiotics.
- An active efflux, which reduces drug accumulation in the bacterial cell. The antibiotic molecules are pumping out across the cell surface before their destructive effect.
- A drug inactivation or modification, such as the production of protective enzymes, β-lactamases for deactivation of penicillin. Bacteria can also change the antibiotic target preventing effective drug binding. This process is associated with a mutational change in the genes encoding the target molecule or the modification of the target by adding a chemical group.

The key to combat the spread and emergence of AMR is to improve antibiotic users' awareness, understand antimicrobial resistance, and develop new tools for the rapid phenotypic and genotypic assessment of AMR and antibiotic susceptibility. A crucial role in

the more responsible and appropriate use of antibiotics play antimicrobial susceptibility testing (AST) systems. They are mostly phenotypic methods as they are based on the detection of bacteria growth or inhibition in the presence or absence of an antimicrobial agent. They provide a direct indication of the susceptibility of a given microorganism to a tested antibiotic. A quantitative feature of bacteria susceptibility delivered by phenotypic AST methods is the value of **minimal inhibitory concentration** (MIC)[13,14]. It is the lowest concentration of the antimicrobial agent, which prevents the visible growth of bacteria.[15]

1.1.4. Heteroresistance

Antibiotic heteroresistance is a phenotype in which the isogenic bacterial population contains a subpopulation of cells with reduced antibiotic susceptibility comparing with the main population[16]. It particularly refers to fraction of the bacterial population displaying a substantial increase in MIC value (at least 8-fold) and ability of cells to grow in the presence of antibiotic (Figure 2)[17]. The variabilities in cells' response to the antibiotic can be attributed to genetic, epigenetic, and nongenetic mechanisms[18–23]. However, most of the described cases of heteroresistance in clinical isolates are related to the genetic heterogeneity of the bacterial population. There is increasing interest in understanding bacterial heteroresistance due to a growing number of data showing that this phenotype leads to antibiotic treatment failure. It concerns both Gram-negative and Gram-positive species. A well-defined and prevalent heterogeneous phenotype is vancomycin-intermediate *Staphylococcus aureus* (hVISA), causing complicated prolonged infections and increased mortality[24–27]. Moreover, the prevalence of heteroresistance was studied, among other things, in *Acinetobacter baumannii*[28], *Klebsiella pneumoniae*[23], *Pseudomonas aeruginosa*[29], *Escherichia coli*[30], *Enterobacter cloacae*[31], and *Clostridium difficile*[32]. For that reason, the sensitive and precise detection of this phenotype is an essential condition for a successful treatment outcome.

A very common type of heteroresistance is unstable heteroresistance, when isolated resistant clone growing in the absence of antibiotic creates a mixed population of susceptible and resistant cells due to resistance phenotype reversibility. One of possible mechanisms of unstable heteroresistance are resistant mutations that are genetically stable but confer a high fitness cost. In the absence of antibiotic a second-site compensatory mutations are selected proving reduced fitness cost and often loss of resistance[16]. A second mechanism underlying heteroresistance involves spontaneous unstable gene amplification of resistance genes and seems to be the most common mechanism in Gram-negative species[21,23].

Staphylococcus aureus is a versatile pathogen known to cause a range of infections which are either acute or chronic and often recalcitrant. The latter are known to be linked with emergence of unstable heteroresistant subpopulation. Those cells are known as small colony variants (SCVs) and emerge during normal bacterial growth cycle but their emergence may be further induced by environmental stress, incl. acidity, intracellular milieu of host cells or subinhibitory concentrations of aminoglycosides[33]. SCVs were firstly described by Bigger in 1944[34]. The growth of SCVs is arrested[35], metabolic activity is reduced, they can colonize infected organs, be protected from the immune system, and therefore show higher tolerance towards antibiotics[36,37]. SCVs can alter their phenotype between non-growing and growing susceptible to antibiotic states, which makes their identification and quantification challenging.

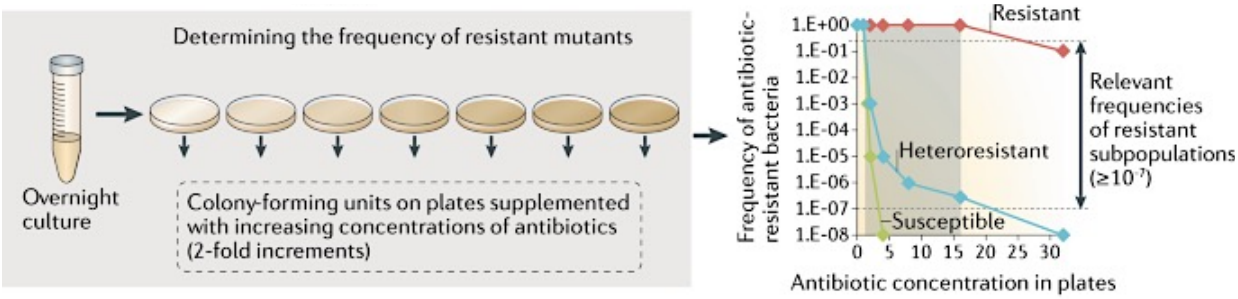

Figure 2. The schematic of the PAP (population analysis profile) test, the gold standard method for the detection of heteroresistance, is shown in the left panel. Briefly, bacteria are spread on agar plates with different concentrations of antibiotics. After one day of incubation, the number of formed colonies is counted to determine the frequency of resistant cells and their resistance level. The right panel presents differences between resistant, heteroresistant, and susceptible bacteria. One frequently accepted definition of heteroresistance is the eightfold increase in resistance (MIC) comparing to the susceptible main population. Figure reproduced from the article published by Andersson et al.[16]

1.2. Bacteria quantification

A precise enumeration of viable bacteria is essential in health care[38], veterinary diagnostics[39], and environmental monitoring[40]. In particular, bacteria counting plays a significant role in antibiotic susceptibility testing and the evolution of mutants. Standards methods for bacteria counting are plate counting, measurement of optical density (OD, turbidity) and flow cytometry.

1.2.1. Plate counting

A traditional and most widely method for bacteria enumeration is a plate counting technique. Figure 3a presents a scheme of a procedure of the method. In the first step, serial logarithmic dilutions are prepared from an initial bacterial sample. Then each dilution is plated on Petri dishes containing solid agar. Grown bacterial colonies represent a single cell in the original

sample, and they are counted where their number on the plate fits in the range 20-300 colony forming units, CFU. Bacteria concentration is calculated based on the number of colonies and the dilution factor. The plate counting method is uncomplicated and inexpensive, but labor-intensive due to plating and analysis usually executed manually and requires long time of incubation for colonies to grow.

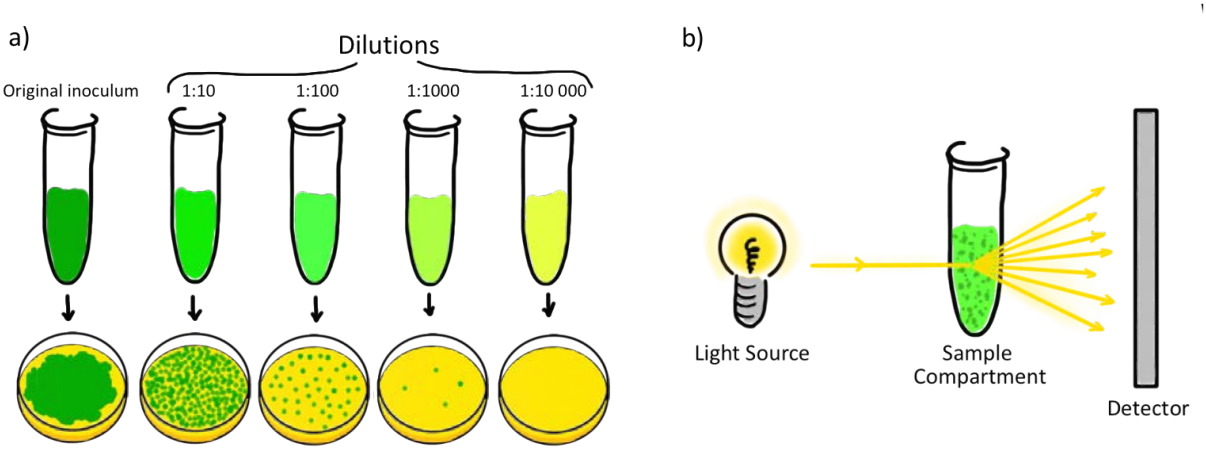

Figure 3. Bacteria counting by a) plate counting technique; b) spectrophotometry.

1.2.2. Turbidimetry

Optical density (OD) measurement is a common technique for determining bacteria concentration in a sample. The measurement is based on the detection of light scattered by cells (Figure 3b). The increasing number of bacteria in the sample decreases light intensity reaching the detector. Sample turbidity measurement is often used to determine bacteria growth curves, and in typical cell density meters, the measurement is performed at 600 nm (OD600) as the 600nm wavelength does little to damage or hinder growth of bacteria. The main features distinguishing OD detection among different techniques are fast and simple measurement. Unfortunately, the reading can be affected by clumping of bacteria; also, this technology does not provide the information about the viability of the cells, and often is not sensitive enough for concentrations below 10^6-10^7 CFU/ml[41].

1.2.3. Flow cytometry

Bacteria can be counted with a wide range of concentrations, in an accurate and fast way by flow cytometry. The bacteria sample is injected into a flow cytometer instrument and focused in a buffer stream to flow one cell at a time through a laser beam. The light is absorbed and then emitted in a characteristic to the cell wavelengths[42]. The cells have to be labeled with fluorescent markers, and additionally, using live-dead staining, the analysis can be enriched by the information about bacteria viability. Flow cytometry is a powerful technique for cell

counting, cell sorting and biomarker detection. The limitation is the high-cost equipment and inevitability of staining of bacteria with fluorescence dyes.

1.3. Bacteria identification

Bacteria identification is an essential task in clinical laboratories. Knowing the pathogen, the right antibiotic can be selected, and the infected patient can be quickly treated. Bacteria can be identified based on cell structure, cellular metabolism, or differences in their genetic sequences. The earliest microbial identification relies on observations of the phenotypic characteristics like size or shape. Staining techniques can detect specific cell structures, and more accurate identification is provided by biochemical tests, gel electrophoresis, mass spectrometry, or methods based on the analysis of genetic material.

1.3.1. Phenotypic identification

Phenotypic identification relies on the determination of the physical characteristics of an unknown organism. The observable features are morphology, developmental processes, metabolism, and biochemical properties.

- **Staining techniques**

The most popular and widely used staining method is the Gram stain technique developed by Hans Christian Gram in 1884. This method is used for microbial classification to Gram-positive or Gram-negative groups of bacteria. Other types of staining methods are Schaeffer-Fulton staining for spores detection, India ink, or nigrosin for checking the presence of capsules and acid-fast staining for mycolic acid detection.

- **Biochemical tests**

Different bacteria behave uniquely in a set of biochemical reactions. This phenomenon helps to select and differentiate microorganisms. For that purpose, selective and differential media are used. They contain specific combinations of nutrients and unique additives[43,44].

Selective media allow the growth of specific microorganisms, while the growth of different bacteria is inhibited. For example, the addition of mannitol salt to agar medium will select *Staphylococcus* species, which can live in a high salt concentration environment. A different example of selective media is Bile Esculin Agar. It tests the ability of bacteria to

hydrolyze esculin in the presence of bile, and it is commonly used for the identification of the genus *Enterococcus*.

Differential media allow the growth of multiple bacteria species, but their characteristic growth patterns can distinguish them. The most popular differential media is blood agar containing 5-10% of sheep or horse blood, where bacteria are distinguished by the type of hemolysis. The biochemical test is a precise and convenient approach for bacteria identification, but it is a versatile method; there is a limited number of available media types.

- **MALDI-TOF MS**

Matrix assisted laser desorption ionization-time of flight mass spectrometry (MALDI-TOF MS) is an accurate and sensitive method for bacteria typing that has been has been recently integrated into the microbiology laboratory workflow. The identification relies on the analysis of the mass spectrum from whole bacterial cells. Bacterial mass patterns are derived from ribosomal or other abundant bacterial proteins which could be used as biomarkers for subspecies discrimination[45]. MALDI-TOF MS is a highly sensitive method but can be expensive, laborious, and requires trained, experienced users.

1.3.2. Genotypic identification

Genotypic methods for bacteria typing rely on the analysis of a genome. The taxonomy and phylogeny of bacteria is based on the sequences of conserved genes, especially those coding for ribosomal ribonucleic acids (rRNA). The most common gene used for species identification is 16S rRNA[46]. It is present in all organisms and performs the same function. The gene is sufficiently long to contain information for identification and short enough to be skillfully sequenced[47]. Molecular methods for bacteria detection are hybridization-based techniques, amplification methods, DNA microarrays and whole genome sequencing[48].

- **Polymerase chain reaction**

The most widely used technique for genotypic bacteria identification among molecular methods is polymerase chain reaction (PCR). It provides fast, accurate, and sensitive bacteria identification even in case of a small concentration of a pathogen's genetic material. PCR amplifies a specific region of the genetic material, usually fragments of between 0.1-10 kbp (kilo base pairs) in length. A basic PCR sample is consisted of:

- a DNA template with the region of amplification interest,
- a *Taq* polymerase, which is a heat-resistant enzyme polymerizing new DNA strands,

- forward and reverse primers, the short nucleic acids complementary to sequences up and downstream of the gene of interest. They play the role of starting points, where DNA polymerase attaches and starts to add new nucleotides,
- deoxynucleoside triphosphates (dNTPs), the building blocks from which DNA polymerase synthesize a new strand,
- a buffer solution to provide a suitable environment for optimum activity and stability of DNA polymerase,
- monovalent and divalent cations like K^+, Mg^{2+}, or Mn^{2+}. They influence the primer-template annealing temperature, fidelity, specificity, and yield.

Figure 4 presents the process of gene amplification by PCR. Typically, PCR consist of 20-40 thermal cycles, which each cycle commonly consisting of three steps:

I. **Denaturation**- genetic material is denatured, the double helix is unwound, and strands are separated by heating at 94-98^{o}C.

II. **Annealing**- the temperature is lowered from 94-98^{o}C to the temperature below the primers' melting point, ~ 55^{o}C. The primers bind to complementary regions of single-stranded DNA.

III. **Elongation**- The reaction temperature is raised to the optimal temperature for polymerase activity, ~68-72^{o}C. The polymerase synthesizes the new strand complementary to the template region by adding free nucleotides (dNTPs) from the reaction mixture in the direction from 5' to 3'.

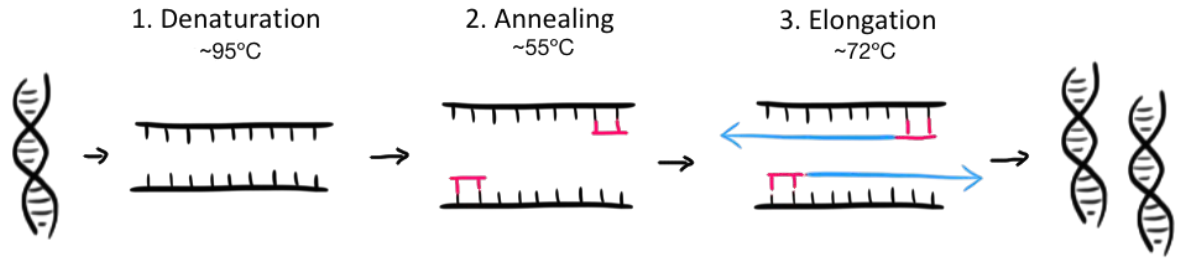

Figure 4. Schematic of DNA amplification by polymerase chain reaction (PCR).

Real-time polymerase chain reaction (real-time PCR), also known as quantitative polymerase chain reaction (qPCR), allows for monitoring the amplification of the target DNA molecule during thermal cycling. There are two standard methods for real-time detection of PCR products. The first one is the non-specific intercalation of a fluorescent dye (SYBR Green) with double-stranded DNA[49]. The second technique is a specific hybridization of a

probe with the complementary sequence of the amplified target[50]. The probe is a short oligonucleotide with covalently bonded fluorophore at 5'-end, and a quencher at 3'-end. As long as the fluorophore and the quencher are in proximity, quenching inhibits any fluorescence signals. As the *Taq* polymerase extends the primer and synthesizes the nascent strand, the 5' to 3' exonuclease activity of the *Taq* polymerase degrades the probe that has annealed to the template. The fluorophore is reveled from the quenching effect and the intensity of fluorescence can be detected.

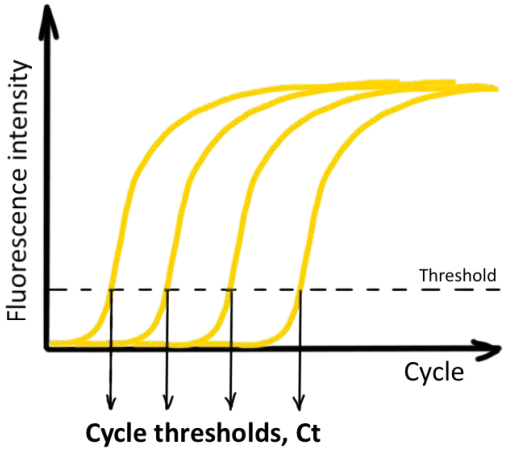

The real-time PCR result is an amplification curve showing increasing fluorescence intensity with an increasing number of thermal cycles. A value that characterizes the amplification curve is a cycle threshold (Ct). It is defined as the number of cycles required for the fluorescent signal to cross the threshold (Figure 5). It is inversely proportional to DNA concentration—a higher concentration of genetic material in the sample results in a smaller Ct value.

Figure 5. Real-time PCR amplification curves with indicated cycle thresholds for four samples containing different concentrations of DNA. Higher concentration of genetic material results in a smaller Ct value.

- **Next-generation Sequencing**

Next-generation sequencing (NGS) is a massively parallel technology used to determine an order of nucleotides in entire genomes or targeted regions of DNA or RNA. The method offers ultra high-throughput, scalability and speed of whole genome sequencing, which can be used for bacteria identification, especially for those novel pathogens, and to study the human microbiome. Besides NGS utilizes RNA sequencing (RNA-Seq) to discover novel RNA variants or to quantify mRNAs for gene expression analysis, analyze epigenetic factors such as genome-wide DNA methylation and DNA-protein interactions. More importantly, NGS can be used to sequence cancer samples (rare somatic variants, tumor subclones, and more).

1.4. Antibiotic susceptibility assays

The issue of antimicrobial resistance (AMR) is now one of the most urgent priorities in public health. In the European Union and United States, AMR causes 25 000 deaths per year. In India, over 58 000 babies died in one year due to infections with resistant bacteria[51].

Antimicrobial susceptibility testing (AST) methods are critical in addressing the issue of bacterial resistance to antibiotics. They are commonly used clinically for the determination of the antibiotic susceptibility profiles of bacterial isolates[52]. The gold-standard AST techniques relies on the detection of bacteria growth in the presence of the antibiotic[53] and a quantitative value evaluating bacteria susceptibility or resistance is a minimum inhibitory concentration (MIC). Suppose measured MIC value is less than or equal to a breakpoint concentration (given annually by national organizations, like the Clinical and Laboratory Standards Institute, CLSI, and the European Committee on Antimicrobial Susceptibility Testing, EUCAST), it means that tested bacteria are considered to be susceptible to the antibiotic. Existing methods for AST are dilution methods, disk diffusion method, E-test, biochemical tests, and genotypic techniques.

1.4.1. Dilution methods

The broth dilution method is a gold-standard AST technique. It is based on the observation of bacteria growth in the presence of a series of antibiotic concentrations. Minimal inhibitory concentration (MIC) value corresponds to the lowest antibiotic concentration, which inhibits bacteria growth[54]. There are macrodilution and microdilution testing types of the method. The difference is in the sample volume, which is ~1.0 ml and 0.05-0.2 ml, respectively. The microdilution technique is used more often due to the higher throughputs of the experiments, where plenty of samples can be analyzed using 96 or 364-well plates.

1.4.2. Disk diffusion method

Disk diffusion method is based on the subjection of commercially available disks (paper disks with a diameter of about 6-13 mm) with a pre-impregnated standard concentration of an antibiotic onto the agar plate with spread pathogen of interest. The antimicrobial agent immediately starts to diffuse outward from the disks, creating a gradient of antibiotic concentration in the agar. The highest concentration is found close to the disk, with decreasing concentrations further away from the disk. The plates are then incubated overnight, and the bacterial growth around each disc is observed. In contrast to resistant bacteria, the susceptible pathogen provides a clear area around the disk with a specific antibiotic (no growth).[55] The disk diffusion method is relatively easy to set up and inexpensive. However, it does not provide quantitative measurements due to visual detection (no possibility of MIC determination), and it is not applicable for some microorganisms[56].

1.4.3. Epsilometer test, E-test

E-test is a commercially available paper strip with an impregnated particular antibiotic, in which concentration gradually decreases along the strip. A printed numerical scale indicates antibiotic concentrations. The E-test is subjected to an agar plate with freshly inoculated bacteria and incubated overnight. The bacterial growth around the strip and a numerical scale of antimicrobial concentrations allow determining MIC value.[57]

1.4.4. Mechanism-specific tests

Resistant bacteria can be detected by establishing their particular mechanism of resistance. There are plenty of examples, like the detection of beta-lactamases, enzymes produced by bacteria able to inactivate beta-lactam antibiotics. Several clinical tests have been devised to detect beta-lactamases. These tests include the iodometric method, the acidometric method, and chromogenic substrates[58]. The most popular is the chromogenic cephalosporinase test. The discs are impregnated with a chromogenic substrate. As a beta-lactamase hydrolyzes the amide bond in a beta-lactam ring, nitrocefin changes color from yellow to red.

1.4.5. Automated antimicrobial susceptibility testing systems

There are existing commercial systems for automated antibiotic susceptibility testing and bacteria identification. They are based on the microdilution method and mechanism-specific tests but provide automated inoculation, reading, and interpretation of data. The difference between different systems is the capacity of sample trays and time of analysis. The most popular is the BioMerieux Vitek® System[59].

1.4.6. Genotypic methods

Resistance is genetically encoded and can be determined by the detection of particular resistance genes. However, the genotypic methods are used just for conformation of a resistance presence in bacteria because susceptibility to antibiotics is also dependent on the mode and level of expression of these genes. Some of the most common molecular methods are utilized for resistance detection. There are polymerase chain reaction (PCR), loop-mediated isothermal amplification assays (LAMP), fluorescence in-situ hybridization (FISH), and next-generation sequencing (NGS).

1.5. Detection of heteroresistance

Heterogenous antibiotic resistance was first described in 1947[60]. Despite these past years, there is a lack of laboratory standards and recommendations for studying that phenomenon.

The main methods currently used to detect bacterial heteroresistance are PAP (population analysis profile) test, Etest, and disc diffusion[18]. In the PAP test, the bacterial population is cultured on the agar plates containing different antibiotic concentrations (usually 2-fold increments), and the grown colonies are counted at each of these concentrations (Figure 2). The PAP test is a gold standard and the most reliable method, but it is used only to confirm specific clinical cases due to its labor-intensity and high costs. The Etest strips (GRD Etest for glycopeptide resistance detection) and disc diffusion assay allow for the detection of heteroresistance by quantifying colonies growing in the inhibition zones. These methods are less tedious and cheaper, but the detection of resistant cells present at low frequency is very challenging due to the low density of bacteria on the plate, and even not possible when the inhibition zone area is too small. Broth microdilution, automated broth (for example, VITEK 2), and growth methods (for example, BACTEC 960) are also used to detect heteroresistance. However, they show low sensitivity, and the results can be affected by the inoculum effect. It is a phenomenon described as an increase of MIC due to a high density of cells in the inoculum[61]. The techniques that can be used to detect heterogeneous antibiotic resistance can be molecular methods providing faster and more sensitive detection limiting to known mutations causing resistance.

Small colony variants (SCVs) are recognized from normal colony phenotypes by the smaller colonies' diameter and reduced pigmentation[35]. When growing on an agar medium containing 5-10% sheep or horse blood, SCVs colonies exhibit lower hemolysis and can be also detected by this feature[62].

An additional powerful single-cell approach for identifying tolerant to antibiotics subpopulation is the utilization of fluorescent reporter constructs and analysis of cells by flow cytometry[63,64]. Differentiation between cells with different growth rates can be provided by tracking the changes in ribosomal RNA content; for example, GFP (green fluorescent protein) inserted at the rRNA locus can be a reporter of ribosome biosythesis[65]. Another approach is a plasmid dilution method. After halting expression of a fluorescent protein, fluorescent signal dilution is observed due to an equal partitioning of a fluorescent protein between non-expressing daughter cells at each cell division[66,67]. An another promising strategy for marking growth phases of bacteria is to use a fluorescent TIMER protein developed number of years ago for measurement of time-dependent expressions in *Caenorhabditis elegans* and *Drosophila*[68,69]. It is a DsRed protein whose fluorescence converts from green to red over time, and the rate of color conversion is independent of protein concentration. TIMER was

already used as a growth rates reporter in *Salmonella* showing the possibility of marking slow-growing subsets[70].

Currently no practical methods are available for simultaneously reliable, sensitive, and not laborious bacterial heteroresistance studies in clinical microbiology. A new clinical ASTs are required, and microfluidics given single-cell analysis can play here an essential part.

1.6. Microfluidics

Microfluidics is considered both as a science and a technology. It allows us to study the behavior of fluids in the microchannels and provides microfluidic devices for plenty of applications in chemical, biological, and biomedical research[71–73]. Microfluidic devices commonly refers to lab-on-a-chip (LoC) technologies and miniaturized total analysis systems (μTASs)[74,75]. They are built with technologies first developed by the semiconductor industry and later expanded by the micro-electromechanical systems (MEMS) field. In the first place, most chips were manufactured in glass and silicon; in the early 2000s, enormously grown the technologies based on molding the microfluidic structures in polymers like polydimethylsiloxane (PDMS).

The fluid phenomena dominates liquids differently at macro- and microscale. In the field of microfluidics the most useful concepts are:

- **Reynolds number (Re)**- a dimensionless quantity that describes a ratio of inertial to viscous forces within a fluid. Re is proportional to flow speed and the system's length scale; it is inversely proportional to the fluid viscosity. A high Reynolds number indicates turbulent flow, dominated by inertial forces tending to create chaotic eddies, vortices, and other instabilities. Laminar flow occurs at low Reynolds numbers, where viscous forces are dominant, the fluid motion is constant and smooth. Laminar flow is characteristic of microfluidics, which allows for highly predictable fluid dynamics.
- **Surface and interfacial tension**- forces playing on a microscale more significant roles than gravity, which dominates on a macroscale. Surface tension is a tendency of liquid-air interface area to shrink to reduce its free energy. Interfacial tension is a similar phenomenon but concerns two immiscible fluids, for example, water and oil.
- **Capillary force**- it is an ability of a liquid to flow in narrow channels, constructions without assistance, or even in opposition to external forces like gravity.

Surface tension and capillary forces enables a variety of tasks in microfluidics; generation of monodisperse droplets[76], passive pumping of fluids in microchannels[77], filtering various of analytes[78], precise placing of user-defined substrates in selected surface[79]. The application of microfluidics is especially promising in biology research and diagnostics. There is a possibility to create excellent candidates to replace traditional laborious and time-consuming traditional experimental approaches. At the beginning of the microfluidic era, researchers focused only on single-phase continuous-flow systems, where the liquid is introduced to the chip and controlled by micropumps, microvalves, micromixers[80] or elektrokinetic effects[81–83]. The continuous-flow microchips have found the applications in a single-cell analysis by studying biophysical properties[84], genomics (DNA and RNA analysis by PCR[85,86]), transcriptomics[87], proteomics[88], and metabolomics[89]. Besides, it found interest in protein crystallization[90,91], electrochemistry[92], and drug screening[93,94]. However, continuous-flow microfluidics is burdened with several issues, like slow reagents mixing[95], low throughput experiments, diffusion of reagents due to the Taylor dispersion obstructing control of the local concentrations[95], contaminations caused by absorption of cells or molecules to the microfluidic channels.

1.6.1. Droplet microfluidics

An alternative approach to continuous-flow systems is droplet microfluidics, where discrete droplets are generated and manipulated through immiscible multiphase flows inside microchannels[96]. At an early stage of development, droplet microfluidics was supposed to generate microreactors for μTAS studies and fabricate droplet-based particles for materials research[97]. However, in the past two decades, enormous progress in theoretical and technical aspects resulted in a massive number of various applications including single-cell analysis[73,98], medical diagnostics[99,100], drug discovery[101,102], and environmental monitoring[103], etc. The application of droplet microfluidics is encouraging due to enhanced mixing and mass transfer within short diffusion distances, lack of boundary effects, for example, axial dispersion, and control of the reactions time on timescale from miliseconds to months[104,105]. Besides, the remarkable advantages are miniaturization, providing a possibility of single-cell and molecular analysis, compartmentalization creating a huge amount of individual reactors which can be manipulated independently, and parallelization making a platform for high-throughput analysis.

1.6.2. Methods of droplets generation

The formation of droplets can be carried out actively or passively[106]. In passive droplet generation, the two-phase flow is controlled by a pressure source located remotely from the droplet formation geometry provided by syringe pumps, pressure regulators, or gravity-based pressure units. In active methods, droplet generation is activated by external forces to exert local actuation and achieve a fast response. According to the type of additional energy, active droplet formation can be classified into thermal, magnetic, electrical, and mechanical methods[107]. Commonly used methods for droplet generation are passive techniques, so that this chapter will be dedicated to their description.

For the last few years we can observe the significant progress in passive droplet generation methods. A frequency for parallelized microfluidic droplet generators of pico- and nanoliter compartments reaches hundreds of kHz[108–111]. There are three standard microfluidic geometries for droplet generation: T-junction[112], flow focusing[76], and co-flowing[113]. The basic principle of operation for each technique is the same. Two immiscible fluids, continuous and dispersed phases, meet at the junction. The design of microchannels determines an interface deformation and droplet breakup. Which fluid become dispersed and which continuous phase is controlled by surface modification of microfluidic channels[114]. The most common case is using hydrophobic channels, where the aqueous phase disperses, and the oil phase surrounds the droplets.

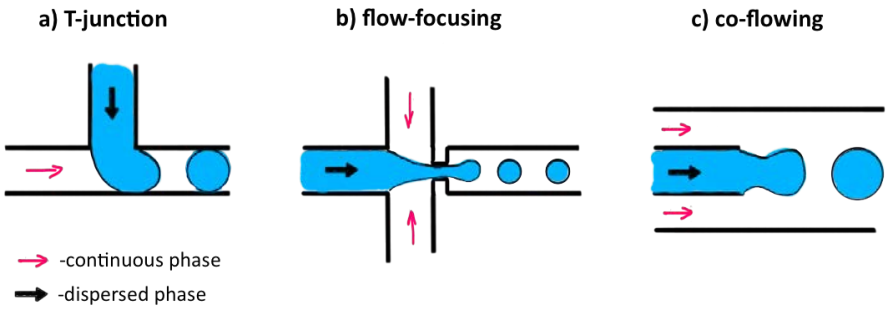

Figure 6. Three principle geometries for droplet formation; a) T-junction, b) flow-focusing junction, c) co-flowing. Pink and black arrows indicate continuous and dispersed phases, respectively.

In the T-junction geometry (Figure 6a), the dispersed and continuous phases flow through orthogonal channels and meet at a cross-junction[106]. A shear gradient appears the dispersed phase elongates and breaks into droplets. In flow-focusing geometry (Figure 6b), the dispersed and continuous phases flow coaxially through a structured region (shear-focusing), causing elongation of fluid, which eventually breaks into droplets. The droplet's size depends

on the channel geometry, flow rate, fluid viscosity, and addition of surfactant. In the co-flowing droplet generation method (Figure 6c), two fluid phases flow through a set of coaxial microchannels. The dispersed phase is introduced into an inner channel, and the continuous phase flows into an outer channel in the same direction. The size of the droplets is affected by fluid properties and flow rates.

In all these cases, the fluid behavior can be characterized by a few important dimensionless numbers calculated by the fluid properties, the geometry of the microfluidic design, and flow conditions[107]. They help to define the importance of different forces in microfluidic channels. The first is the Reynolds number (Re) indicating the inertial to viscous forces, Next one, the capillary number (Ca) represents the ratio of viscous shear stress to interfacial tension forces, which are the most significant in the droplet microfluidics:

$$Ca = \frac{\mu U}{\gamma},$$

where:
μ- dynamic viscosity of the fluid $[Pa \cdot s]$
U- characteristic velocity $[{}^{m}/_{s}]$
γ- surface tension $[J \cdot m^2]$

The capillary number helps predict droplet formation and its dimensions[115–118]. The third number is the Weber number, which measures inertial to interfacial tension. It indicates whether the kinetic or the surface tension energy is dominant.

1.6.3. Single-cell encapsulation

Encapsulation of cells within monodisperse droplets provides new means to perform quantitative biological experiments on a single-cell basis for large cell populations. The encapsulation is usually performed in a random process called Poisson distribution given by:

$$p(k, \lambda) = \frac{\lambda^k e^{-\lambda}}{k!},$$

where k is a number of cells in a droplet, and λ is the average number of cells per droplet volume.

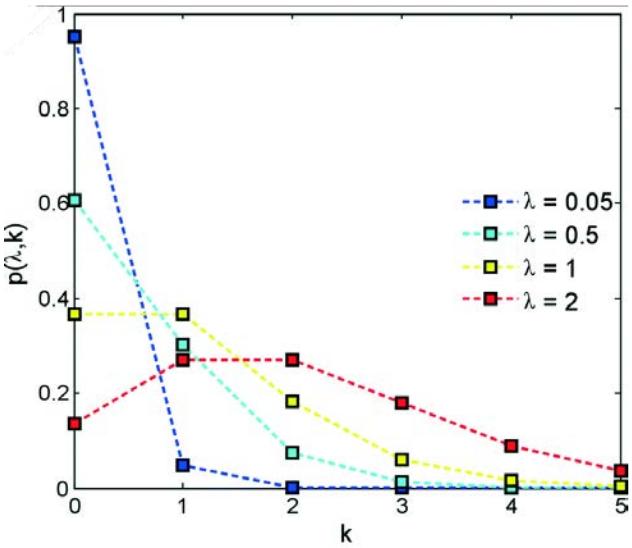

Figure 7. The Poisson distribution representation as a proportion of droplets p(λ, k) containing a given number of cells k for different values of average number of cells in the droplets λ. Figure reproduced from the article published by Collins et al.[119]

The cell suspension is directly emulsified into droplets, and cells are encapsulated stochastically. To provide single-cell encapsulation, cell suspension is highly diluted. It ensures that droplets do not contain no more than one cell, but it also results in a high number of empty compartments. Figure 7 represents the Poisson distribution for different cellular densities expressed by λ. The amount of cells per droplet increases with rising cellular concentrations with a maximum located on λ. Single-cell encapsulation is the most effective in a specific range of cell concentrations when $\lambda<1$[119].

1.6.4. Droplet stability and aging mechanisms

Droplet microfluidics is undoubtedly very attractive platform for high-throughput assays thanks to the utilization of a vast amount of discrete droplets behaving as separate reactors. These droplets are formed by combining two immiscible fluids (most often water compartments in oil) in microfluidic channels etched in silicon, glass and polymers. The last ones are mostly used in microfluidics, where PDMS is the most known material[120]. The generation of stable aqueous droplets requires hydrophobic modification of microfluidic channels. The continuous phase wets the channel surface and creates a thin layer preventing water droplets' contact with channel walls. There are many methods for surface treatment of microfluidic devices[120]. In the frame of research presented in this thesis, the internal channels surface in PDMS chips were modified using fluorosilane polymer by flowing the solution into microchannels and heating[121,122].

The stability of the droplet interface is provided by amphiphilic molecules, surfactants. They adsorb at the water-oil interface preventing droplet coalescence[123]. The flow of the droplets causes the heterogeneous distribution of surfactant molecules at the droplet-oil interface. This gradient of surface density induces a Marangoni effect (Figure 8a, b), which is opposite to the droplet flow and counteracts drainage of continuous phase film between droplets upon their collision[124] (Figure 8c, d). It stabilizes emulsion before coalescence. Apart from stabilization, surfactants are involved in the molecular exchange between droplets and biocompatibility of the system, which is essential in biochemical applications. The whole droplet system should be biocompatible, as must the surfactant and carrier oil. For that reason, many biochemical experiments rely on the use of fluorinated oils and fluosurfactants[125–128]. Despite biocompatibility, the choice of fluorinated oils is driven by the low solubility of organic compounds and high solubility of gases from which oxygen is an essential reagent for growing cells inside droplets.

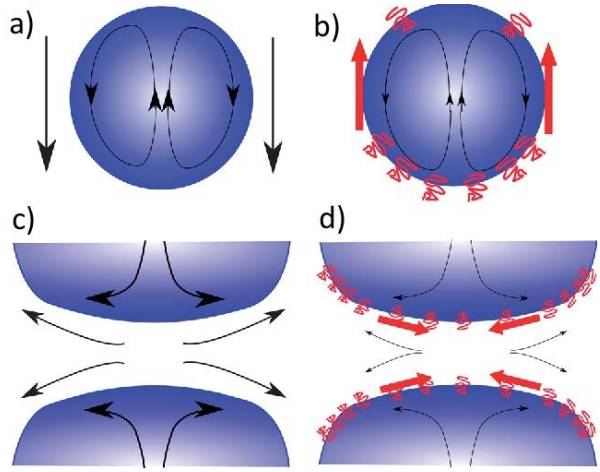

Figure 8. Marangoni effect on the motion of a droplet covered with surfactant. a) a moving droplet in the absence of surfactant, black arrows indicate the flow patterns; b) a moving droplet in the presence of surfactant, red arrows indicate a Marangoni stress reversed to the flow caused by a heterogeneous distribution of surfactant at the interface droplet-oil phase; c) draining of continuous phase upon collision of droplets before coalescence; d) stabilization of the droplets against coalescence. The Marangoni stress (red arrows) counteracts the drainage of a thin layer of carrier oil between droplets. Figure reproduced from the article published by J.-Ch. Baret[129].

One aging mechanism in droplet-based microfluidics is coalescence. The thin oil film between two adjacent droplets is raptured, and the droplets are fused. The second mechanism is Ostwald ripening[130,131]. It relies on diffusion of the aqueous phase from small droplets with higher Laplace pressure through carrier oil to larger droplets. It increases the average droplet size, reduces their number, and eventually leads to a total emulsion disruption.

1.6.5. Droplet microfluidics for microbiology

Droplet microfluidics finds application in several fields of microbiology: counting, detection, and identification of bacteria, analysis of bacterial physiology, antibiotic susceptibility testing, biotechnological evolution, and selection of strains[132]. The use of droplets in microbiology presents an advantage of bacteria compartmentalization in a small volume of liquid, which favors the fast accumulation of growing cells or molecules secreted by cells providing earlier detection compared to bulk culture. The second unique feature of droplet microfluidics is the facilitation of complex experimental protocols by performing iterative operations on droplets, like their formation, merging, splitting, mixing, sorting, injection of additional reagents. It creates a possibility to conduct many measurements on the same droplets[133,134] or observation of cells behavior in controllably changing environment[135]. The third significant advantage is the possibility of creating an enormous number of separate bioreactors providing single-cell and high-throughput bacteria examination.

1.6.6. Fluorescence-based bacterial growth detection methods

Monitoring bacterial growth in droplets is usually performed by introducing fluorescent labels[136,137]. One example of commonly used label is resazurin, which is a redox indicator and it is transformed to resorufin by metabolically active cells[138,139]. Unfortunately, dyes can leak out of the droplets making bacteria growth detection either impossible or limiting the incubation time within which the method can discriminate between proliferation and lack of it[140–142]. Another approach is to use enzymatic activity of microbes[128,143,144]. Enzymes produced by bacteria degrade a substrate to its fluorescent form. Sometimes bacteria has to be genetically modified to express specific enzyme and product of enzymatic activity can leak to the continuous phase. Another commonly used method relies on genetic modification of bacteria. The clone contains gene encoding fluorescent protein and its stable form is produced during the bacteria growth[145,146]. Detection of fluorescence of expressed proteins is widely popular and it has been used for example for the analysis of *Escherichia coli*[147] and *Staphylococcus aureus*[137] (Figure 9).

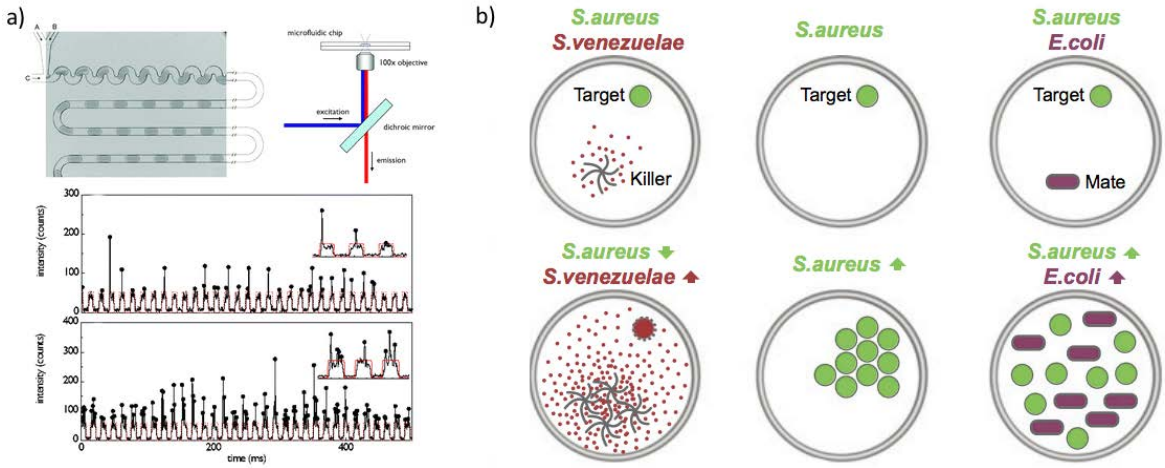

Figure 9. Bacteria detection based on fluorescent proteins readout. a) a microfluidic device for generation of aqueous droplets (top left), schematic of the optical setup for fluorescence detection (top right), and exemplary fluorescence readout for low (central scheme) and high (bottom scheme) cell loading conditions. Each arch-shaped signal indicates a droplet with a weakly fluorescent LB medium. A vertical spike corresponds to the droplet containing cells expressing the fluorescent protein. Figure reproduced from the article published by Huebner et al.[147]; b) Screening of bacteria inhibiting *S. aureus* growth. *S. aureus* expressing green fluorescent protein was encapsulated with a killer *S. venezuelae* producing red fluorescent metabolites or mate *E. coli* with a far-red fluorescent reporter (top). *S. venezuelae* inhibits *S. aureus* growth, which yields distinct combinations of fluorescent signals (bottom) in the droplets. Selection of the droplets with the lowest intensity of green fluorescence results in the enrichment of killers. Figure reproduced from the article published by Terekhov et al.[137]

1.6.7. Label-free methods for bacterial growth detection

Parts of this chapter are published as: Pacocha N., Bogusławski J. et al., *High-throughput monitoring of bacterial cell density in nanoliter droplets: label-free detection of unmodified Gram-positive and Gram-negative bacteria*, *Analytical Chemistry*, 2020[148]

Detection of fluorescence intensity in the droplets is very common approach, but either way it is an additional step to introduce necessary substrates or to modify cells. There is thus an important need for development of label free technique that would allow detecting proliferation of unlabeled bacteria in nanoliter droplets. Some steps towards this goal have already been demonstrated. For example, Jakiela et al.[135] and Horka, Sun et al.[149] presented methods of measuring of optical density in microliter volume droplets. While these results show that in principle the readout of optical density in droplets is possible, the size of the droplets does not allow for high-throughput applications. L. Boitard et al. presented an interesting method for cell detection in picodroplets[150]. In this contribution the droplet composition changes during bacteria growth and it results in the change of osmotic pressure. Water molecules start to migrate between droplets causing their shrinking or swelling. The

decrease in volume can be correlated with a number of cells. Unfortunately, the method does not provide high-throughput screening of the droplets right now. Similarly, Liao et al. showed a label-free and sensitive method for bacteria detection in picoliter droplet using micro-Raman spectroscopy, but the method was not used for droplet screening[151]. On the other hand, Zang et al. presented a method for detection the growth of bacteria in picoliter droplets based on real-time image processing[152]. They achieved a 100 Hz frequency of readout and growth-dependent droplet sorting. A promising alternatives to the techniques mentioned above are methods based on detection of scattered light intensity. A direction of propagation of a laser beam illuminating bacteria is changed upon scattering. The intensity of scattered light is proportional to the number of cells. Liu et al.[153] proposed an assay based on detection of light scattered by bacterial cells in picoliter droplets with the screening frequency of 243 Hz (Figure 10). In this approach the light is collected by fiber optic components, which makes the whole system more compact and cost-effective. Similarly, Hengoju et al.[154] presented an optofluidic detection system based on the readout of absorbance and scattered light in picoliter droplets with frequency of approx. 40 Hz.

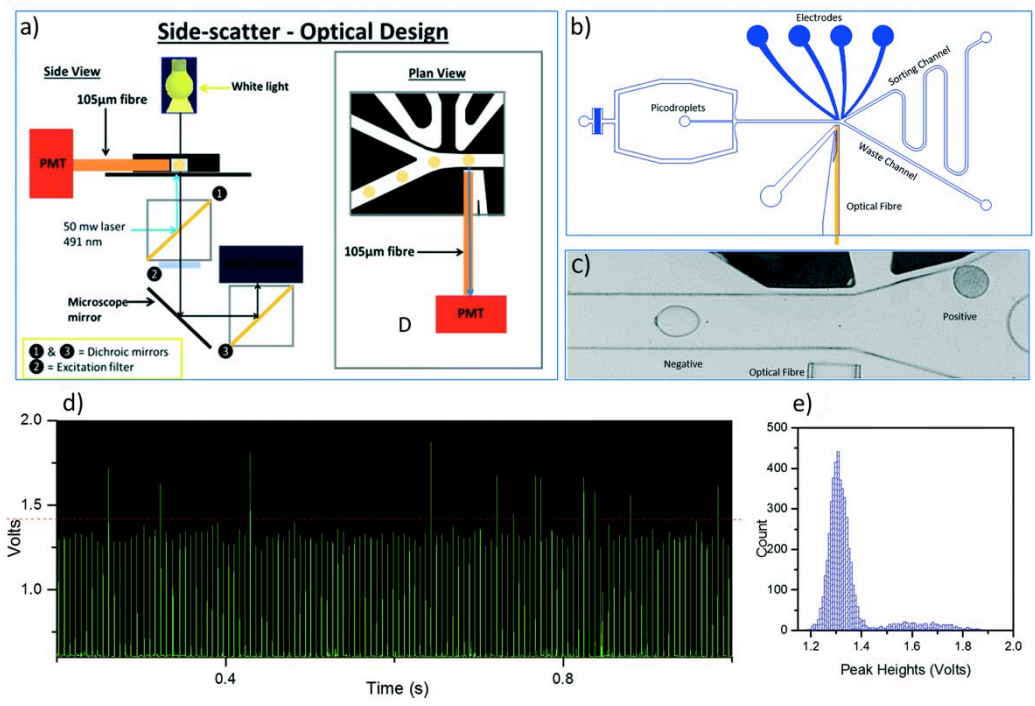

Figure 10. Screening of droplets based on scattered light intensity. a) schematic representation of the optical setup; b) scheme of the microfluidic chip to detect scattered light and droplet sorting; c) micrograph presenting picodroplets flowing in the sorting region of the chip; d) exemplary scattered light signal from the picodroplets. The dotted red line indicates a sorting threshold; e) histogram of the droplets' scatter light intensity. Figure reproduced from the article published by Liu et al.[153]

1.6.8. Identification and quantification of bacteria in droplets

The most common approach for highly specific bacteria identification is the detection of bacterial genes and genomes. Droplet microfluidics refined this research area by introducing a droplet digital PCR (ddPCR) [155]. It brings a possibility of analyzing bacterial genomic content at a single-cell level. A DNA sample is randomly partitioned across discrete droplets so that each droplet contains no more than one copy of DNA. Specific gene sequences are amplified, providing an increasing fluorescence intensity (Figure 11). According to Poisson distribution, the number of 'positive' droplets meaning compartments with high fluorescence intensity, indicates absolute DNA content in the initial sample. Droplet digital PCR allows to quantify and identify nucleic acids with high specificity and precision[156–158].

Lim et al. presented a method, PCR-activated cell sorting (PACS), for separation of target microbial cells based on their genomic content[159]. Bacteria are encapsulated together with PCR reagents, among which primers and TaqMan probes provide high specificity of target bacteria detection. The amplification of specific gene sequences during PCR leads to increasing fluorescence intensity allowing sorting of the droplets containing a desire bacteria. In another work, Ziegler et al. showed a quantitative ddPCR method for detection of *Staphylococcus aureus*, *Streptococcus pneumoniae*, and *Escherichia coli* on blood samples from patients with bloodstream infections[160].

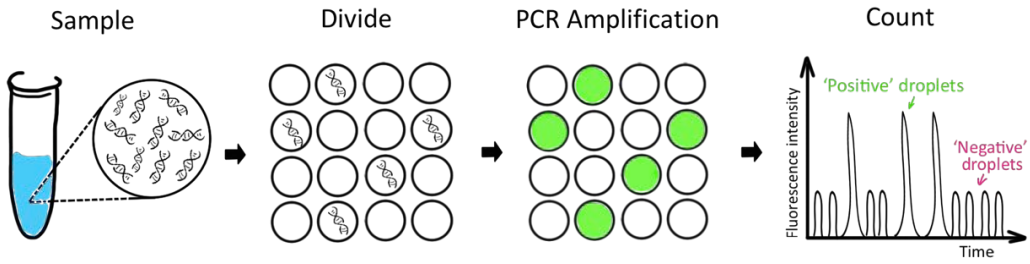

Figure 11. Droplet digital polymerase chain reaction (ddPCR). An initial DNA sample is split into discrete droplets, such that each droplet contains one ('positive' droplet) or no copy ('negative' droplet) of template DNA. The fluorescence signal is generated during PCR in the droplets containing target gene sequence. DNA concentration in the initial sample is calculated based on the number of 'positive' droplets and Poisson distribution.

Kang et al. presented an attractive approach for rapid bacteria detection in clinical samples using DNAzymes sensor technology and 'Integrated Comprehensive Droplet Digital Detection' (IC 3D)[161]. DNAzymes are short catalytic oligonucleotides that specifically react with the lysates of target bacteria, leading to a rapid increase of fluorescence signal (Figure 12). The system provides absolute quantification of both stock and clinical *E. coli* isolates.

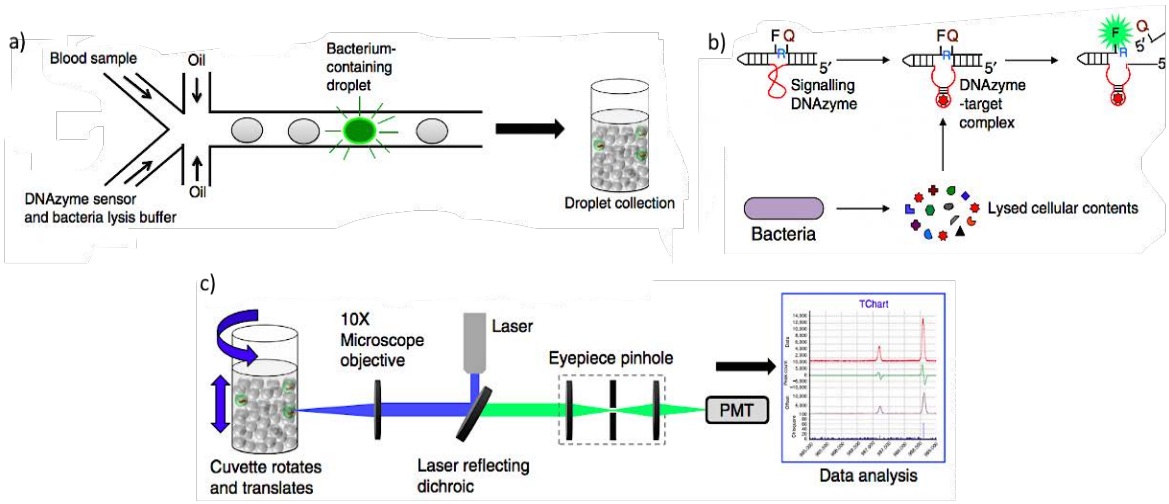

Figure 12. Detection of bacteria using a DNAzyme sensor and IC 3D technology. a) Encapsulation of blood sample with DNAzyme sensor and bacteria lysis buffer; b) schematic representation of the mechanism of target and DNAzyme sensor interaction. A cellular bacterial content binds to the inactive DNAzyme sequence (red), which actives DNAzyme to catalyze the fluorogenic substrate at the ribonucleotide junction (R). It results in cleavage of the fluorophore (F) and the quencher (Q), producing a high fluorescence signal; c) Droplets detection by IC 3D counter. The cuvette with collected droplets rotates and moves vertically while the laser beam illuminates the droplets, and emission light is collected by a photomultiplier tube (PMT). Figure reproduced from the article published by Kang et al.[161]

Lyu et al. demonstrated a quantitative detection method of *Mycobacterium tuberculosis* cells expressing a β-lactamase enzyme, BlaC148. The number of bacteria encapsulated at the single-cell level together with a fluorogenic probe for BlaC detection can be counted by enumerating fluorescent droplets. Bacteria can also be detected by micro-Raman spectroscopy as shown in the work of Liao et al.[151]. A droplet with bacteria is transported to the detection area, where cells are accumulated at the tips of an energized quadrupolar microelectrode array by means of electroosmosis and dielectrophoresis. Then, the droplet is removed and bacteria are detected by Raman spectra. The disadvantage of this method is lack of high-throughput droplet screening.

1.6.9. Microfluidic antimicrobial susceptibility testing

Multiple microfluidic platforms for testing bacteria susceptibility to antibiotics were developed. They can be divide into categories by the approach of liquid handling: static chamber arrays, flow chamber arrays, droplet arrays, a system with flowing droplets, and a separate category of phenotypic-molecular tests. The first four categories rely on bacteria growth detection (phenotypic ASTs) in the absence or presence of antibiotic, the last category is the hybrid of phenotypic and genotypic assessments.

In the static chamber systems, the sample firstly fills the entire device. Then the chambers are separated by oil (Figure 13a), creating discrete bioreactors. After incubation stimulating the growth of colonies, we can assess the outcome visually[162]. It is a rapid and easy-to-use device but hardly scalable, which limits its use in heteroresistance studies.

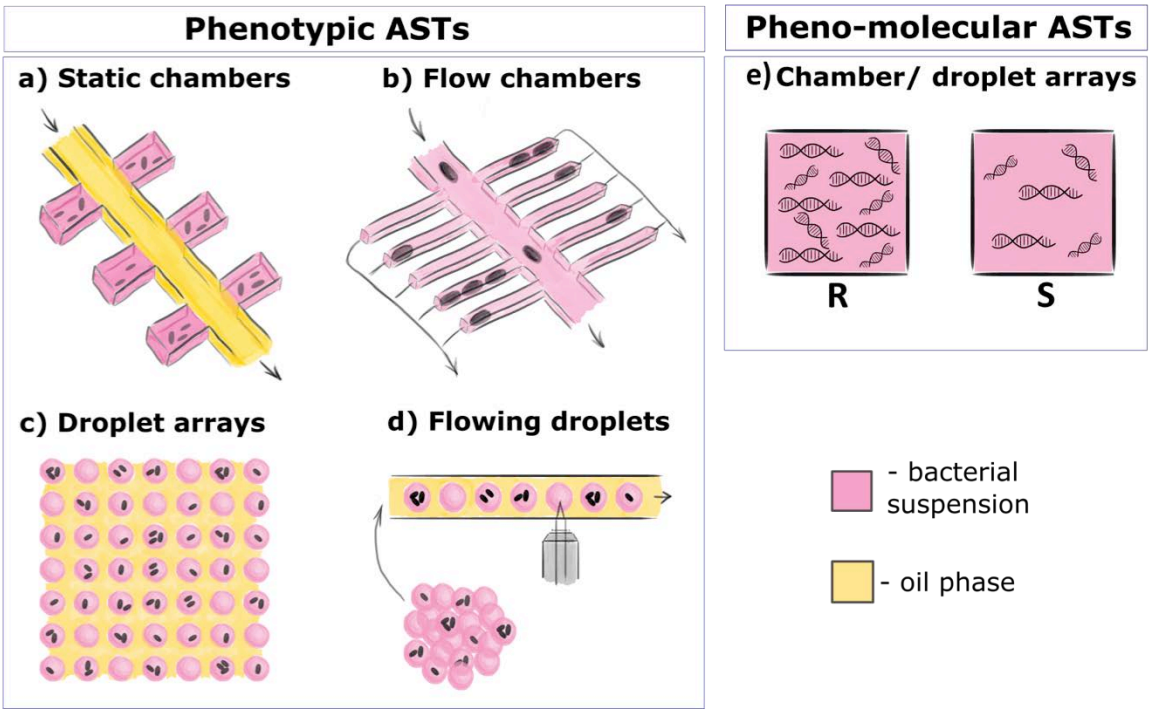

Figure 13. Schematic representation of microfluidic antimicrobial susceptibility testing in the form of a) static chambers providing a relatively easy and rapid measurement of bacteria growth considering a low number of chambers and detection of bacteria division at the level of single cells using optical microscopy; b) flow chambers, similar to static chambers with the exception that we can change their content over the course of the experiment; c) droplet arrays offering greater throughput and multiplexing with still relatively convenient detection as the droplets are immobile. The limiting factor is the high complexity of changing the conditions inside the droplets and possible transport of matter between compartments; d) system based on flowing droplets, providing excellent throughput and multiplexing capabilities. Complex operations resulting in the change of droplet composition are possible even at the level of single compartments. The detection of bacteria growth is more difficult as the cells move. The incubation increasing number of bacteria is indispensable. Besides, the transfer of matter between droplets has to be considered; e) 'pheno-molecular' tests offering high-speed measurements of bacteria susceptibility based on DNA or RNA concentration.

Similar properties offer the flow chamber arrays (Figure 13b) combining microfluidic devices with microscopy, where the growth of many individual cells is observed over time[163,164]. The most interesting design is the *mother machine*[165,166]. It is a microfluidic chip consisted of plenty of 1D channels, which width match the width of a bacterial cell. One *mother* bacterial cell is trapped per one growth channel. It continuously divides, and the excess of cells is flushed away at the end of the channel by a nutrient supply stream. The *mother machine* enables long-term experiments with a single cell over many generations under precisely

controlled conditions. The droplet arrays (Figure 13c, 2D array of droplets placed in microwells)[167–169] and system based on flowing droplets[170,171] (Figure 13d) are more laborious, and time-consuming but offers high scalability and high-throughput bacteria screening. The bacterial suspensions can be split into enormous number of droplets enabling analysis of considerable number of cells. The last category is the 'pheno-molecular' test outstanding by rapid pathogen identification and verification of its susceptibility to antibiotics (Figure 13e). They exploits the concentration of DNA or RNA molecules as a proxy for the growth of bacteria which is the phenotype detected by optical AST[172–174]. The limiting factor of 'pheno-molecular' tests is their difficulty of use.

1.6.9.1. Droplet-based antimicrobial susceptibility testing

Among all microfluidic antimicrobial susceptibility testing, the droplet-based assays provide the highest throughput of bacteria screening. It is especially essential when a considerable amount of cells need to be analyzed, for example, towards heteroresistance of the bacterial population. For that reason the following chapters focus on platforms based on flowing droplets.

Researchers have reported various droplet-based systems for determining bacteria susceptibility to antibiotics. Boedicker et al. demonstrated a plug-based platform for sensitivity testing of *Staphylococcus aureus* to many antibiotics via a fluorescence assay[138]. The single bacterial cells were encapsulated in 4nL droplets along with viability indicator, resazurin. Then, the plugs were incubated for 7h to increase the number of bacterial cells for their reliable detection. Kaushik et al. presented a similar AST fluorescence assay (dropFAST) with the difference in droplet size and system integration[174]. The 20 pL droplets can be generated, incubated, and screened using one microfluidic platform (Figure 14a). The concept of antimicrobial susceptibility assessment using the dropFAST system was illustrated by testing the antibacterial effect of gentamicin on *E.coli* growth. Liu et al. presented a label-free method for detection and sorting of *E. coli* mutants resistant to fusidic acid[153]. Bacterial samples with fusidic acid were split into 330 pL droplets and incubated for 8h before screening towards scattered light intensity detection. Postek et al. presented a system with improved throughput where dozens of droplet libraries of ca. 2000 compartments were generated semi-automatically. Each library contained a different antibiotic concentration (Figure 14b)[171].

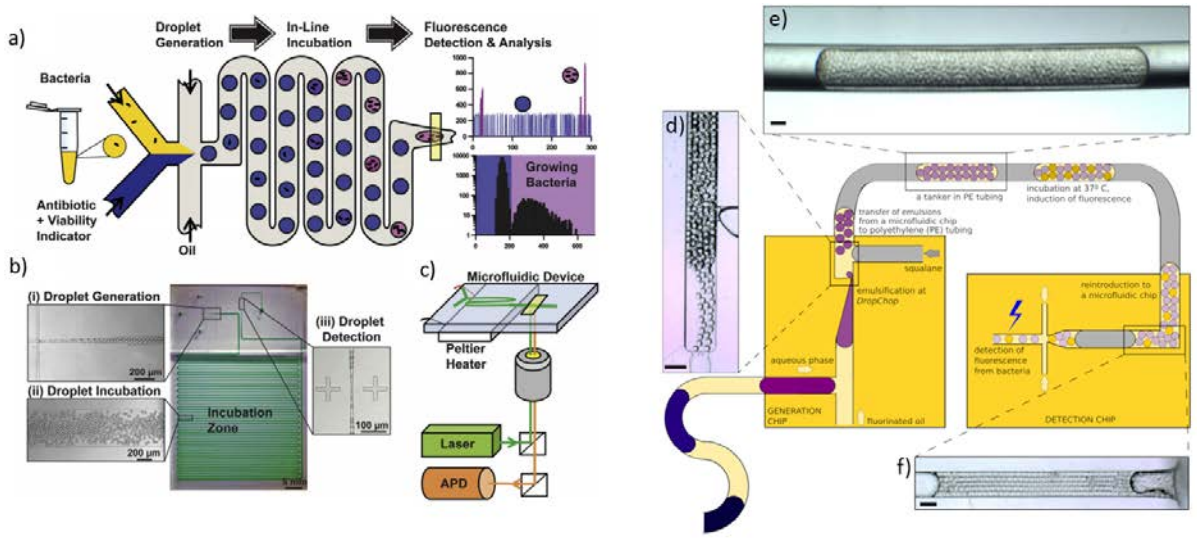

Figure 14. dropFAST platform for bacterial growth detection and antimicrobial susceptibility testing. a) dropFAST system allows for encapsulation of single bacterial cells with antibiotic and fluorescent growth indicator dye (resazurin) into picoliter droplets, on-chip droplets incubation for a few bacteria replication, and droplet screening for fluorescence intensity detection. Empty droplets emit weak fluorescence intensity, while droplets with growing bacteria emit strong fluorescence. The number of growing bacteria is calculated based on the histogram of droplets' fluorescence intensities; b) micrographs of the integrated dropFAST platform for droplet generation, incubation, and detection of the droplets in a continuous flow; c) schematic representation of the dropFAST platform's instrumentation. Droplet incubation is conducted using a Peltier heater, and fluorescence detection utilizes a laser excitation source and an avalanche photodiode (APD) detector. Figure reproduced from the article published by Kaushik et al.[174]; d) Large droplets of bacteria suspension with different antibiotic concentrations are generated using T-junction or vertically oriented *DropChop* emulsifying geometry; e) The subsequent libraries of nanoliter droplets (*tankers*) are separated by immiscible squalane oil (grey) and collected in PE tubing; f) The *tankers* are then incubated to allow bacteria to grow and increase the droplets' fluorescence intensity, which is measured in the detection chip after incubation. Scale bars: 400 µm. Figure reproduced from the article published by Postek et al.[171]

1.6.9.2. Droplet-based detection of heteroresistance

Parts of this chapter are published as: Scheler O., Makuch K., Debski P., Horka M., Ruszczak A., Pacocha N., Sozański K., Smolander O.-P., Postek W., Garstecki P., *Droplet-based digital antibiotic susceptibility screen reveals single-cell clonal heteroresistance in an isogenic bacterial population*, *Scientific Reports*, 2020[175]

Droplet microfluidics allows for high-throughput and faster antibiotic susceptibility testing comparing to standard AST methods. Also, as described in the previous chapter it brings essential innovations in the testing of bacteria behavior in the presence of antibiotics at the single-cell level. Traditional determination of minimum inhibitory concentration is not always informative enough to guide effective antibiotic treatment. Artemova et al. demonstrated that measured MIC can strongly depend on the initial bacterial density (inoculum effect), particularly in case of antibiotic resistance mediated by degradation[176]. The superior

quantitative feature of antibiotic resistance is the measurement of single-cell minimum inhibitory concentration (scMIC). Eun et al. presented a single-cell analysis of the bacteria population by encapsulating *E. coli* cells in agarose nanoparticles with different serial concentrations of rifampicin[177]. The minimum inhibitory concentration was determined, and spontaneous resistant mutants were isolated by fluorescence-activated cell sorting (FACS). Sun et al. presented a digital droplet PCR to detect resistance genes and point mutations in *H. pylori* cells in stool samples[178]. Lyu et al. demonstrated a digital quantification of the heteroresistance based on single-cell MIC determination using fluorescent viability probe alamarBlue[175,179].

The measurement of scMIC is an excellent platform for quantifying the distribution of each cell's phenotypic responses in bacterial populations to antibiotics. Phenotypic variation of genetically identical cells remains poorly studied compared to the genetic mechanisms of drug resistance[180,181]. The cells differ from each other with respect to gene expression and other phenotypic traits[182–184]. Phenotypic heterogeneity can be medically relevant due to the persistence of bacterial individuals in the face of antibiotic exposure causing unsuccessful treatment. Scheler et al. demonstrated a droplet-based digital antibiotic susceptibility method for screening of each cell in isogenic bacterial population towards heteroresistance[175].

Escherichia coli DH5α carrying a yellow fluorescent protein (YFP) gene for the detection was encapsulated in water-in-oil droplets with different cefotaxime concentrations. The starting inoculum suspension was diluted so that the vast majority of non-empty droplets contained only one cell. After incubation, each droplet's fluorescence intensity was measured providing a total number of droplets, N and the number of positive compartments, N_+ (containing fully grown bacteria) for each droplets' library with a particular concentration of antibiotic, c (Figure 15a, b).

Authors presented the results of single-cell antibiotic susceptibility testing in the form of fraction of individual cells that grow as a function of antibiotic concentration (Figure 15c) and as a probability distribution density, p(MIC), of cells exhibiting a given MIC (Figure 15d). The results suggest that heteroresistance is not a phenomenon where there are two strictly different sub-populations (resistant and susceptible with clear threshold), but it is a continuous gradient of susceptibility among the population.

The probability distribution of individual MICs allows for precise analysis of phenotypic heterogeneity of the bacterial population. The response of single-cells to antibiotics helps to avoid the failure of the antibiotic treatment. It allows for a more precise analysis of tolerant to antibiotics sub-populations.

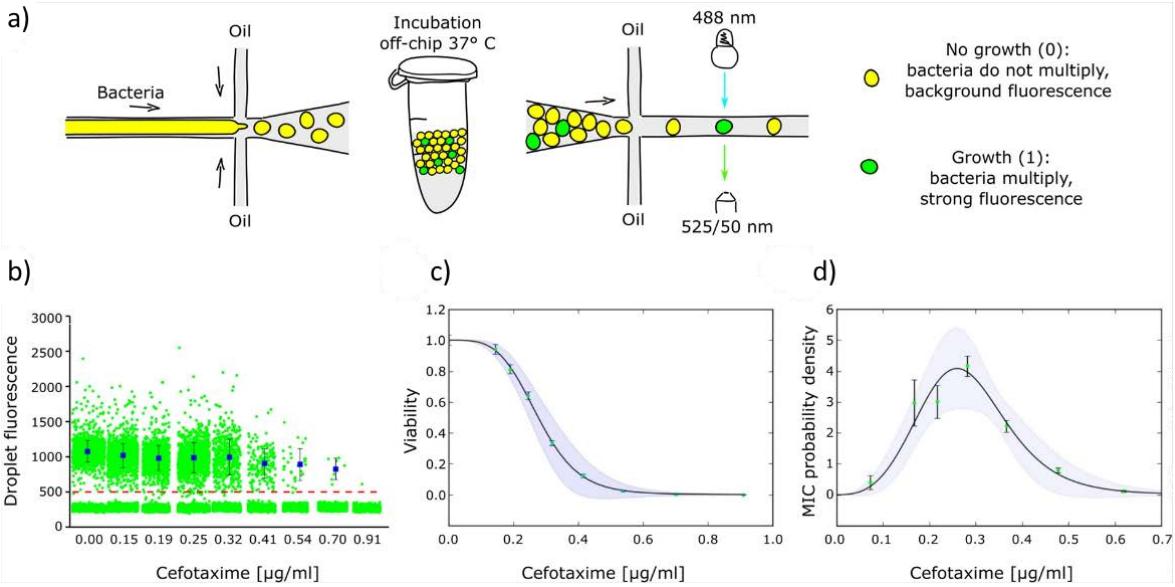

Figure 15. Droplet digital cefotaxime susceptibility screen of isogenic *E. coli* population. a) An experimental workflow for the single-cell assay, in which water-in-oil droplets consisting of bacteria, culture medium, and antibiotic are generated. Each antibiotic concentration is a separate library of nanoliter droplets. During incubation, encapsulated bacteria replicate YFP (yellow fluorescent protein) unless the antibiotic inhibits the growth. After incubation, the droplets are screened for fluorescence intensity using a confocal microscope. The readout has a binary characteristic, bacteria proliferate (1- positive droplet) or does not (0- negative droplet); b) fluorescence signal intensities of each droplet in nine samples containing different concentrations of the antibiotic. The red dashed line indicates a threshold for positive droplets. Blue rectangles with error bars mark the average signal of positive droplets with standard deviations; c) cell viability as a function of antibiotic concentration c; d) probability distribution of individual MICs in the bacterial population received from a numerical derivative of the data points in c). Figure reproduced from the article published by Scheler et al.[175]

2. Materials and Methods

This chapter describes the materials, microfluidic chip fabrication methods, sample preparation, detection, experimental procedures, and data analysis processes used in the following projects:

I. *Droplet digital CFU (ddCFU) assay for precise quantification of bacteria over a broad dynamic range.*
II. *Species specific, accurate and precise quantification and identification of bacteria in mixed samples.*
III. *High-throughput label-free readout of bacteria density in nanoliter droplets.*
IV. *Droplet-based assay for quantitative characterization of bacterial population.*

2.1. Fabrication of microfluidic chips

This procedure was used in all projects performed in this doctoral dissertation.

Fabrication of microfluidic chip consists of three steps. First, the channel network is designed and milled in polycarbonate (PC) plate using a CNC machine (MSG4025, Ergwind, Poland). In the next step, polydimethylsiloxane (PDMS, Dow Corning, USA) is poured onto the PC chip and polymerized at 75^{o}C for 1 hour. Then, the newly created positive mold's surface is activated by Laboratory Corona Treater (BD 20AC, Electro-Technic Products, USA) and silanized in the vapors of tridecafluoro-1,1,2,2-tetrahydrooctyl-1-trichlorosilane (United Chemical Technologies, USA) for 30 min under 10 mbar pressure. In the last step, the PDMS chips are fabricated using the salinized positive mold and bonded to 1mm thick glass slides using oxygen plasma. The microfluidic channels are modified to enhance their hydrophobicity by introducing Novec 1720 solution (3M, USA), evaporation at room temperature, and baking the chip at 75^{o}C for 1 hour.

2.2. Generation of droplets

This procedure was used in all projects performed in this doctoral dissertation.

Generation of the droplets was conducted using a setup shown in Figure 16a. The heart of the system is a PDMS microfluidic chip with a flow-focusing junction (Figure 16b) operated by neMESYS syringe pumps (Cetoni, Germany). The syringes (Hamilton, USA) contained Novec HFE 7500 fluorocarbon oil (3M, USA) and 2% triblock PFPE-PEG-PFPE surfactant. One syringe was a source of the continuous phase, and the second one was providing the sample. The volume of one sample was 10-100 μl. Such small volumes were sucked into the microfluidic Teflon tube and then pushed by the oil filling the syringe. The continuous phase passes the filters and split the sample into droplets at a frequency of ~500 Hz. The droplet formation process was monitored in real-time using uEye camera (IDS Imaging Development Systems GmbH, Germany).

The dimensions of a microfluidic chip for droplet generation are following:

- channel for disperse phase at inlet, width 800 μm x height 800 μm,
- channel for continuous phase, width 200 μm x height 200 μm,
- flow-focusing junction, width 100 μm x height 120 μm,
- outlet channel, width 800 μm x height 800 μm.

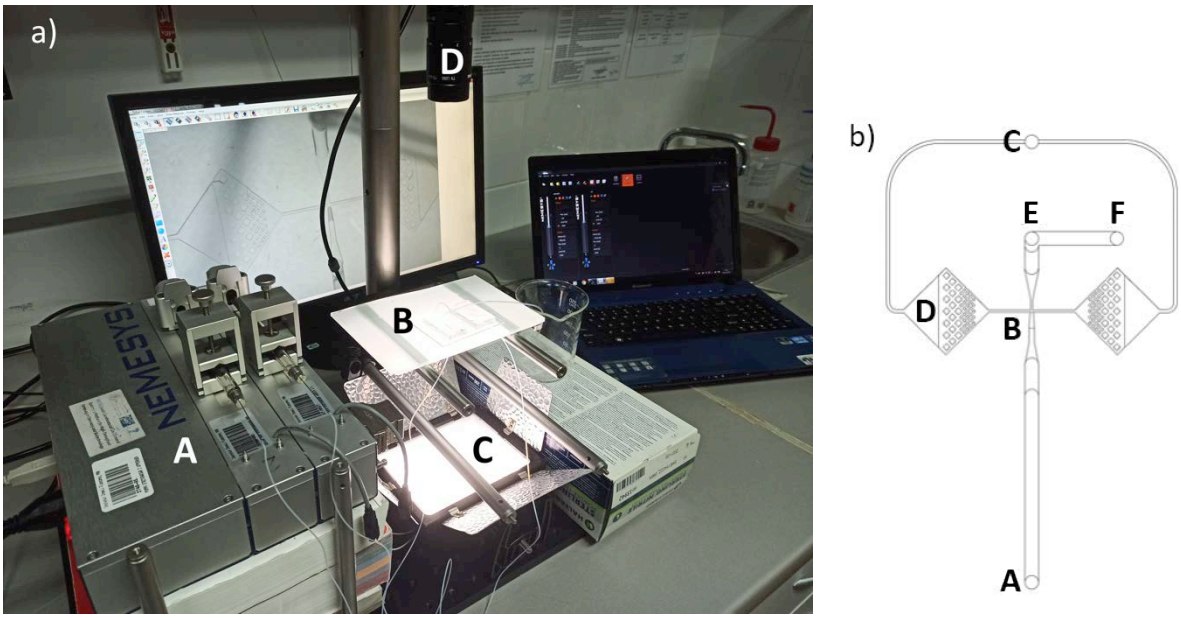

Figure 16. The setup for droplet generation. a) photograph showing a station for droplet formation. The syringes containing oil and surfactant operated by syringe pumps (A) provides the flows of a continuous and dispersed phase in the microfluidic chip (B). The light source (C) allows for real-time monitoring of the droplet generation process with a uEye camera (D); b) scheme of a microfluidic chip used for droplet generation. The sample is introduced through an inlet (A), split into droplets in flow-focusing (B) by the continuous phase flowing by side channels (C) and passing the filters (D). The droplets are collected in an outlet (E). The additional channel (F) can be used to separate the droplets by air plugs.

2.3. Fluorescence detection in droplets using confocal microscope

This chapter concerns the projects no. I and II.

We used following dye substrates to measure metabolic activity of bacteria: resazurin sodium salt (Sigma-Aldrich, USA) and C12-resazurin (part of Vybrant Cell Metabolic Assay Kit, Life Technologies, USA). Besides, we measured fluorescence intensity in droplets originated from TaqMan probes and enhanced green fluorescent protein (EGFP). Table 1 presents a distribution of fluorescent markers into individual projects where fluorescence intensity was measured with confocal microscope.

Table 1. Fluorescent markers used in I and II projects where fluorescence intensity was measured using confocal microscope.

Project	Fluorescent marker
I. Droplet digital CFU (ddCFU) assay for precise quantification of bacteria over a broad dynamic range	C12-resazurin, EGFP plasmid in *E. coli* DH5α
II. Species specific, accurate and precise quantification and identification of bacteria in mixed samples	TaqMan probes with 6-FAM (6-Carboxyfluorescein) fluorophore

The fluorescence intensity in the droplets was measured using a confocal microscope (Nikon, Japan) (Figure 17a) and a microfluidic chip with flow-focusing (Figure 17b) operated by syringe pumps. The droplets are injected into the chip, and the additional oil streams separate them further apart from each other. Then, the droplets are illuminated by the laser beam. We acquired the fluorescence of TaqMan probes and EGFP at excitation/detection wavelengths of 488 nm/ 500-550 nm. In the case of resorufin/C12, at 561 nm/ 570-620 nm, respectively.

Figure 17. An experimental setup for detection of fluorescence intensity in droplets. a) the detection chip (A) operated by syringe pumps (B) is mounted on the stage on the confocal microscope (C) and all the data generated during fluorescence intensity measurement are collected by the computer (D); b) a scheme of a microfluidic chip for droplet screening. The droplets are introduced through an inlet (A) and separated in flow-focusing (B) by oil stream (C). The oil passes the filters (D) to be free of clogging particles. Fluorescence intensity is measured just after the junction (red rectangle), and then the droplets are disposed of through an outlet (E).

The dimensions of a chip for fluorescence intensity reading in droplets are following:

- channel for droplets, width 1200 µm x height 1200 µm
- channel for continuous phase, width 114 µm x height 100 µm
- flow-focusing junction, width 124 µm x height 100 µm

2.4. Scattered, autofluorescence and fluorescence light detection using self- built optical detector

This chapter concerns the project no. III, High-throughput label-free readout of bacteria density in nanoliter droplets.

The measurement of scattered, autofluorescence, or fluorescence light intensity was conducted using a self-built detector. Figure 18a shows the complete optical setup. The droplets are introduced to the microfluidic chip (Figure 18b) and illuminated by a 473 nm laser beam delivered by a fiber. The laser beam is first collimated with a lens (L1, focal length 19 mm) and then focused by an objective (MO, Olympus RMS20X) into the middle of the detection channel. The scattered light is collected with a multimode optical fiber positioned at 90^{o} to the laser beam. We use a 105 µm fiber with a low numerical aperture (0.1) to restrain the detection area. An aspheric lens (L2, focal length 8 mm) then focuses the guided light onto an avalanche photodiode (APD, Thorlabs APD120A, bandwidth: 50 MHz). We use a bandpass filter (BP1, central wavelength of 470 and 10 nm of bandwidth) to filter out the fluorescence and pass the scattered light only. The autofluorescence or fluorescence signal collected by the objective is reflected on a dichroic mirror (DM, a cut-off wavelength of 490 nm), passes a bandpass filter (BP2, a central wavelength of 530 and 43 nm of bandwidth) then the light is focused by a lens (L3, focal length 30 mm), passes a pinhole and targets a photomultiplier (PMT, Hamamatsu H5783-20). The photomultiplier is placed in a confocal configuration, which allows rejecting out-of-focus light (e.g., light reflected from other surfaces, stray light). Both collected signals (scattering and fluorescence/ native fluorescence) are recorded simultaneously with a data acquisition card (National Instruments, USB-6212, sampling frequency: 500 kHz) and processed by custom-written LabVIEW software.

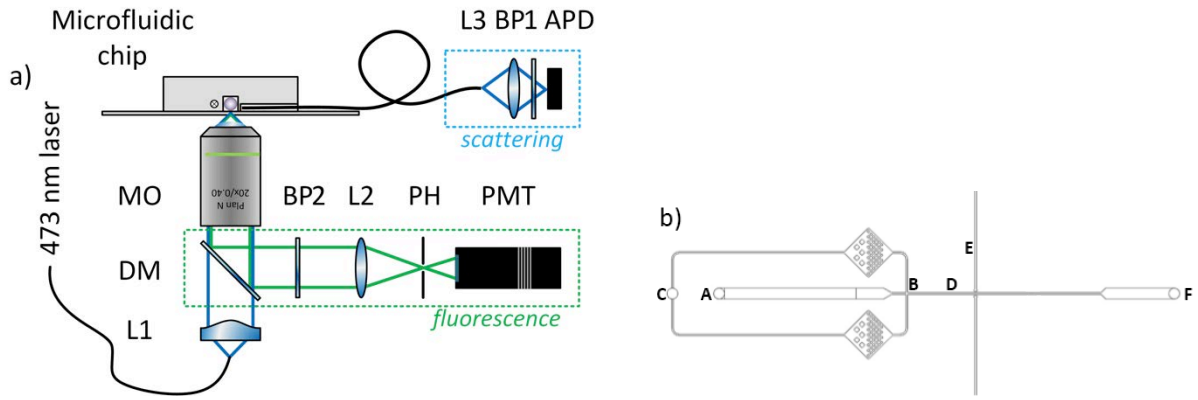

Figure 18. Schematic representation of experimental setup. a) Scheme of the optical setup. L1-L3-lenses, BP1 and BP2-bandpass filters, MO-microscope objective, DM-dichroic mirror, PH-pinhole, APD-avalanche photodiode, PMT-photomultiplier; b) scheme of a microfluidic chip for scattered, autofluorescence and fluorescence light detection. The droplets are introduced through an inlet (A), separated from each other in a flow-focusing (B) by oil without surfactant (C) and illuminated by laser beam in the detection channel (D). The scattered light is collected by an optical fiber (E), and the droplets are discarded through an outlet (F). Figure reproduced from the article published by Pacocha, Bogusławski et al.[148]

The dimensions of a chip for scattered and fluorescent light detection are following:

- channel for droplets, width 800 µm x height 100-1200 µm,
- channel for continuous phase, width 120 µm x height 100 µm,
- flow-focusing junction, width 120 µm x height 100 µm,
- detection channel, width 120 µm x height 100 µm

2.5. Data analysis

Data acquired using confocal microscope (project no. I and II): the raw fluorescence data were analyzed using MS Office Excel (Microsoft, USA) with Real Statistics Resource Pack (http://www.real-statistics.com/).

Data acquired using self-built detector (project no. III): the scattering, fluorescence, or autofluorescence signal intensities were analyzed using custom-written LabVIEW software. The positive droplets were distinguished from negative ones by a two-level threshold-based approach. The first threshold allows counting all the droplets, and the second one determines negative form positive compartments (Figure 19).

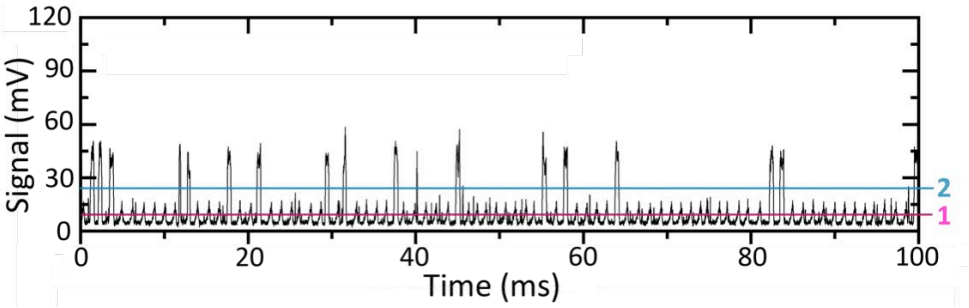

Figure 19. Exemplary scattered light signal from nanodroplets with two thresholds, the lower one for counting all the droplets (pink), and higher one for positive droplets determination (blue).

2.6. Real-time and direct droplet digital PCR

The chapter concerns project no. II, Species specific, accurate and precise quantification and identification of bacteria in mixed samples.

2.6.1. Reagents

We used the same reagents in real-time PCR and dddPCR experiments to ensure the same reaction conditions for a better comparison of both methods. We used 2x ddPCR™ Supermix for probes (BioRad, USA), forward and reverse primers (Genomed, Poland), TaqMan® probe (Genomed, Poland), and nuclease-free water (A&A Biotechnology, Poland).

The sequences of used primers and probes for *Staphylococcus aureus* were following:

- forward primer: GACAAGGTACCGGAAGC,
- reverse primer: TCCAACCTGATCCAAATAATGT,
- probe: 6-*FAM*-AGGATGTCAGTCCGTAATAATGGCGGT-*BHQ*-1.

The sequences of used primers and probes for *Staphylococcus capitis* were following:

- forward primer: GCTAATTTAGATAGCGTACCTTCA,
- reverse primer: CAGATCCAAAGCGTGCA,
- probe: 6-*FAM*-TTCAAACTGCAGTACGTAATAATGGTGGC-*BHQ*-1.

The sequences of used primers and probes for *Staphylococcus epidermidis* were following:

- forward primer: GCTAATTTAGATAGTGTGCCATCTA,
- reverse primer: CCTGAACCAAATCGTGCT,
- probe: 6-*FAM*-AAACAGCTGTTCGTAATAATGGCGGT-*BHQ*-1.

2.6.2. Sample preparation

The total volume of one sample in real-time PCR and dddPCR was 20 µl. It contained 10 µl of 2x ddPCRTM BioRad Supermix for probes, 1.4 µl of 10 µM forward primer, 1.4 µl of 10 µM reverse primer, 0.3 µl of 10 µM TaqMan® probe, 2 µl of bacteria solution, and 4.9 µl sterile, nuclease-free water. Samples (bulk or droplet samples) were introduced to a 96-well PCR plate, covered with PCR strips (Figure 20b), and plated in thermocycler LightCycler 96 (Roche, Germany) (Figure 20a).

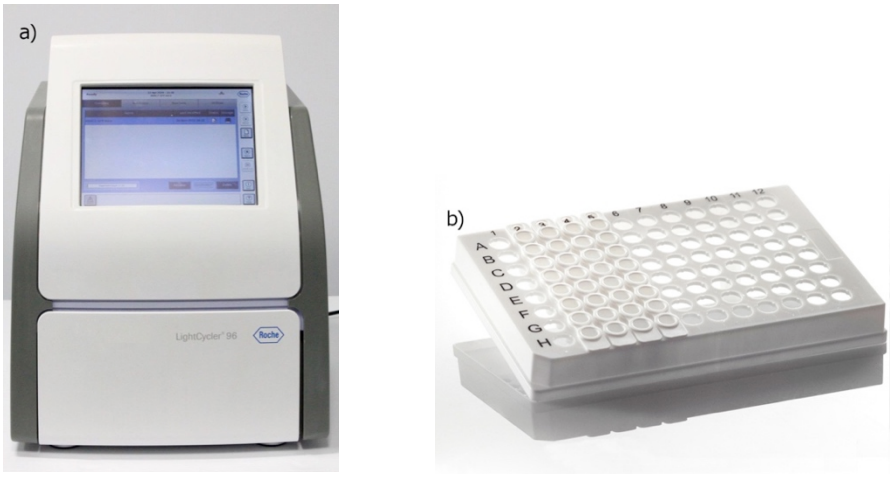

Figure 20. Photographs of PCR experimental set components. a) Roche Light Cycler® 96 System used for real-time PCR and direct droplet digital PCR, b) 96-well plate with covering strips for PCR samples.

2.6.3. Thermocycling process

The protocol for direct droplet digital PCR was optimized for the reduction of variabilities in droplet fluorescence intensities. We used the following final cycling conditions: 10 min at 95^{o}C, followed by 60 cycles of 94^{o}C for 60s and 60^{o}C for 120s.

For real-time PCR, we used the following thermocycling process: 10 min at 95^{o}C, followed by 45 cycles of 94^{o}C for 30s, 60^{o}C for 60s.

2.7. Bacterial strains and culture mediums

We used different bacterial species in each of four projects (Table 2):

Table 2. Bacterial strains and culture mediums used in the microbiological parts of the projects.

Project	Bacterial strains and culture mediums
I. Droplet digital CFU (ddCFU) assay for precise quantification of bacteria over a broad dynamic range	*Escherichia coli* DH5α placEGFP, *Enterobacter aerogenes* PCM183. Bacteria were cultured using LB-Lennox media (Roth, Germany). With *E. coli*, the media contained 100 μg/ml ampicillin and 1 mM isopropyl β-D-1-thiogalactopyranoside IPTG (both from Thermo Fischer Scientific, USA) for EGFP plasmid retention and expression, respectively.
II. Species specific, accurate and precise quantification and identification of bacteria in mixed samples	*Staphylococcus aureus* NCTC8325-4, *Staphylococcus capitis* DSM20326, *Staphylococcus epidermidis* DSM20044. Bacteria were cultured in Brain Heart Infusion media (Biocorp, Poland).
III. High-throughput label-free readout of bacteria density in nanoliter droplets	*Escherichia coli* ATCC 25922, Escherichia coli TOP 10 placEGFP, *Staphylococcus aureus* LS1, *Staphylococcus aureus* SH1000, *Corynebacterium simulans* DSM 44392, *Pseudomonas aeruginosa* ATCC 27853, *Staphylococcus intermedius* ATCC 29663, *Klebsiella pneumoniae* ATCC 13883, *Acinetobacter baumanii* ATCC 19606, *Salmonella arizonae* ATCC 13314, *Shigella sonnei* ATCC 29930, *Listeria monocytogenes* ATCC 1915. Bacteria were cultured in Tryptic Soy Broth (Biocorp, Poland) or Brain Heart Infusion media (Biocorp, Poland). For fluorescence-based screening, we cultured *E. coli* TOP 10 placEGFP

	in LB medium (Roth, Germany) with 100 μg/ml ampicillin and 1 mM isopropyl β-D-1-thiogalactopyranoside IPTG (from Sigma-Aldrich, USA and Thermo Fischer Scientific, USA, respectively).
IV. Droplet-based assay for quantitative characterization of bacterial populations	*Staphylococcus aureus* SH1000, *Staphylococcus aureus* MSSA 476, *Pseudomonas aeruginosa* PAO1. Bacteria were cultured in Tryptic Soy Broth (Biocorp, Poland), and Tryptic Soy Agar (Biocorp, Poland).

2.8. Antibiotics

In the antibiotic kill tests, determination of MIC and scMIC values we used the following antibiotics (Table 3):

Table 3. Antibiotics used for MIC, scMIC and time kill tests.

Project	Bacterial strains and culture mediums
I. Droplet digital CFU (ddCFU) assay for precise quantification of bacteria over a broad dynamic range	Norfloxacin (Sigma-Aldrich, USA)
II. Species specific, accurate and precise quantification and identification of bacteria in mixed samples	No antibiotics were used in this project.
III. High-throughput label-free readout of bacteria density in nanoliter droplets	Gentamicin sulfate solution (TOKU-E, Japan and Sigma-Aldrich, USA)
IV. Droplet-based assay for quantitative characterization of bacterial populations	Gentamicin sulfate solution (TOKU-E, Japan and Sigma-Aldrich, USA), ciprofloxacin (TOKU-E, Japan), tobramycin sulfate (TOKU-E, Japan), vancomycin hydrochloride from Streptomyces orientalis (Sigma-Aldrich, USA), amikacin sulfate (Sigma-Aldrich, USA), rifampicin (TOKU-E, Japan), oxacillin sodium salt (Sigma-Aldrich, USA)

2.9. Small colony variants triggering

The procedure was applied in project no. IV, Droplet-based assay for quantitative characterization of bacterial populations.

Small colony variants of *S. aureus* SH1000 were triggered and isolated based on a protocol previously described by Edwards[33]. Tryptic soy broth containing gentamicin at a concentration of 2 mg/ml was inoculated with a single *S. aureus* colony and incubated at 37^{o}C

for 18h. SCVs were isolated by plating serial dilutions of the culture on tryptic soy agar plates with 2 mg/ml gentamicin, not permitting the growth of normal cells but selecting tolerant to antibiotic small colony variants additionally characterized by small colony size reduced pigmentation and deficiency in beta-hemolysis. The SCVs colonies were harvested with a loop, suspended in 30% (v/v) glycerol solution, or directly subjected to experimental procedures described.

2.10. In vitro biofilm formation

The procedure was applied in project no. IV, Droplet-based assay for quantitative characterization of bacterial populations.

Biofilms were grown in microtiter plates (Nunclon™ Delta Surface, Thermo Scientific Nunc). For plasma pre-coated wells a total of 100 µL of 20% (v/v) blood plasma in 50 mM carbonate buffer, pH 9.6, was incubated in the wells for 2h at 37°C prior inoculation with bacteria. Overnight cultures of *S. aureus* were diluted 1:200 in TSB (tryptic soy broth) and inoculated at 100 µL in microtiter wells. Biofilms were formed for either 24h or 72h at 37°C. Unattached bacteria were washed out. To disperse the biofilm, proteinase K was added to the wells at 100 µL and incubated for 30 min at 37°C. Digested biofilms were subjected to thorough pipetting and a viable count to determine their densities.

2.11. Determination of minimum inhibitory concentration (MIC)

The procedure was applied in project no. III and IV.

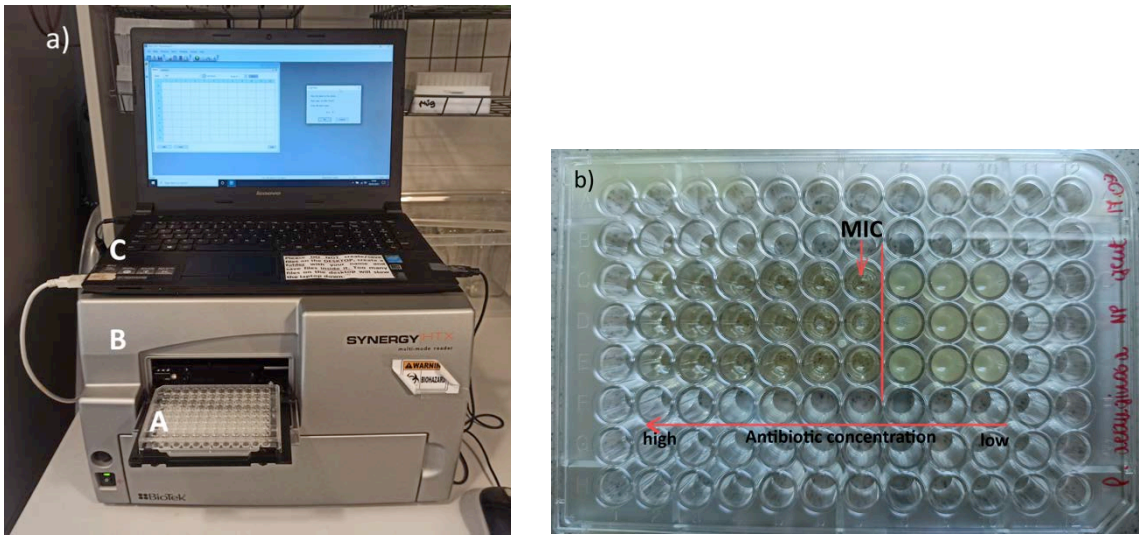

Figure 21. Experimental setup for MIC determination. a) setup for bacteria growth reading, a 96-well plate (A) is placed in a plate reader (B). Growth curves of bacteria are collected by a computer (C) for each of 96 wells; b) photograph of the 96-well plate with samples containing bacteria and antibiotic at

serially changing concentration, from the lowest (right) to the highest (left). MIC value is obtained as the lowest antibiotic concentration inhibiting bacteria growth. Every sample is prepared in three replicates.

A minimum inhibitory concentration was obtained using a 96-well plate and a plate reader (BioTek Instruments, USA) connected to the computer (Lenovo, China) (Figure 21a). Samples containing bacteria and antibiotic at various concentrations were incubated, and optical density was measured over time. The MIC value was the lowest antibiotic concentration with inhibited growth of bacteria (Figure 21b).

2.12. Determination of single-cell minimum inhibitory concentration (scMIC)

The procedure was applied in project no. III and IV.

A single-cell minimum inhibitory concentration (scMIC) was determined using a droplet-based approach. Initially, the bacteria sample was diluted to the concentration providing a high probability of single-cell encapsulation in the range of 0.5×10^5 to 2×10^5 CFU/ml. Next, the antibiotic was added, resulting in a series of samples with various antibiotic concentrations (Figure 22a), which were then split into 1 nl droplets and collected in 0.5 ml Eppendorf tubes (Figure 22b). The droplet samples were incubated at 37^{o}C. After around 18 hours, all the droplets were screened for scattered or autofluorescence light intensity measurement (Figure 22c). The percentages of positive compartments were determined for each sample, and the distributions of scMICs were obtained (Figure 22d).

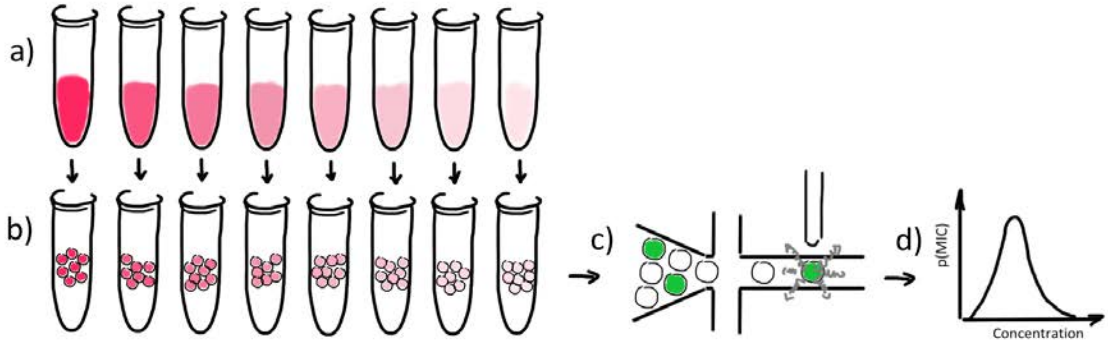

Figure 22. Scheme of a method for scMIC determination. a) Preparation of samples containing bacteria and various concentrations of antibiotic; b) splitting of the samples into 1nl droplets and incubation at 37^{o}C; c) measurement of scattered or autofluorescence light intensity in each droplet in all samples; d) data analysis towards heterogenic response of bacteria to antibiotic treatment.

2.13. Data analysis towards phenotypic heterogeneity of bacterial population

The procedure was applied in project no. III and IV.

Data analysis method was already used and described in details in the following publication: Scheler, O.; Makuch, K.; Debski, P. R.; Horka, M.; Ruszczak, A.; Pacocha, N.; Sozański, K.; Smolander, O.-P.; Postek, W.; Garstecki, P. *Droplet-Based Digital Antibiotic Susceptibility Screen Reveals Single-Cell Clonal Heteroresistance in an Isogenic Bacterial Population. Sci. Rep.* 2020, *10* (1), 3282.[175]

As a result of single-cell antibiotic susceptibility testing we receive a total number of droplets, N and the number of positive compartments, N_+ (containing fully grown bacteria) for each droplets' library with a particular concentration of antibiotic, c. The measurement of distribution of antibiotic susceptibility in the population is obtained by normalization of the number of positive droplets by their number in the absence of antibiotic, to determine the fraction of individual cells that grow as a function of antibiotic concentration (Figure 23a):

$$F_R(c) = f_+(c)/f_+(0), \text{ where } f_+(c) = N_+(c)/N(c)$$

Another well-defined measurement of bacteria heterogeneity in a population is a probability distribution density, p(MIC), of cells exhibiting a given MIC (Figure 23b). Bacteria which can grow at a given antibiotic concentration c are characterized by MIC level m≥c; using the equation $F_R(c) = \int_c^\infty p(m)dm$, the probability can be calculated from the identity:

$$p(c) = -\frac{d}{dc}F_R(c).$$

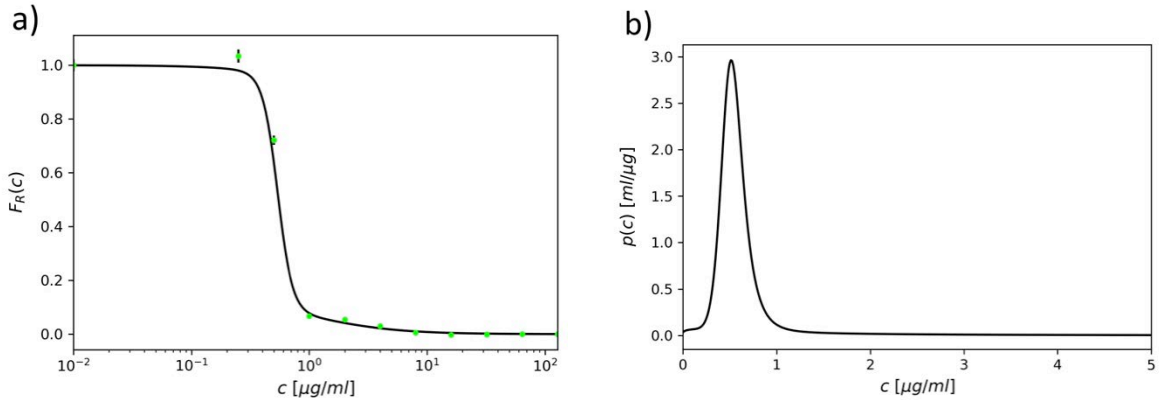

Figure 23. Analysis of bacterial phenotypic heterogeneity at the single-cell level. a) Fraction of recovering cells (fraction of positive droplets normalized by the value of positive compartments without antibiotic) as a function of antibiotic concentration; b) probability distribution of individual MICs obtained from a numerical derivative of the data points in a).

3. Results and Discussion

This chapter describes four projects concerning precise bacteria quantification (I and II), identification (II), antibiotic susceptibility testing (III and IV), and detection of bacteria subpopulation able to survive treatment with a high dosage of antibiotics (IV):

I. *Droplet digital CFU (ddCFU) assay for precise quantification of bacteria over a broad dynamic range (3.1).*
II. *Species specific, accurate and precise quantification and identification of bacteria in mixed samples (3.2).*
III. *High-throughput label-free readout of bacteria density in nanoliter droplets (3.3).*
IV. *Droplet-based assay for quantitative characterization of bacterial population (3.4).*

3.1. Droplet digital CFU (ddCFU) assay for precise quantification of bacteria over a broad dynamic range

Parts of this chapter are published as: Scheler O., et al., *Optimized droplet digital CFU assay (ddCFU) provides precise quantification of bacteria over a dynamic range of 6logs and beyond*, *Lab on a Chip*, 2017[145]

The droplet digital CFU (ddCFU) method is an optimized version of the standard digital assay for bacteria quantification. It is characterized by a significantly reduced number of used compartments and a broad dynamic range of quantification (over a 9log range). Using classical droplet digital assays, the bacterial sample is split into droplets, and the cells are encapsulated at the single-cell level according to Poisson distribution. The initial target concentration is determined by the fraction of positive droplets. The number of compartments is proportional to the dynamic range, so the standard approach needs a vast number of compartments for operating over a wide dynamic range of target concentrations.

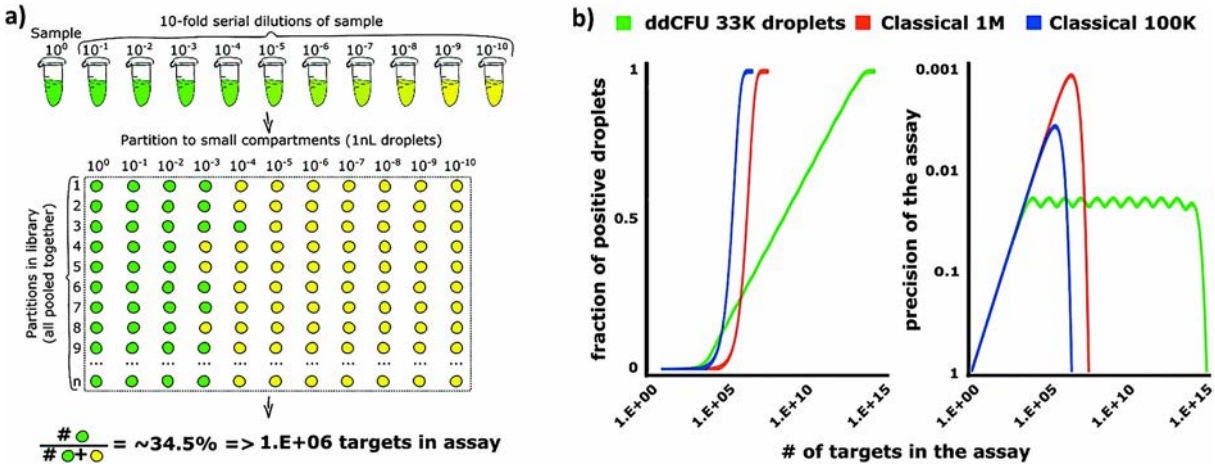

Figure 24. The theoretical background of optimized droplet digital CFU assay (ddCFU) for bacteria counting. a) The overview of the ddCFU approach. The serial 10-fold dilutions of the initial bacterial sample are prepared, and each sample is partitioned into libraries of ~ 3000 nanoliter droplets. After incubation, the number of positive compartments characterized by high fluorescence intensity is determined. The fraction of positives is then used to calculate the initial number of targets in the sample via statistical algorithms based on the most probable number method and Bayes probability; b) The performance of ddCFU assay compared to classical single-volume digital approaches. The left graph presents the response in the fraction of positive droplets with a logarithmically increasing number of targets in the sample. The right graph illustrates the comparison of the precision of three quantification assays in the wide range of target concentrations. Classical 1M and 100K stand for classical digital assays with one million and 100 thousand compartments, respectively. Figure reproduced from the article published by Scheler et al.[145]

We developed an alternative method by implementing a rational design[185] of digital droplet assays. The logarithmic dilution series of the initial bacterial sample is generated and divided

into one nl droplet. All 11 libraries (initial bacterial sample plus 10 dilutions) are pooled together in one test tube, incubated, and analyzed (Figure 24a). Our assay's performance was verified numerically via grand canonical Monte Carlo simulations and compared to the performance of standard single-cell approaches. The precision of bacteria quantification by optimized ddCFU is better than 5% and comparable to the classical assays (Figure 24b).

3.1.1. Droplet digital CFU technology

Bacteria quantification by ddCFU technology starts with manual dilutions of the initial sample. The 10-fold dilutions are prepared and, together with the undiluted sample, are transferred to a 96-well plate. Next, the 3 µl plugs of 11 samples separated by 3 µl oil droplets are aspired into microfluidic tubing using an automated positioning system tray and syringe pumps (Figure 25a).

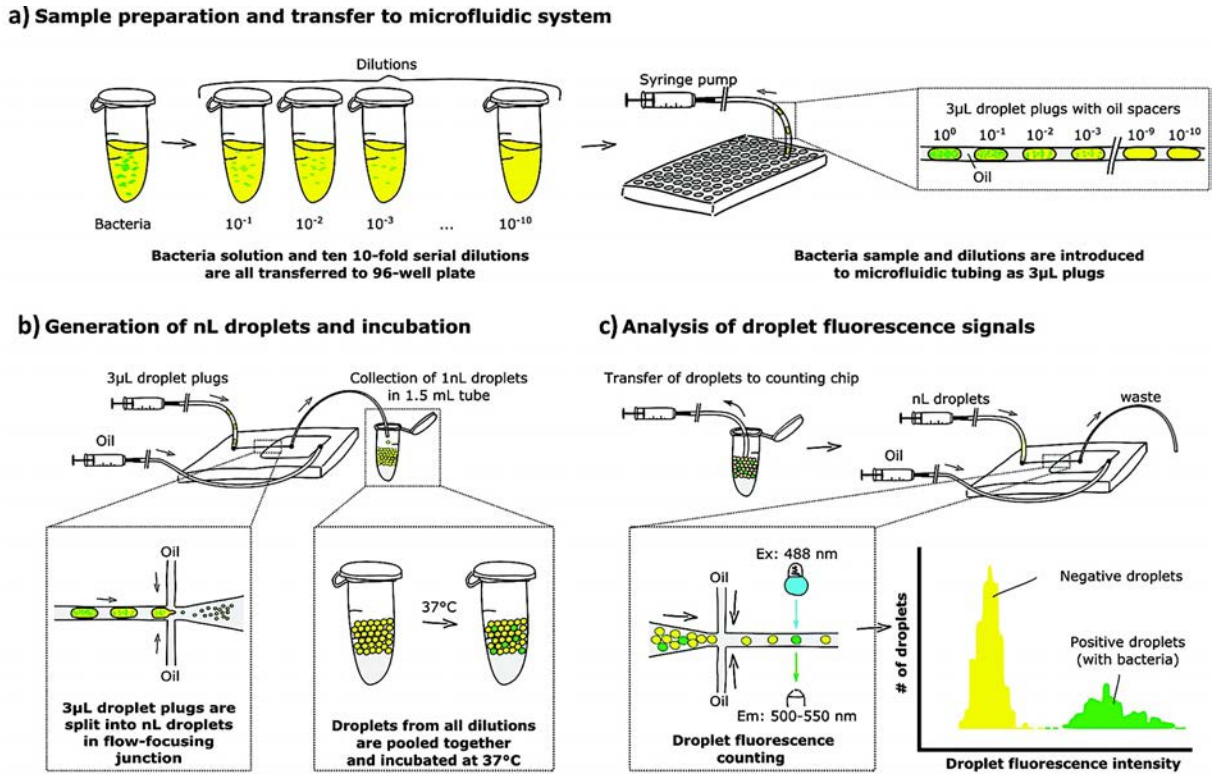

Figure 25. Schematic of the ddCFU workflow. a) Initial bacterial sample is serially diluted. The initial suspension and ten 10-fold serial dilutions are transferred to a 96-well plate where 3 µl plugs of each sample are aspirated into microfluidic tubing and separated by additional oil spacers; b) Each plug is split into 1 nL droplet in the microfluidic chip with a flow-focusing junction, collected in a 1.5 ml test tube, and incubated at 37°C; c) measurement of fluorescence intensity in each droplet by flowing them by detection chip and determination of the initial sample concentration using rational algorithms. Figure reproduced from the article published by Scheler et al.[145]

In the next step, the sample plugs are split into ~1 nl droplets using a microfluidic chip with a flow-focusing junction. The droplets from all dilutions are collected in one 1.5 ml tube and

incubated at 37^{o}C (Figure 25b). After incubation, the droplets are screened by flowing them through the detection chip mounted in a confocal microscope stage (Figure 25c). An additional stream of continuous phase spaces the droplets in the flow-focusing junction of the detection chip just before the image acquisition area.

3.1.2. Comparison of digital CFU assay and standard plate counting

We verified the performance of rational design for digital quantification of bacteria by comparing the results obtained by our optimized assay and gold standard enumeration method commonly used in microbiological laboratories, plate counting (Figure 26a). An overnight culture of an enhanced green fluorescent protein (EGFP)-producing *Escherichia coli* DH5α was diluted serially. In detail, six samples with bacteria concentrations ranged over six orders of magnitude – from overnight stationary culture to the 6th 10-fold logarithmic dilution were prepared. The viable bacteria were quantified by both methods. The droplet samples and Petri dishes with plated bacteria were incubated at 37^{o}C for 16 and 20 hours, respectively. In case of optimized droplet method, bacteria concentration was established based on the number of positive droplets (high intensity of fluorescence) and rational algorithms. For the reference assay, grown bacterial colonies were counted and multiplied by dilution factors.

We compared the number of bacteria determined by our ddCFU assay and conventional plate counting. Figure 26b shows that both methods yield highly correlated results. The least-squares exponential fit indicates a linear relationship between each two obtained variables in the entire range of bacteria concentrations. A coefficient of determination, R^2, also proves the fit's satisfactory quality, which qualifies the ddCFU approach as a promising tool for the bacteria enumeration. The lowest concentration that can be detected with our ddCFU method depends on the initial sample volume. It means that in our case it is one cell per 3 µl, which corresponds to $3.33 \cdot 10^2$ CFU/ml.

We observed that the results obtained by the ddCFU approach are very often slightly lower than those obtained by plate counting (~25% on average in our case). A similar difference in the number of viable detected cells using droplet-based systems has already been demonstrated with *E. coli*. It has been speculated that this is due to shear forces on the cells during the encapsulation process[186]. As a matter of caution thus, the effect of bacteria encapsulation on the viability of the cells should be tested before using ddCFU assay for bacteria quantification.

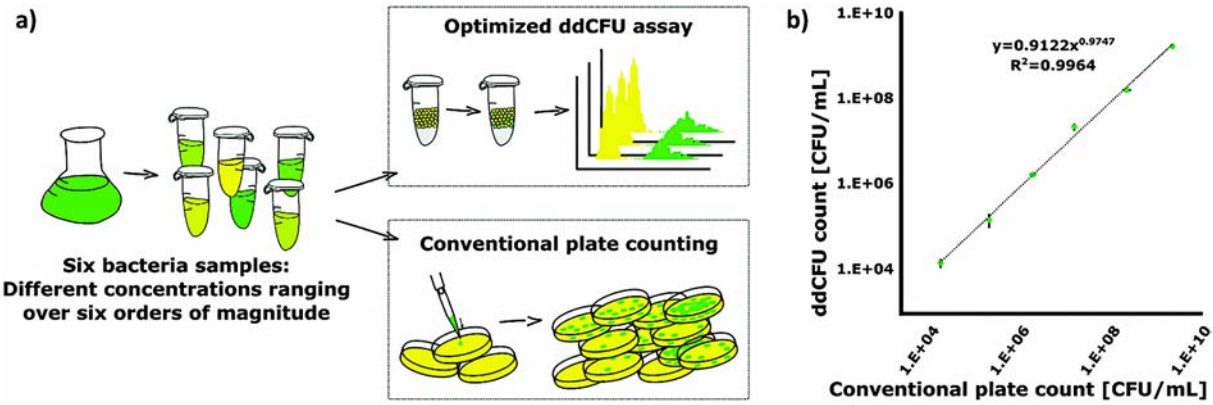

Figure 26. ddCFU assay provides results in high correlation with traditional plate counting enumeration. a) schematic experimental workflow of bacteria quantification. Viable cells in six different samples with bacteria concentrations of six orders of magnitude were counted by ddCFU assay and conventional plate counting; b) the graph showing the bacterial concentration on a logarithmic scale in the samples measured by plate counting and ddCFU approach. Figure reproduced from the article published by Scheler et al.[145]

3.1.3. Bacteria detection time

We investigated the time needed to detect viable bacteria using our optimized droplet-based system. We tested the growth time of two bacterial species, *Escherichia coli* and *Enterobacter aerogenes* using three different fluorescent labeling approaches: I) genetic modification of bacteria towards EGFP expression, II) metabolic marker dye resazurin, III) metabolic marker dye C12-resazurin. The working principle of C12-resazurin is similar to resazurin but it has been shown to retain in water droplets for an extended period of time[139].

We encapsulated both species in 1 nl droplet at the single-cell level and monitored the fluorescence intensity over time. Bacteria were counted using ddCFU assay. For EGFP expressing *E. coli*, we could detect positive containing cells droplets in six hours. Metabolic activity signals for resorufin and C12-resorufin were detected in four and five hours, respectively. Next, we tested *E. aerogenes*, bacteria associated with nosocomial infections. In that case, the minimum incubation time using marker dyes resorufin and C12-resorufin was three and four hours, respectively. Such detection time is similar to that already shown, for example, for detecting *Staphylococcus aureus*[138]. These results demonstrate an enormous advantage over the traditional plate counting method, where the incubation period is at least 16-20 hours long. In droplet assays, compartmentalization of cells in small volumes allows for the faster accumulation of target to detectable concentration.

3.1.4. Antimicrobial time-kill testing

The Time Kill Test or Time Kill Analysis is carried out to evaluate antimicrobial agents' efficiency to reduce the viability of bacterial population[187]. We conducted an antimicrobial time-kill test using our ddCFU technology. We inoculated EGFP *E. coli* DH5α in ~30 ml culture medium to the concentration ~2×10^6 CFU/ml. We added norfloxacin with one minimum inhibitory final concentration, 0.2 μg/ml (Figure 27). Norfloxacin is a quinolone that targets DNA gyrase (an enzyme catalyzing structural changes in DNA) in bacteria and leads to the death of the cells over time[188]. After the addition of antibiotic, we collected the samples over time ranging from 0 to 25 hours, changed culture media to fresh one without antibiotic, and counted the viable cells using ddCFU assay.

Figure 27 shows the immediate effect of norfloxacin on bacteria viability. After 30 min, more than half of the bacterial population was killed by the antibiotic. The number of viable bacteria continued to decrease. After 4 hours, we could not detect any viable cells in the culture.

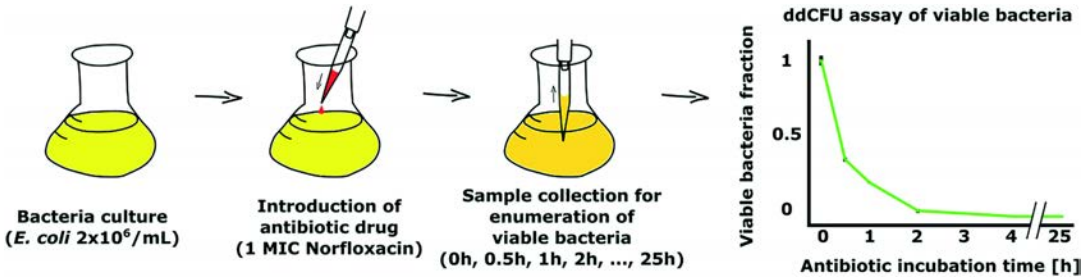

Figure 27. Demonstration of ddCFU assay application for antibiotic susceptibility testing. The antibiotic, norfloxacin, was added to *E. coli* culture and the bacteria viability was measured over time. The results are presented in the graph showing bacteria viability as a function of incubation time of cells in the presence of antibiotic. Figure reproduced from the article published by Scheler et al.[145]

3.2. Species specific, accurate and precise quantification and identification of bacteria in mixed samples

Parts of this chapter are published as: Pacocha N., et al., *Direct droplet digital PCR (dddPCR) for species specific, accurate and precise quantification of bacteria in mixed samples*, *Analytical Methods*, 2019[189]

A direct droplet digital polymerase chain reaction (dddPCR) assay allows for simultaneous identification and quantification of bacteria in a bacterial mixture. The method is designed to detect *Staphylococcus aureus, Staphylococcus epidermidis, and Staphylococcus capitis*, both alone as mono-cultures and in a mixture. We encapsulate bacteria together with PCR reagents

to amplify specific target genes. The method is calibration-free digital assay with eliminated tedious DNA isolation and purification protocols. Besides, the process of extraction and purification of genetic material from bacteria is time-consuming and has fluctuating efficiency[190].

The combination of identification and enumeration of bacteria in one method is challenging, particularly for analyzing a sample containing many different bacterial species. The sufficient specificity for bacteria recognition in a mixture is provided by genotypic methods headed by real-time PCR, where quantification of bacteria is performed using a laborious preparation of calibration curve. We propose a solution that alleviates the need for calibration and extraction of genetic material from cells by direct encapsulation of bacteria, specific gene amplification, and quantification of targets using droplet digital PCR.

3.2.1. Direct droplet digital PCR (dddPCR) technology

Recognition and quantification of target bacteria in a sample using dddPCR technology (Figure 28a-d) starts with a dilution of the initial sample with 10 mM TRIS buffer (pH 8.5) to reduce the potential inhibition of amplification by culture medium. Then, bacteria are mixed with PCR reagents providing amplification of a gene in target cells, and the sample is split into 1nl droplets. We introduce PCR tubes with collected droplets into thermocycler and apply optimized for droplet PCR a temperature cycling protocol. The increasing number of amplicons results in higher fluorescence intensity deriving from the hydrolysis probe's cleavage and releasing fluorophore from the quencher. The final step is to measure the fluorescence signal's intensity in all droplets using a microfluidic detection chip mounted on a confocal microscope. The droplets with high fluorescence intensity are considered positive (means containing target bacteria), while low signal intensity indicates negative compartments. The threshold between negative and positive droplet populations is determined halfway between the minimum measured signal and maximum intensity due to the high difference (at least four times) between positive and negative droplets' fluorescence signal. According to the Poisson distribution, a concentration of the target bacteria concentration corresponds to the number of positive droplets.

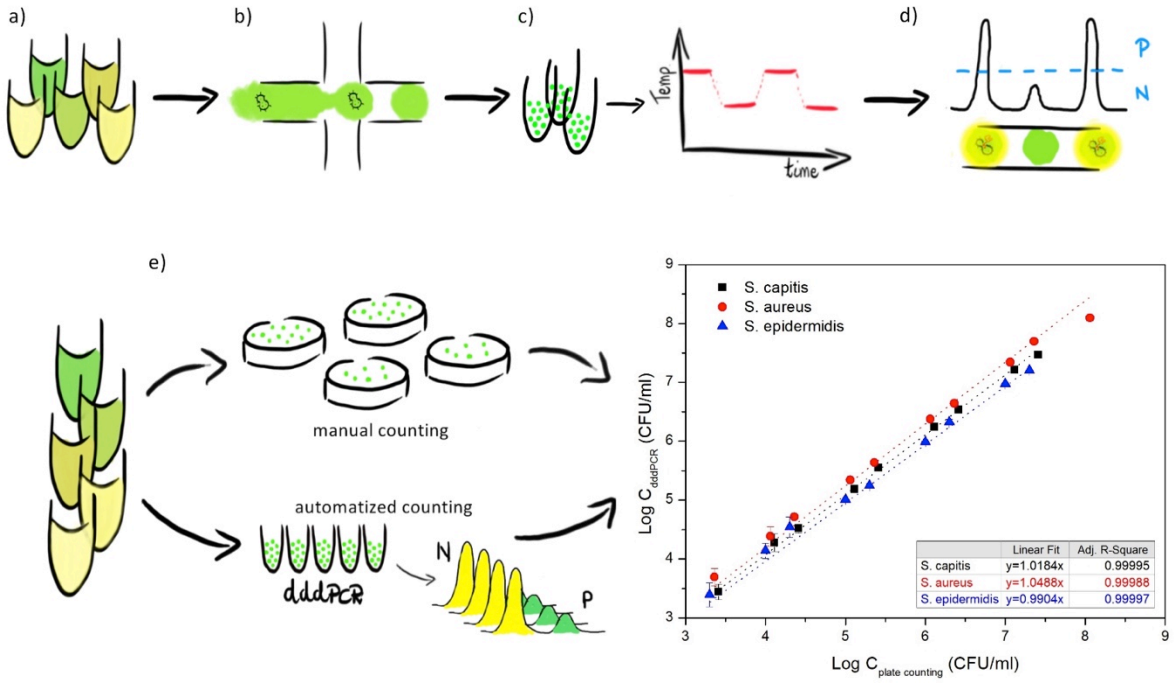

Figure 28 . Schematic of the dddPCR technology and experimental workflows. a) dilution of an initial bacterial sample; b) generation of nanoliter droplets containing bacteria and PCR reagents and collection of formed compartments in a PCR tube; c) lysis of bacteria and amplification of target specific gene during direct droplet digital polymerase chain reaction; d) screening of droplets and counting of positive, containing target bacteria (P) and negative (N) droplets based on the fluorescence intensity, dashed line indicates the signal threshold; e) workflow of an experiment comparing dddPCR assay with standard plate counting. The overnight bacterial sample was diluted to enumerate bacteria in each dilution by plate counting and dddPCR technique, N and P indicates the fraction of negative and positive droplets, respectively. The graph shows the bacterial concentration obtained by plate counting as a function of concentrations determined by dddPCR assay. Figure reproduced from the article published by Pacocha et al.[189]

DddPCR technology does not require a calibration curve for determination of target bacteria concentration, for that the only information we need is a fraction of positive droplets. The difference in fluorescence signal between positive and negative compartments has to be clear and explicit. Therefore, when the temperature cycling protocol is not optimized it provides poorly separated droplet populations called droplet rain[191]. We conducted an experiment showing an improvement of droplet separation by modification of PCR thermal protocol. We amplified *S. epidermidis* DNA (encapsulated concentration $1.5 \cdot 10^{-3}$ ng/µl) in the droplets using two different PCR temperature profiles:

I. 95°C for 10min, 40 cycles of 94°C for 30s, 60°C for 60s and final 37°C for 30s,
II. 95°C for 10min, 60 cycles of 94°C for 60s, 60°C for 120s and final 37°C for 30s.

Figure 29a presents a result of the shorter PCR protocol. The droplet populations are not clearly separated which hinders threshold setting and falsify final outcome. The second PCR program yields improved droplet distribution with distinctive two fractions and significantly

reduced number of droplet with intermediate fluorescence intensity (Figure 29b). The extended protocol was used in dddPCR technology.

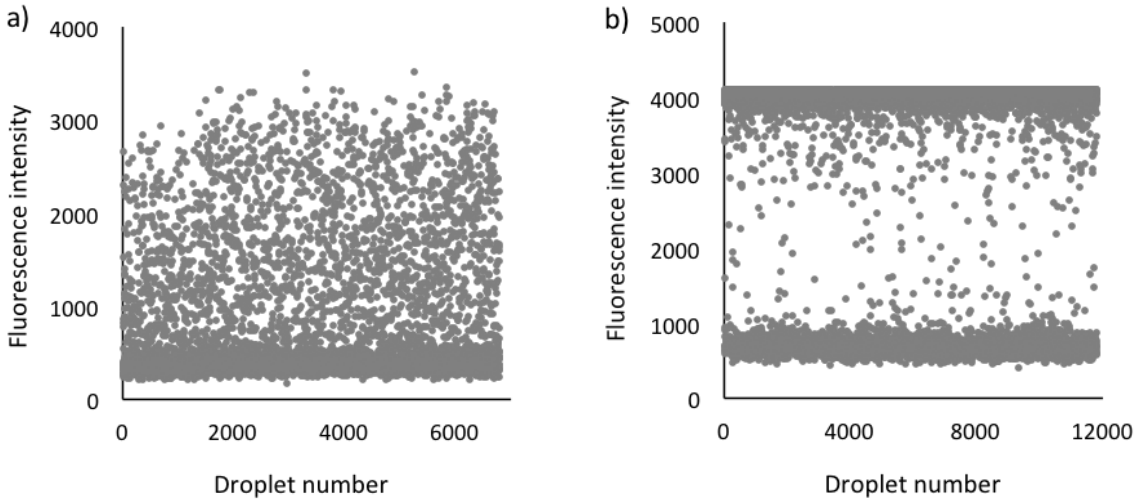

Figure 29. Cycling conditions strongly influence the efficiency of ddPCR. The droplets containing *S. epidermidis* DNA were exposed to two different PCR thermal conditions. a) graph shows the distribution of fluorescence intensity of the droplets after following thermal treatment 95°C for 10min, 40 cycles of 94°C for 30s, 60°C for 60s and final 37°C for 30s; b) graph presents fluorescence intensities of the droplets treated at 95°C for 10min, 60 cycles of 94°C for 60s, 60°C for 120s and final 37°C for 30s. Figure reproduced from the article published by Pacocha et al.[189]

3.2.2. Comparison of dddPCR and standard plate counting

We tested the reliability of dddPCR technology by comparing the results of bacteria quantification by our method and gold standard plate counting (Figure 28e). We used three different bacterial species (*S. aureus*, *S. epidermidis*, *S. capitis*) at various concentrations. We compared both methods using a very fresh bacterial suspensions to eliminate an error related to detecting both alive and dead cells in the dddPCR approach. The cells from the edge of the freshly cultured colony on the agar plate were suspended in a liquid medium and incubated at 37°C to OD_{600} 0.2.

Bacteria enumeration by plate counting method was conducted by sample dilution with culture medium, bacteria spreading on agar plates, overnight incubation at 37°C, and counting of grown colonies. In the dddPCR experiment, an initial bacterial sample was diluted with TRIS buffer, mixed with PCR reagents, split into droplets, and analyzed towards the number of positive droplets after DNA amplification. Each bacterial dilution for each species was analyzed in three replicates. We found that both methods provide highly correlated results, which is proved by the linear regression equations and the determination coefficients (R^2)

(Figure 28e). DddPCR technology allows counting bacteria over a dynamic range of at least five orders of magnitude with the possibility to extend it. In low bacteria concentration, the cells can be centrifuged and resuspended in a smaller volume of liquid. For highly concentrated samples, bacteria can be encapsulated using a higher number of droplets, or the optimized droplet digital CFU assay described in one chapter above can be engaged.

3.2.3. Specificity of hydrolysis probes in real-time PCR and dddPCR

A specificity of bacteria recognition in a mixture by dddPCR technology is provided by TaqMan® hydrolysis probes and flanking primers, which target a *sodA* gene (prevalent marker gene in microbiological diagnostics). We design probes and primes using sequences from NCBI GenBank. We aligned the gene sequences of each bacterium together using *ApE* and *ClustalX* software to receive suitable gene regions to assert high specificity.

The specificity of designed probes was tested using reference qPCR and our dddPCR approach. For both methods, we prepared samples containing just target bacteria and the samples of the target bacteria with background cells. Table 4 presents the sample composition for the qPCR experiment. Ten different samples were prepared for each species: four concentrations of target bacteria, four samples with target and background cells, and two controls (one without any cells and one consisting of background bacteria). The concentration of interfering cells was selected to avoid inhibition of amplification due to too high content of genetic material in the sample. Bacteria were added directly to the samples and lysed at high temperature before the amplification process. We found that recognizing the target bacteria for all three species using the probes and primers is clear and specific (Figure 30a) with slightly more challenging bacteria detection at low concentrations. We can see from Figure 30a that these concentrations are affected by greater standard deviations.

Table 4. Concentrations of target and background bacteria in the samples analyzed by real-time PCR. Number of cells in PCR wells is estimated on basis of standard plate counting.

		Concentration of bacteria [CFU/ml]								
Target	***S. capitis***	$1.0 \cdot 10^6$	$1.0 \cdot 10^5$	$1.0 \cdot 10^4$	$1.0 \cdot 10^3$	0	$1.0 \cdot 10^6$	$1.0 \cdot 10^5$	$1.0 \cdot 10^4$	$1.0 \cdot 10^3$
Background	*S. aureus* *S. epidermidis*	0				$1.75 \cdot 10^5$				
Target	***S. aureus***	$2.5 \cdot 10^6$	$2.5 \cdot 10^5$	$2.5 \cdot 10^4$	$2.5 \cdot 10^3$	0	$2.5 \cdot 10^6$	$2.5 \cdot 10^5$	$2.5 \cdot 10^4$	$2.5 \cdot 10^3$
Background	*S. epidermidis* *S. capitis*	0				$1.0 \cdot 10^5$				
Target	***S. epidermidis***	$2.5 \cdot 10^6$	$2.5 \cdot 10^5$	$2.5 \cdot 10^4$	$2.5 \cdot 10^3$	0	$2.5 \cdot 10^6$	$2.5 \cdot 10^5$	$2.5 \cdot 10^4$	$2.5 \cdot 10^3$
Background	*S. capitis* *S. aureus*	0				$1.0 \cdot 10^5$				

We also tested the specificity of bacteria recognition in a mixture by dddPCR. We compared samples of target bacteria as monocultures and mixtures with two remaining species (Table 5). We split the sample into droplets and collected them in PCR tubes for dddPCR (each bacteria dilution in three replicates). After amplifying target genes, we measured fluorescence intensity and counted the fraction of positive droplets in each sample. Figure 30b demonstrates the high specificity of bacteria recognition. The concentration of target bacteria obtained in the presence of interfering cells does not differ from the concentration determined in the absence of background bacteria.

Table 5. Concentrations of target and background bacteria in the samples analyzed by dddPCR. Number of cells in PCR wells is estimated on basis of standard plate counting.

		Concentration of bacteria [CFU/ml]					
Target	***S. capitis***	$5.0 \cdot 10^5$	$5.0 \cdot 10^4$	$5.0 \cdot 10^3$	$5.0 \cdot 10^5$	$5.0 \cdot 10^4$	$5.0 \cdot 10^3$
Background	*S. aureus* *S. epidermidis*	0			$1.0 \cdot 10^7$		
Target	***S. aureus***	$2.0 \cdot 10^6$	$2.0 \cdot 10^5$	$2.0 \cdot 10^4$	$2.0 \cdot 10^6$	$2.0 \cdot 10^5$	$2.0 \cdot 10^4$
Background	*S. epidermidis* *S. capitis*	0			$1.7 \cdot 10^7$		
Target	***S. epidermidis***	$5.0 \cdot 10^4$	$5.0 \cdot 10^3$	$5.0 \cdot 10^2$	$5.0 \cdot 10^4$	$5.0 \cdot 10^3$	$5.0 \cdot 10^2$
Background	*S. capitis* *S. aureus*	0			$1.0 \cdot 10^7$		

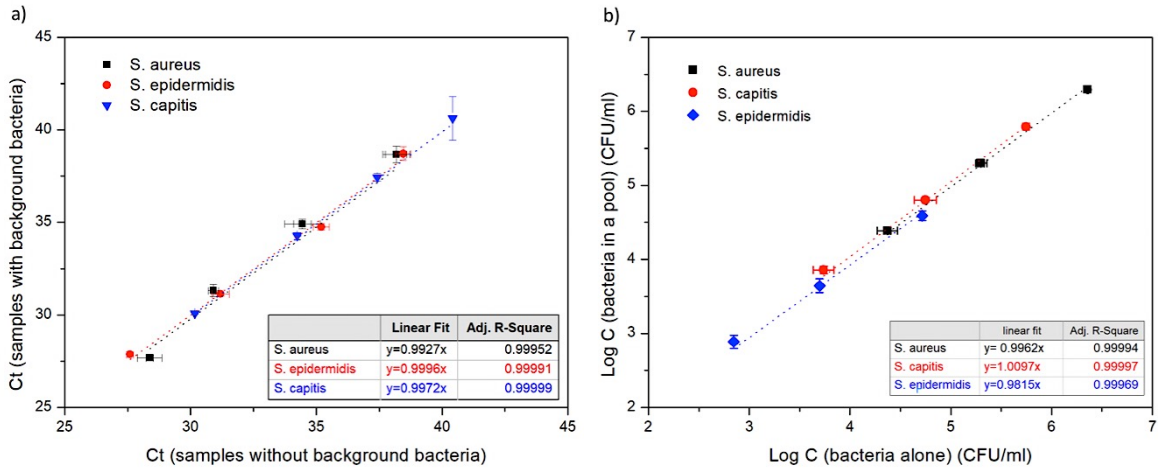

Figure 30. The specificity of TaqMan® hydrolysis probes in real-time PCR and dddPCR. a) recognition of target bacteria in a mixture of three bacterial species using real-time PCR. The X-axis represents the cycle threshold for the samples containing a different number of target bacteria; Y-axis indicates the cycle threshold for the samples, including different concentrations of target bacteria and a superior number of interfering cells. Black, red, blue symbols show the effectiveness of recognizing *Staphylococcus aureus, Staphylococcus epidermidis, and Staphylococcus capitis*, respectively. b) target bacteria detection using dddPCR technology in samples containing only target bacteria ($C_{\text{bacteria alone}}$) and samples with target and background cells ($C_{\text{bacteria in a pool}}$). Black, red, blue symbols show the quantified number of *Staphylococcus aureus, Staphylococcus capitis, and Staphylococcus epidermidis*, respectively. Figure reproduced from the article published by Pacocha et al.[189]

Table 6 presents the robustness of bacteria identification by dddPCR in mixed samples. The relative standard deviations (%SD) of target bacteria enumeration in the presence of interfering cells were calculated by multiplying an absolute error by 100% and dividing by the average of three independent measurements of target bacterial concentration. The SD% remains within a few percent, with the most extensive spread of 20% for *S. epidermidis*. The results demonstrate that dddPCR assay allows for tracking even small changes in bacteria content. It creates a possibility to follow an evolution of bacterial consortia composition upon treatment with diverse sets of compounds.

Table 6. Robustness of bacteria recognition in mixed samples, b/t indicates the ratio of densities of background (b) to target (t) bacteria, %SD indicates relative standard deviation.

S. aureus			***S. capitis***			***S. epidermidis***		
Average concentration of target bacteria [CFU/ml]	Ratio b/t	%SD	Average concentration of target bacteria [CFU/ml]	Ratio b/t	%SD	Average concentration of target bacteria [CFU/ml]	Ratio b/t	%SD
$2.0 \cdot 10^6$	8,5	4.4	$6.2 \cdot 10^5$	20	3.9	$3.9 \cdot 10^4$	20	15.0
$2.0 \cdot 10^5$	85	4.6	$6.4 \cdot 10^4$	200	6.5	$4.4 \cdot 10^3$	200	21.5
$2.4 \cdot 10^4$	850	4.3	$7.2 \cdot 10^3$	2000	11.4	$7.7 \cdot 10^2$	2000	20.2

3.2.4. Inhibition of PCR by background bacteria and culture medium

DddPCR technology enables bacteria identification and quantification in the presence of background cells. We experimented with comparing the influence of different concentrations of interfering bacteria in the sample on target bacteria recognition by conventional qPCR and dddPCR assay. We found that dddPCR is more tolerant to the non-specific background (Figure 31a), and we speculate that it can be a result of compartmentalization. There is a small restricted volume of inhibitors influencing the amplification of target DNA. Besides, the detection of droplets is binary. None or very low intensity of fluorescence indicates a negative droplet without target bacteria. High fluorescence intensity corresponds to a positive droplet, and the level of fluorescence is not critical. The high concentration of inhibitors can influence PCR, causing a reduction of fluorescence intensity, but the droplet is still detected as positive.

The factor which can also inhibit PCR is a too high concentration of growth medium in the final PCR sample. We tested how much of culture medium the PCR sample may contain to do not influence amplification. We prepared seven samples containing different volume percent of BHI (broth heart infusion) broth, from 0% to 30% v/v, and purified DNA of *S. aureus*. After real-time PCR, we obtained cycle thresholds for each sample. Figure 31b shows that the

growth medium is a potent inhibitor of the amplification reaction. The concentration should not exceed 1% v/v. Higher content inhibits or ultimately hinders PCR. Using dddPCR technology initial bacterial sample has to be diluted, or the growth medium has to be removed by centrifugation and resuspension of the pellet in the non-inhibiting buffer, for example, TRIS buffer.

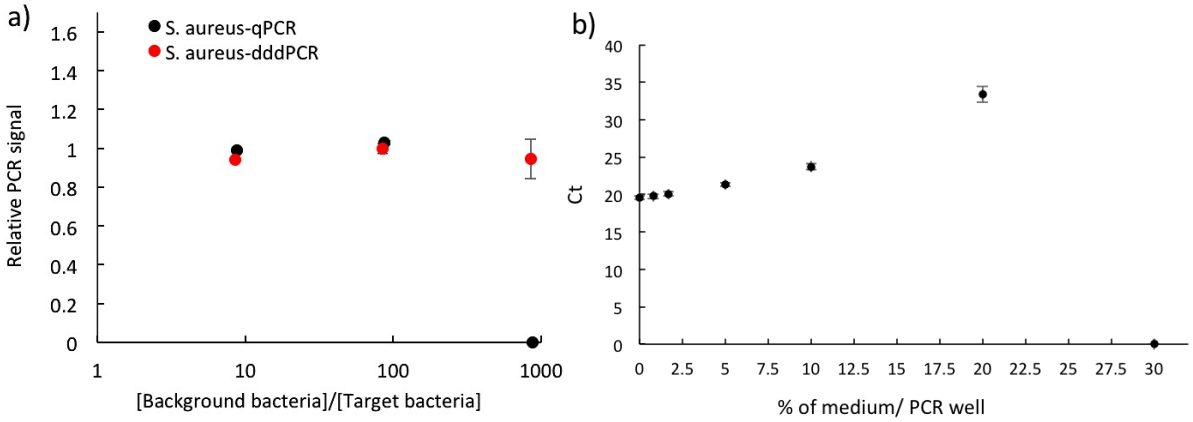

Figure 31. Background bacteria and culture medium inhibit DNA amplification. a) Graph presents a comparison of real-time PCR and dddPCR assays for samples containing different ratios of background to target bacteria (X-axis). Y-axis shows a relative PCR signal calculated as a ratio of a signal obtained in a sample containing the target and interfering cells to signal determined in a sample with just target bacteria. b) Graph shows the percentage of growth medium in the PCR sample as a function of PCR cycle threshold. Figure reproduced from the article published by Pacocha et al.[189]

3.3. High-throughput label-free readout of bacteria density in nanoliter droplets

Parts of this chapter are published as: Pacocha N., Bogusławski J. et al., *High-throughput monitoring of bacterial cell density in nanoliter droplets: label-free detection of unmodified Gram-positive and Gram-negative bacteria*, *Analytical Chemistry*, 2020[148]

Droplet microfluidics brings innovative possibilities in analyzing bacteria, including sequencing and antibiotic susceptibility testing at the single-cell level. It requires high-throughput methods for droplet generation and detection. Despite the significant progress in droplet formation techniques, the detection methods have lagged. The most common approach is the detection of fluorescence light, which naturally is not highly intense. The chemical markers of metabolism have to be added to enhance fluorescence intensity, or bacteria have to be genetically modified. We developed a high-throughput label-free system for monitoring of bacteria growth in nanoliter droplets with frequency of 1.2 kHz. The measurement is based on the intensity of light scattered by bacterial cells, Gram-positive, and Gram-negative with various structures, shapes, and growth characteristics. We present the

applicability of our system in analysis of phenotypic heterogeneity of *Staphylococcus aureus* population by determination of minimum inhibitory concentrations (scMIC) at the single-cell level.

3.3.1. Readout of bacteria density by measurement of scattered light

3.3.1.1. Experimental setup

A schematic description of the experimental workflow used in this work is presented in Figure 32a. An optimization of our system was performed using samples containing different ratios of 1 nL droplets containing culture medium only (negative) and the droplets containing a high concentration of bacteria (positive). The droplets with high bacteria density were prepared by splitting an overnight bacteria suspension (OD ~5.0). Both types of freshly generated droplets were collected in a 1.5 mL Eppendorf tube and mixed by gentle rotations. The percentage content of positive droplets in the sample is indicated by ρ_{pos}, while the percentage content of negatives is indicated by ρ_{neg}. The experiments conducted at the single-cell level were performed according to the procedure shown in Figure 32b. The bacterial sample was first diluted to a concentration of 10^5 CFU/mL (high probability of single-cell encapsulation) and then split into droplets to be collected in a 1.5 mL Eppendorf tube for incubation at 37 °C in the microbiological incubator.

Our detection system utilizes a microfluidic chip with a flow-focusing junction, shown in Figure 32c. The droplets are introduced to the chip through an inlet on the left side, and then they are separated further apart from each other by two additional oil streams without surfactant. The absence of surfactant in the continuous phase causes dilution of its high concentration in the original emulsion and reduces the background scattered light between droplets. In the final step, the droplets get to the detection channel, where a focused laser beam illuminates them.

The general principle of detection of bacteria growth in droplets is based on Mie scattering theory. Bacterial cells approximate spheroids with a size comparable to the wavelength of light. The light illuminating bacteria changes the direction of propagation and can be collected by an optical fiber positioned off the optical axis, in this case, perpendicularly to the laser beam (Figure 32d). The system is also equipped with the optical setup for the detection of fluorescence light. It was primarily used to validate a label-free approach as the detection of bacteria growth based on detection of fluorescence is well-established.

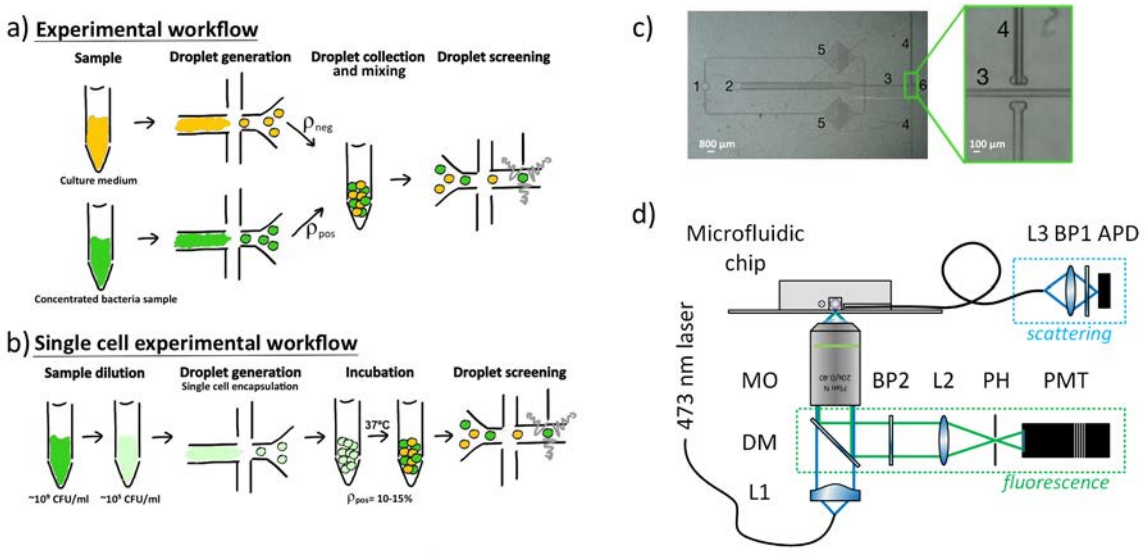

Figure 32. Schematic of experimental workflows and optical setup. a) overview of experimental workflow; b) schematic of experimental workflow for single-cell experiments; c) scheme of microfluidic chip for droplet screening, 1-inlet for continuous phase, 2-inlet for droplets, 3-detection channel, 4-guiding channel for optical fiber, 5-filters, 6-outlet; d) schematic of optical setup for detection of scattered and fluorescence light, L1-L3-lenses, BP1 and BP2-bandpass filters, MO-microscope objective, DM-dichroic mirror, PH-pinhole, APD-avalanche photodiode, PMT-photomultiplier. Figure reproduced from the article published by Pacocha, Bogusławski et al.[148]

3.3.1.2. Comparison of label-free system with standard approach of fluorescence intensity detection

The detection of bacteria growth in droplets is usually conducted using fluorescent metabolism markers, or bacteria has to be genetically modified to express fluorescent proteins. We compared results obtained by a well-established readout of the fluorescence signal with our label-free approach to validate our method and present the reliable detection of bacteria growth without additional labeling. For that purpose, we prepared eight samples containing a range of different percentages of negative (ρ_{neg}) and positive droplets (ρ_{pos}). The negative compartments had only a growth medium, and positive droplets were prepared by encapsulating a high concentration of genetically modified *E. coli* expressing a green fluorescent protein, which resulted in around 800 cells per droplet. Those samples contained ρ_{pos} of 0, 10, 30, 50, 60, 80, 90, 100%, respectively, and were analyzed in three replicates by simultaneous readout of scattering and fluorescence intensities. The droplets were screened with a frequency of 1200 Hz. Figure 33a presents an exemplary fluorescence and scattered light signals from nanodroplets with clearly distinguishable peaks with high intensity (positive droplets) and low intensity (negative droplets).

To quantify positive and negative droplets based on the recorded signals, we used a two-level threshold-based approach. The first level concerns counting all of the droplets in the sample. The threshold is located above the signal noise and below the highest intensity of negative droplets. The second threshold (roughly in half of the signal of positive droplets) allows enumerating positive compartments. The positive and negative droplets can be easily differentiated. In two exemplary histograms presented in Figure 33b, we can see two widely separated populations of droplets. Figure 33c,d shows the correlation between the theoretical and measured number of positive droplets in the sample based on detection of fluorescence and scattered light, respectively. The scattered light readout allows for precise detection and counting of droplets containing bacteria as the fluorescence-based method. The results obtained by both ways correlate highly, as proved by the linear regression equation and determination coefficient (R^2=0.9996) (Figure 33e).

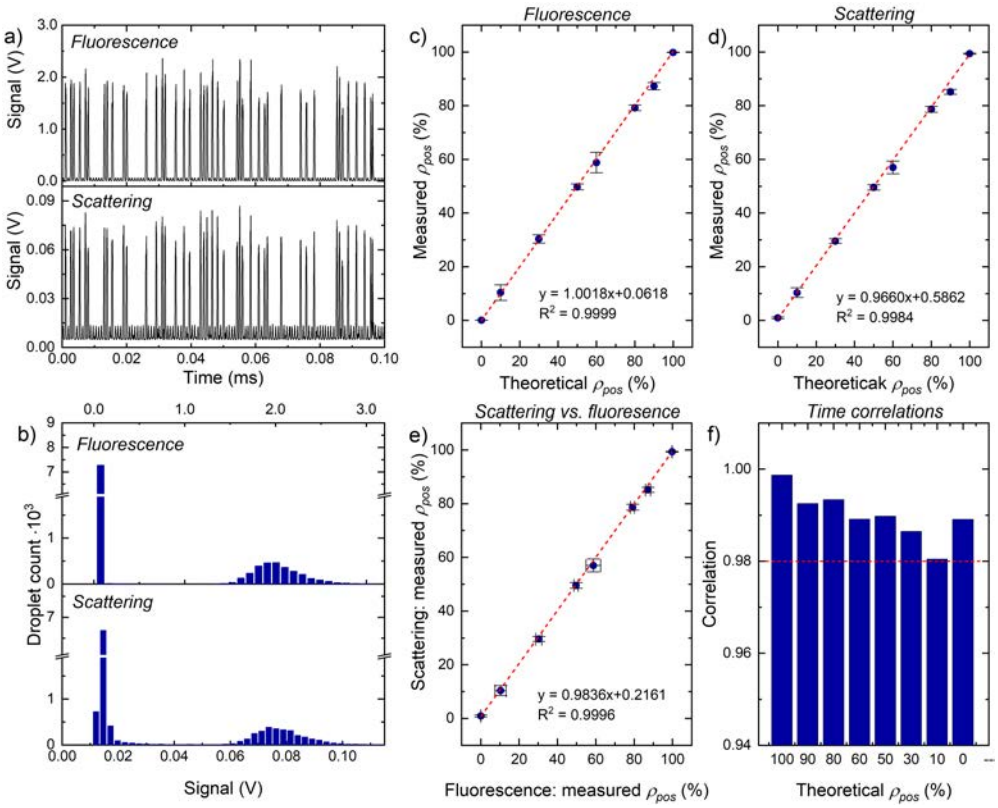

Figure 33. Label-free system provides reliable results as the method based on the detection of fluorescence light. a) exemplary fluorescence and scattered light signals from negative (low intensity of signal) and positive (high intensity) nanodroplets; b) histograms of fluorescence and scattered light intensities with two clearly distinguishable populations of droplets; c) correlation of theoretical and measured percentages of positive droplets obtained based on the intensity of fluorescence intensity; d) correlation of theoretical and measured percentages of positive droplets determined by label-free method; e) measured percentage of positive droplets determined by detection of fluorescence intensity as a function of the percentage of positive droplets obtained by the method based on scattered light; f) time correlation of fluorescence and scattered light signals. Figure reproduced from the article published by Pacocha, Bogusławski et al.[148]

The fluorescence and scattered light are recorded simultaneously. We checked the time correlations between both signals. The previously defined threshold for differentiation of positive and negative droplets was selected to convert numerical values of droplets amplitude peaks to 0 and 1 labels for negative and positive droplets, respectively. The compatibility of results in scattering and fluorescence traces was checked by calculation of the correlation metric. The number of compliant pairs was divided by the total number of droplets in the sample. We found that the detection of scattered light contains the same information as the detection of fluorescence. The correlation coefficient is larger than 0.98 for each sample, as shown in Figure 33f.

3.3.1.3. Frequency of droplet screening

The most prominent advantage of the application of droplet microfluidics is the possibility of high-throughput analysis. To reduce the undesirable effects during droplet screening, for example, droplet merging or splitting up, we optimized a microfluidic detection chip design. According to the work of Rosenfeld et al., the small entrance angle to the detection channel and its width comparable to the width of the droplets is advantageous for droplet stability and their stable flow in narrow constriction[192]. Comparing to the system presented by Liu et al. we have reduced the entrance angle to the detection channel from 45 to 25^{o}[193]. Moreover, the width of the detection channel was selected to fit 1 nl droplets with diameter of 120 μm.

We tested the maximum frequency at which droplets can be screened using our label-free system. We aimed to reduce spacing oil between the droplets resulting in the minimal distance between the droplet's amplitude peaks. We tested different ratios of flow rates of continuous and droplet phase. This way, we found the most favorable conditions when the maximum number of droplets pass by optical fiber in a given time, which is 1200 Hz (droplets/s).

3.3.1.4. Qualitative readout and resolution of the method

Phenotypic screening of bacteria in the droplets is based on measuring the number of negative (only culture medium or dead non replicating cells) and positive droplets containing growing bacteria. We tested the reliability of qualitative readout of droplets using our label-free detector. We prepared eight samples composed of different ratios of 1 nl empty droplets and compartments containing a very high concentration of non-fluorescent *E. coli* (overnight culture, ~10^9 CFU/ml, which corresponds to around 1000 cells per droplet). We analyzed all samples at a maximum frequency of 1200 droplets/s. Figure 34a presented the high

correlation between theoretical (prepared) and measured percentage content of positive droplets in the samples. The empty compartments are easily distinguishable from positive containing high concentration of bacteria droplets, which allows for a reliable readout in a label-free manner.

We also determined the method's resolution by measuring the minimum number of bacteria in the droplet allowing its detection as a positive compartment. We prepared nine samples consisted of 30% droplets with tryptic soy broth and 70% droplets with a range of different non-fluorescent *E. coli* densities, from 1 to 800 CFU/droplet. Figure 34b shows a relative error of discrimination of positives from negatives as a function of the number of bacteria per droplet. The satisfactory recognition of positive compartments starts from 400 cells per droplet. The relative error is an absolute error divided by the actual number of positive droplets. We also found that increasing the number of bacteria per droplet results in increased scattered signal intensity, as shown in 34c.

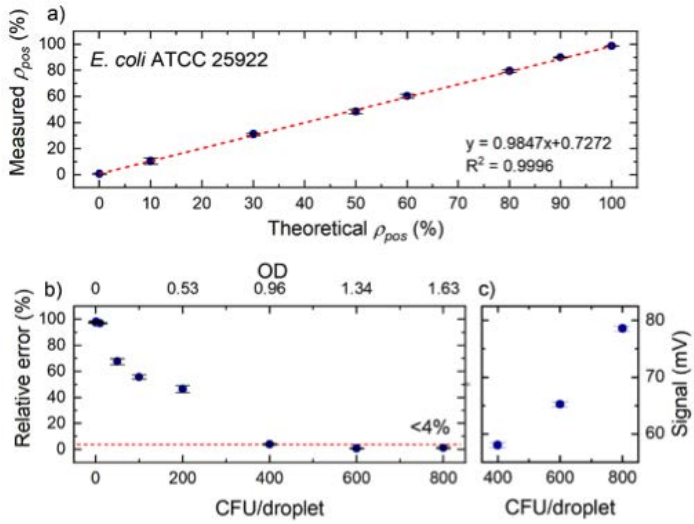

Figure 34. Our label-free detection system allows for qualitative readout of droplets containing at least 400 bacterial cells. a) the graph presents theoretical (X-axis) versus measured (Y-axis) percentages of positive droplets in the samples; b) the graph shows relative error as a function of the number of bacterial cells per droplet c) linear correlation of scattered light signal and number of bacterial cells per droplet. Figure reproduced from the article published by Pacocha, Bogusławski et al.[148]

3.3.1.5. Screening of different strains of bacteria

Our label-free scattering-based detection system should be able to monitor the growth of many bacterial species. The only potential limitations would be the difficulty of encapsulation into droplets bacterial cells, which exhibit a filamentous phenotype or grow slowly. These features restrict bacteria analysis in droplets at a single-cell level, and the detection of slow growers becomes impossible after some time of incubation due to limited droplet stability.

We verified our system's versatility by testing five samples containing different ratios of negative and positive droplets with a high concentration of tested bacteria: *Escherichia coli*, *Corynebacterium simulans*, *Pseudomonas aeruginosa*, and two strains of *Staphylococcus aureus*. Figure 35a shows the linear correlation between theoretical and measured percentages of positives within each sample regardless of variations in size, shape (round-shape, rod-shape, and club-shaped), and behavior of bacteria. *S. aureus* SH 1000 tends to form clumps. We hypothesize that this aggregation can increase the number of false-positive signals manifesting in slightly higher standard deviations, as shown on the graph 35a.

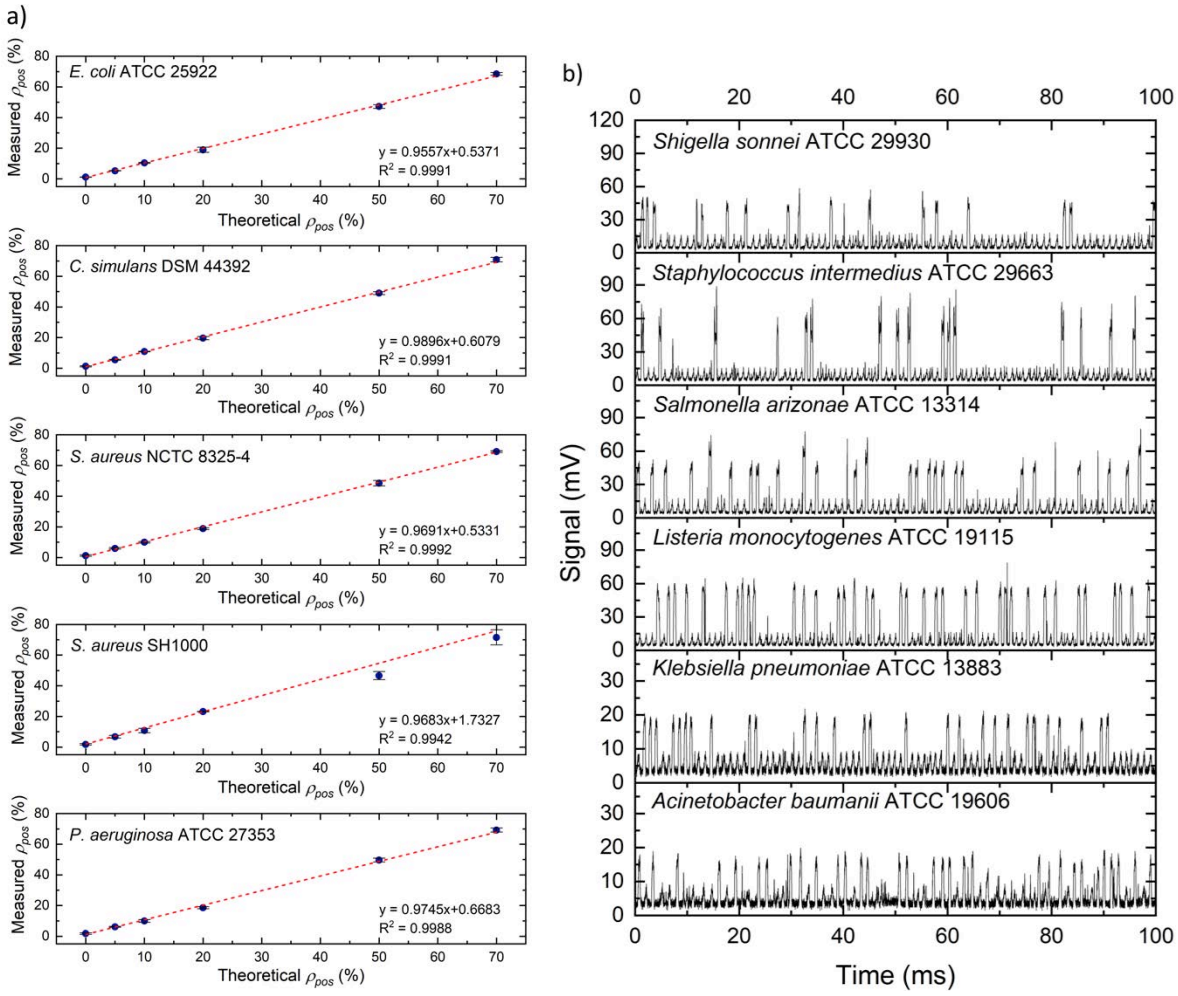

Figure 35. The system allows for monitoring of the growth of different bacteria species/ strains in the droplets. a) graphs show the correlation of theoretical and measured percentage of positive droplets containing *E. coli*, *C. simulans*, two strains of *S. aureus*, *P. aeruginosa*, respectively from top to bottom graph; b) exemplary scattered light signals of six unlabeled samples containing *S. sonnei*, *S. intermedius*, *S. arizonae*, *L. monocytogenes*, *K. pneumonia*, *A. baumanii*, respectively from top to bottom graph. Figure reproduced from the article published by Pacocha, Bogusławski et al.[148]

We also tested *Shigella sonnei*, *Staphylococcus intermedius*, *Salmonella arizonae*, *Listeria monocytogenes*, and *Klebsiella pneumoniae* by analyzing only one sample consisting of 30% of negative and 70% positive droplets (high concentration, overnight culture) per species.

Figure 35b shows the exemplary droplet signals. We found that the intensities originating from negative droplets are easily distinguishable from positive compartments. Our system allows for monitoring the growth of a wide range of bacterial species of clinical, research, and industrial interest.

3.3.1.6. Bacteria proliferation in droplets

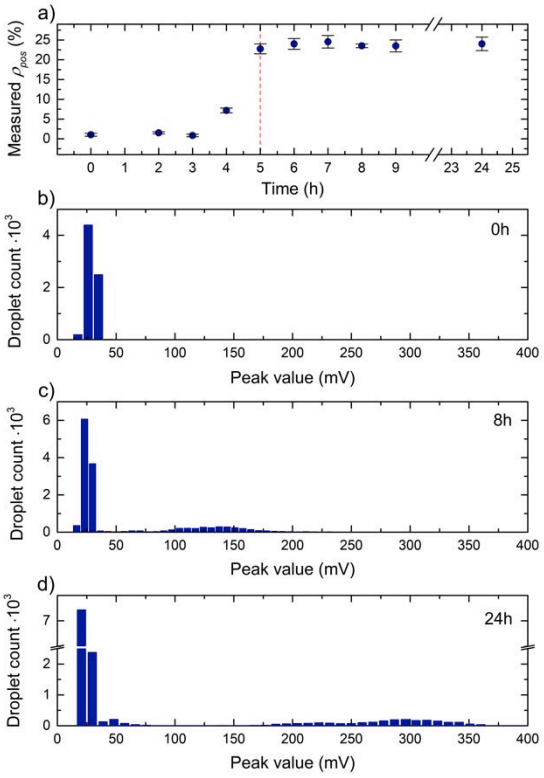

Figure 36. The system allows for detection of bacteria proliferation in the nanoliter droplets. a) detection of percentage of positive droplets in time; b-d) histograms of scattered light intensities after 0, 8 and 24 hours of droplet incubation at 37°C, respectively. Figure reproduced from the article published by Pacocha, Bogusławski et al.[148]

We checked the ability of our system to monitor bacteria proliferation in the droplets, and we determined the minimum incubation time required to distinguish positive droplets containing growing *E. coli* from negative compartments. We encapsulated bacteria at a single-cell level, as shown in Figure 32b. The overnight *E. coli* culture was diluted to the concentration, which, based on Poisson distribution, results in around 20% positive compartments. We used one nl droplets, and the bacterial sample was diluted to 2×10^5 CFU/ml. The bacterial suspension was split into droplets, and then the samples were incubated at 37°C. We monitored the bacterial growth in time by measuring the percentage of positive droplets based on scattered light intensity. We found that the number of droplets containing growing bacteria saturates at the level of 23.7% after 5 hours of incubation. For this particular species, this is the minimum time required to detect all positives in the sample (Figure 36a). Histograms presented in Figure 36b-d shows changes in the number of positive and negative compartments over time. When bacteria are freshly encapsulated, we can observe only negative droplets (Figure 36b); single bacterial cells are not detectable by our system. After 8 and 24 hours of incubation, the fraction of droplets with growing and replicating cells is visible and easily distinguishable from a population of negatives (Figure 36c,d). The average

signal intensity of positive droplets grows in time, associated with an increasing number of cells during the incubation. More scatters give higher scattered light intensity, but the overall number of positive droplets remains unchanged. The average scattered light intensities equal 75.6 ± 2.0, 117.1 ± 13.0, 232.8 ± 18.4 mV after 5, 8, 24 h of incubation, respectively. The variability in signal values of positive droplets increases with time. We speculate that it can be related to the phenotypic diversity of cells and various bacteria growth in droplets.

3.3.1.7. Screening of bacteria towards heterogeneity

Our label-free system can be used for bacteria screening towards phenotypic heterogeneity of the bacterial population. We characterized the response of individual cells in the isogenic bacterial population of *Staphylococcus aureus* LS1 to gentamicin. *S. aureus* is a versatile pathogen causing a range of infections, which are either acute or chronic and often recalcitrant. Gentamicin was chosen due to its known effect on the heterogeneous growth of *S. aureus*. First, we determined the scMIC using a wide range of antibiotic concentrations. Figure 37 shows the decrease of fraction of recovering bacteria with the increasing concentration of gentamicin with complete growth inhibition at 1 μg/ml concentration. Next, we treated bacteria with a narrow range of gentamicin concentrations, emphasizing the subMIC area, where the heterogeneous growth of bacteria is most likely to be observed. Figure 38a presents the decreasing fraction of recovering bacteria in the population, $F_R(c)$, as a function of increasing antibiotic concentration, c. The data were fitted with the Gompertz function. The cells in the isogenic population of *S. aureus* does not respond to the gentamicin in the same way. It is presented in Figure 38b (a derivative of the data from Figure 38a), which shows the distribution of the probability of scMIC in the bacterial population. It visualizes that a range of antibiotic concentrations inhibits bacteria growth. Testing bacterial heterogeneity in response to antibiotics is crucial for a better understanding of resistance mechanisms and more effective antibiotic treatment.

The number of positive droplets measured by our scattering-based approach is affected by some percentage of false positives, which is around 1.5%. To provide reliable results, we applied a mathematical model to remove false-positive droplets from our data. Therefore, we can observe a few negative values of the fraction of resistant bacteria in Figure 37 and 38a caused by this operation.

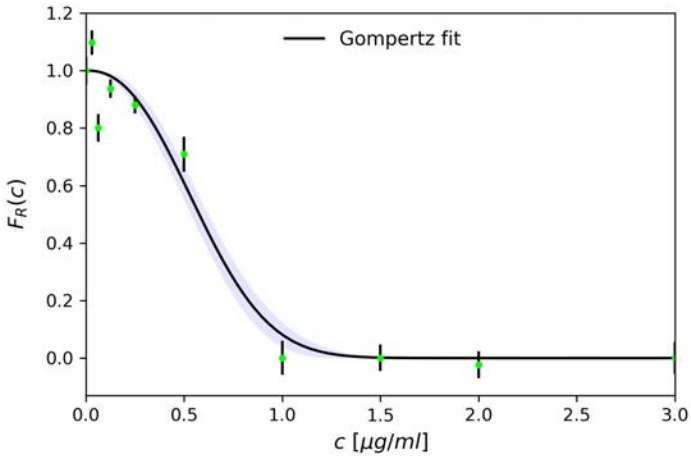

Figure 37. Testing of *S. aureus* susceptibility to gentamicin. The graph presents the fraction of recovering bacteria as a function of gentamicin concentration. The shaded area represents errors related to the curve fitting parameters determined by the least-squares method. Figure reproduced from the article published by Pacocha, Bogusławski et al.[148]

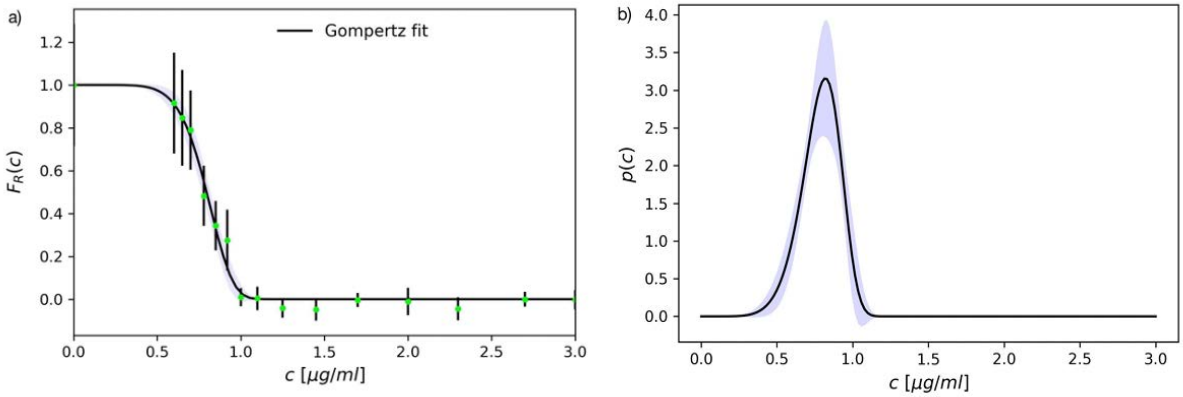

Figure 38. Determination of scMIC profile allows for analysis of phenotypic heterogeneity of bacterial population. a) the graph shows the change of bacteria recovery as a function of antibiotic concentration. b) probability density distribution of single-cell MICs in bacterial population. Figure reproduced from the article published by Pacocha, Bogusławski et al.[148]

3.3.2. Readout of bacteria density by measurement of native fluorescence

We observed that some bacterial species naturally emits fluorescence which can be detected by our detector described above. It creates an additional possibility to perform label-free reliable qualitative readout of bacteria growth in the droplets. The measurement based on detection of native fluorescence is less sensitive in the sense of detection of background particles (for example, dust), and the difference in signal peaks of positive and negative droplets does not strongly depend on the laser position in the detection channel comparing to the scattering-based method. We measured the autofluorescence signal utilizing the fluorescence channel used before for scattered-based method validation. We tested the reliability of qualitative measurements. We checked the maximum frequency of droplet

screening, and we monitored bacteria proliferation in nanoliter droplets over 24 hours of incubation.

3.3.2.1. Experimental setup

Detection of autofluorescence signal in nanoliter droplets is conducted using a microfluidic chip with flow-focusing junction (Figure 39a) and the experimental setup schematically presented in Figure 39b. Droplets are introduced to the chip by microfluidic tubing, where they are separated from each other in the junction with a continuous phase without surfactant. The droplets are then illuminated by the 473 nm lasers beam (20 mW) focused by a 20x microscope objective in the middle of the channel. The autofluorescence light is collected by the same microscope objective and directed by a dichroic mirror (490 nm cutoff) through a band-pass filter (central wavelength 530 nm, bandwidth 43 nm) to the photomultiplier tube in a confocal configuration. The PMT signal is recorded using a data acquisition card and processed using a custom-written computer program.

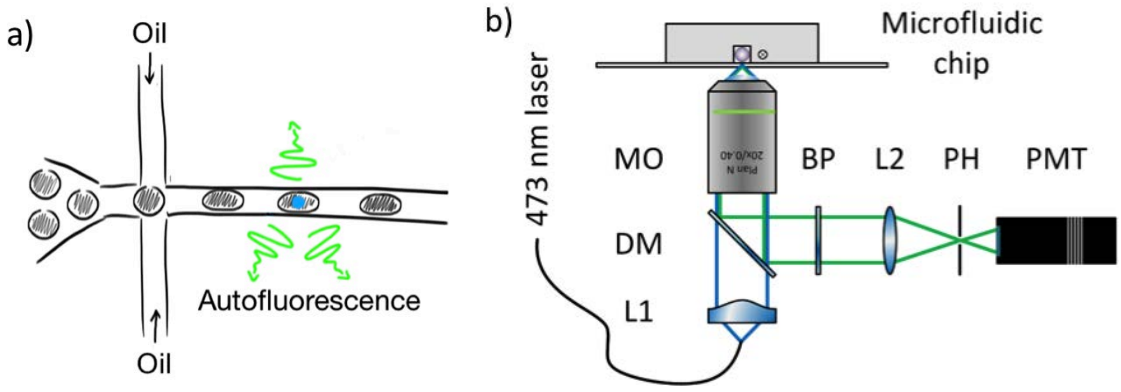

Figure 39. Schematic of the experimental setup. a) scheme of the optical setup for detecting autofluorescence signal in nanoliter droplets; L1-lens no. 1, L2-lens no. 2, DM-dichroic mirror, MO-microscope objective, BP-bandpass filter, PH-pinhole, PMT-photomultiplier; b) scheme of detection microfluidic chip with a flow-focusing junction. The blue dot and green arrows indicate the point where the laser beam is focused and the autofluorescence signal originating from bacterial cells, respectively. Figure reproduced from the article published by Pacocha, Bogusławski et al.[148]

3.3.2.2. Qualitative readout

We tested the qualitative readout performance of the number of positive and negative droplets by detecting bacterial native fluorescence. We prepared seven samples to consist of 0, 10, 30, 50, 70, 90, and 100% of positive compartments (ρ_{pos}) with a high concentration of *Escherichia coli* cells. Negative droplets (ρ_{neg}) contained only LB culture medium. Each sample was analyzed in three replicates at a frequency around 1.2 kHz (similarly to the scattered light detection). Figure 40a presents exemplary waveforms of droplet signals. The

top and bottom graphs present autofluorescence signal of only negative and positive populations of droplets, respectively. The middle one concerns a mixture, where peaks with higher intensity indicating compartments containing cells are easily distinguishable from peaks with lower signal intensity (negative droplets). To distinguish both populations and enumerate the droplets, we used a two-level threshold-based approach, as explained before in Chapter 3.3.1.2. We found that the theoretical and measured values of percentages of positives within each sample determined based on autofluorescence signal are highly correlated, as shown in Figure 40b. It is proved by the linear regression equation and coefficient of determination. The detection of bacterial native fluorescence is an alternative system for label-free qualitative monitoring of bacterial growth in nanoliter droplets.

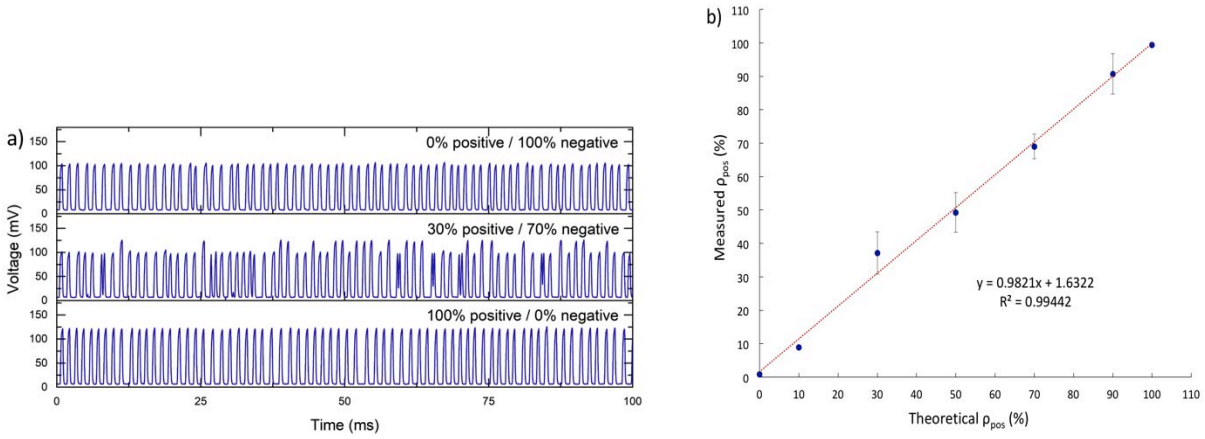

Figure 40. The autofluorescence-based detection system allows for qualitative readout of nanoliter droplets. a) Exemplary autofluorescence signals from nanodroplets. The top, central, and bottom graphs concern samples containing 0%, 30%, and 100% positives, respectively. b) the graph showing a correlation between theoretical and measured values of percentages of positives in each of seven samples based on the autofluorescence intensity.

3.3.2.3. Frequency of screening

We tested whether the maximum frequency of droplet scanning based on autofluorescence intensity measurement can be higher compared to the scattered-based method. We used the same design of the detection microfluidic chip (Figure 32c), and we encapsulated bacteria into one nl droplets. The final sample contained 30% positive (overnight culture of *E. coli*) and 70% negative compartments (culture medium). We screened the droplet with a range of different flows of droplets and oil phase. Figure 41a presents the exemplary waveforms for three different scanning frequencies where the most optimum is 1100 droplets/s. The droplets are distinctly separated, and populations of positives and negatives are distinguishable, as shown in the top histogram in Figure 41b. For the frequency as high as 2100 Hz, we observed droplet signal disturbance and difficulty to determine the threshold for positive droplets

counting. It is presented in the bottom histogram in Figure 41b showing the range of different droplet signal intensities without a clear separation of two distinct droplet populations.

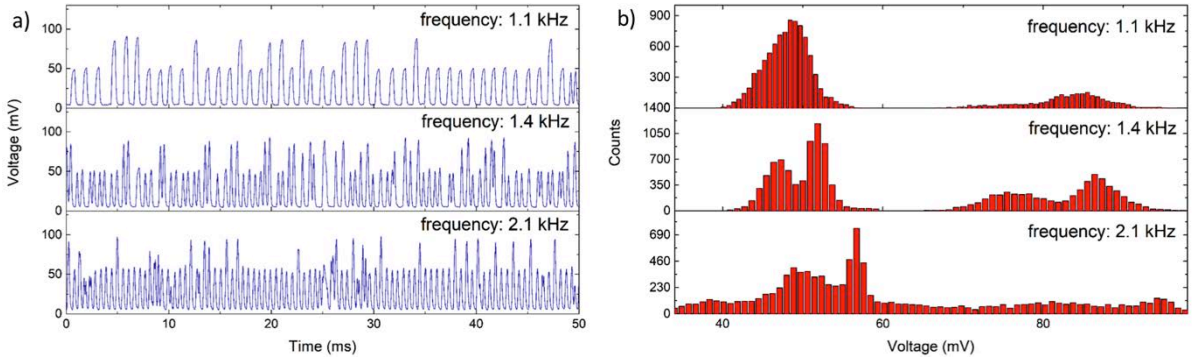

Figure 41. The screening system based on detection of native fluorescence in the nanoliter droplets allows for high-throughput analysis of bacteria. a) The exemplary waveforms of droplets screened at frequency of 1.1 (top), 1.4 (central), and 2.1 kHz (bottom). b) Histograms of autofluorescence intensity for samples scanned at frequency of 1.1 (top), 1.4 (central), and 2.1 kHz (bottom).

3.3.2.4. Screening of different strains of bacteria

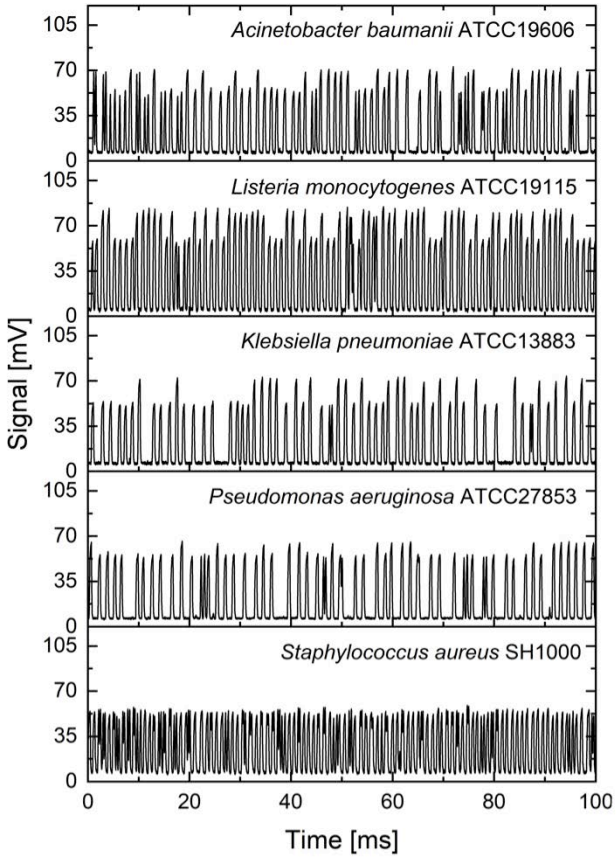

Figure 42. The system allows for monitoring of growth of different bacterial species in nanoliter droplets. The exemplary native fluorescence signals of five samples containing *A. baumanii*, *L. monocytogenes*, *K. pneumoniae*, *P. aeruginosa*, and *S. aureus*, respectively from top to bottom.

We tested the applicability of our autofluorescence-based system for screening different bacterial species. We chose bacteria of clinical, research, and industrial interest, providing an extensive overview of various species. Bacteria were cultured overnight at 37^{o}C, mostly in LB medium. Some species were cultivated in BHI (nutrient-rich medium) for more favorable growth. We prepared samples to consist of 70% negative droplets and 30% of positive compartments with a high concentration of tested species. Then, the native fluorescence intensity was measured in each droplet (Figure 42), and the positive to negative peak ratio was calculated for each bacteria. Table 7 presents the results of the screening. We found that many of the tested species show higher autofluorescence

intensity than the culture medium. It is mostly observable for Gram-negative bacteria. We could not determine the number of positive droplets containing most of the gram-positive species except *Listeria monocytogenes*. We hypothesize that used excitation wavelength and bandpass filter can preclude the detection of mentioned species. A new optical setup should be created for that purpose. The inability to detect some bacterial species can be advantageous in microbiological experiments where polymicrobial culture is tested, and only one species exhibit higher native fluorescence than the culture medium.

Table 7. Detection of different bacterial species by measurement of autofluorescence intensity. (G-)- Gram-negative bacteria, (G+)- Gram-positive bacteria, LB- lysogeny broth, BHI- brain heart infusion.

Bacterial species	G-/G+	Culture medium	Positive to negative peak ratio
Escherichia coli	G-	LB	1.304 ± 0.109
Klebsiella pneumoniae	G-	LB	1.368 ± 0.007
Acinetobacter baumanii	G-	LB	1.294 ± 0.015
Pseudomonas aeruginosa	G-	LB	1.176 ± 0.005
Salmonella arizonae	G-	BHI	1.116 ± 0.005
Listeria monocytogenes	G+	BHI	1.357 ± 0.010
Shigella sonnei	G-	BHI	1.0913 ± 0.0004
Enterococcus faecalis	G+	LB	-
Staphylococcus aureus Newman	G+	LB	-
Staphylococcus aureus SH1000	G+	LB	-
Staphylococcus epidermidis	G+	LB	-
Staphylococcus intermedius	G+	LB	-

3.3.2.5. Bacteria proliferation in droplets

We checked the possibility of using natural emission of light by bacteria to monitor their growth in the nanoliter droplets. We encapsulated *E. coli* cells at a single-cell level. Then we incubated the samples at 37^{o}C (see Figure 32b for experimental workflow). We measured the number of positive droplets just after droplet formation and after 2, 3, 5, 6, 7, 8, 9, 24 hours of incubation. We analyzed around 60 000 droplets at each time point at a frequency of 1.2 kHz.

The signal intensity originating from positive droplets increases as bacterial cells proliferate during incubation (Figure 43a). We expected to detect 20% positive and 80% negative droplets according to the bacteria concentration prepared before droplet generation. After 6 hours of incubation, we observed a sufficiently large difference in droplet intensities to count consistent with our expectations number of positive compartments. After 24 hours of incubation, this number slightly changed and was determined to be 20.8%, as shown in Figure 43b. The histograms of autofluorescence intensities for three different time points are shown

in Figure 43c. They present changes observed in the populations of negative and positive droplets over time. Before incubation (0h), only negative droplets were determined in the sample. After 5 hours, we observed the rising population of positive droplets without clear distinction from the negatives' population. The clear separation is visible after 6 hours of incubation, with negative droplets located on the left- and positive droplets on the right-hand side.

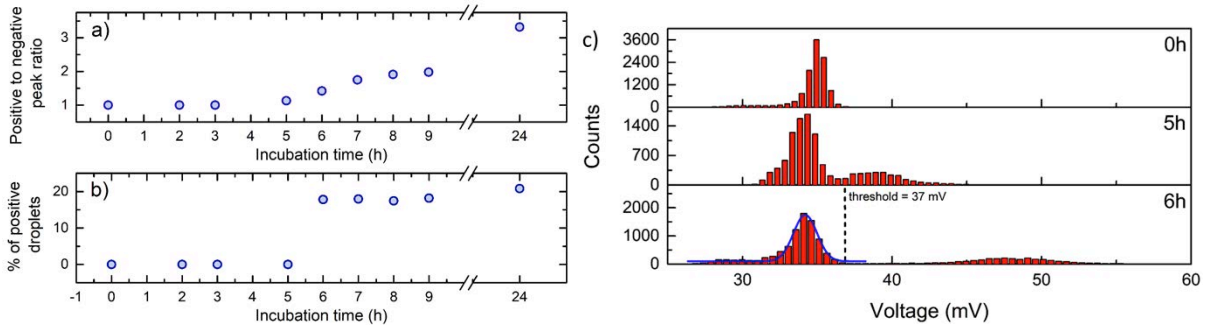

Figure 43. The system allows for monitoring of the proliferation of *E. coli* cells in nanoliter droplets. a) The graph showing changes of positive to negative peak ratio over time. b) The graph presents the percentage of positive droplets as a function of time. c) Histograms of native fluorescence intensity after 0h (top), 5h (central), and 6h (bottom) of incubation at 37^{o}C.

3.4. Droplet-based assay for quantitative characterization of bacterial populations

Parts of this chapter will be published as: Pacocha N., et al., *You will know by its tail: a method for quantitative characterization of heterogeneity of bacterial populations using single-cell MIC profiling.* In preparation.

Phenotypic and genetic heterogeneity of bacterial response to antibiotics is recognized as a critical aspect for selecting effective treatment against infecting pathogens. Even a clonal population of bacteria can contain antibiotic tolerant subpopulations of persisters or small colony variants. There is a lack of label-free, precise, and high-resolution methods for quantification and analysis of heterogeneous bacterial populations.

We developed a droplet-based approach for the analysis of diverse bacterial samples based on single-cell MIC profile determination. We measure the response of single cells to various antibiotic concentrations. Bacterial growth in the droplets is measured by the detection of scattered light intensity. An obtained susceptibility profile is then used for analysis and quantification of tolerant to antibiotic subpopulations in the bacterial population. The detection of native fluorescence light intensity simultaneously with scattered light

measurement creates an even more comprehensive scope of the method's application, which is the analysis of polymicrobial samples.

3.4.1. Heterogeneity profiles of normal cells and small colony variants

We have already verified that the detection of scattered light can be used to determine scMIC distribution within bacterial population[148]. We decided to utilize label-free bacteria growth detection and scMIC profiling to analyze bacterial heterogeneity in response to antibiotics and quantification of small colony variants (SCVs) subpopulation. We chose *Staphylococcus aureus* strain SH1000 to investigate its antibiotic response at the single-cell level. Firstly, we obtained heterogeneity distributions of normal colonies (normal colony phenotype, NCP) and small colony variant phenotype (SCV) as separated populations of bacteria. NCPs are bacteria cultured under optimum conditions, while SCVs were triggered by antibiotic stress. The growing culture of *S. aureus* was pre-exposed to 2 μg/ml gentamicin following the selection of small tolerant to gentamicin colonies on agar plates (Figure 45a). The phenotypic differences observed for the gentamicin-triggered SCVs population were aminoglycosides tolerance (Table 8), colony size (Figure 45b), longer lag time (Figure 44), and reduced pigmentation.

Table 8. MIC values of various antibiotics for bulk suspensions of NCPs, half and half mixture of NCPs and SCVs, and SCVs.

	Gentamicin [μg/ml]	**Vancomycin** [μg/ml]	**Amikacin** [μg/ml]	**Rifampicin** [μg/ml]	**Oxacillin** [μg/ml]
NCPs	2	2	16	0.0156	0.25
50% NCPs + 50% SCVs	32	2	256	0.0156	0.25
SCVs	32	2	256	0.0156	0.25

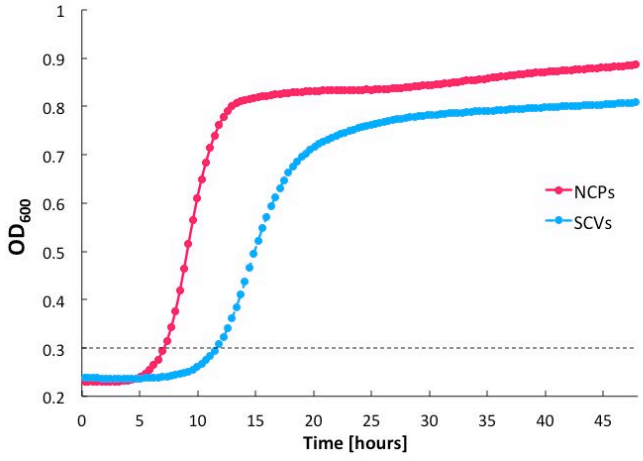

Figure 44. The growth of SCVs (blue line) compared to normal cells (pink line) is delayed in time, probably caused by the delay in the first division at the level of single cells. Growth curves of NCPs and SCVs cultures measured at 600 nm wavelength over 46 hours in a rich medium.

Homogenous type colonies of NCPs and SCVs were harvested with a loop and subjected to the single-cell MIC measurement (Figure 45c). Suspensions of cells either phenotype at ca. 1×10^5 CFU/ml were split into 1nl droplets at a range of gentamicin concentrations (around 30 thousand droplets per one sample). According to Poisson distribution, we encapsulated bacteria where approximately 10% droplets were single-cell bacteria-occupied. After incubation at 37^{o}C for 18 hours, the scattered light intensity was measured in each droplet compartment. The number of droplets with multiplying bacteria (positive droplets) was detected based on high signal intensity and used to calculate the fraction of recovering bacteria, $F_R(c)$, for each antibiotic concentration. The $F_R(c)$ value is the number of positive droplets normalized by the number of positive compartments obtained in the sample where bacteria were not exposed to the antibiotic.

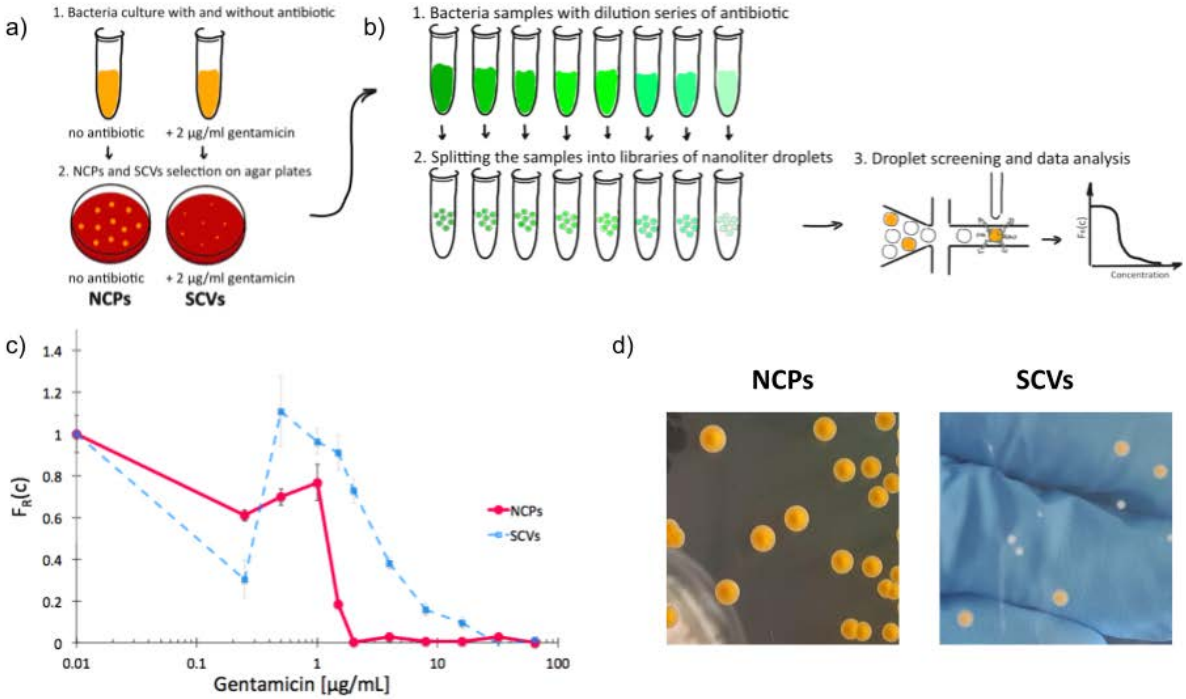

Figure 45. The scMIC profiles for NCPs and SCVs are very distinctive and consist of two regions. a) Overview of SCVs triggering process by antibiotic stress. Firstly, *S. aureus* was incubated in the absence and presence of gentamicin; then, both suspensions were plated on agar plates without and with antibiotics for NCPs and SCVs selection; b) schematic workflow of scMIC and phenotypic heterogeneity profile determination. Shades of green indicate a range of antibiotic concentrations; d) comparison of scMIC curves obtained for the population of NCPs (red bold) and SCVs (blue bold). X-axis and Y-axis indicate gentamicin concentration and a fraction of recovering bacteria, respectively; d) photographs of NCPs (left) and SCVs (right) colonies on tryptic soy agar plates. The phenotypes of NCPs and SCVs differ significantly. The gentamicin-triggered SCVs population has increased tolerance to aminoglycosides, reduced colonies size, and pigmentation;

The scMIC profiles of NCPs and SCVs were obtained separately and compared (Figure 45d,e). The NCPs complete growth inhibition was observed at 2 µg/ml, and scMIC for SCVs was determined at 32 µg/ml of gentamicin, consistently with MIC values established using

the standard microdilution method (Table 8). The scMIC profiles for NCPs and SCVs are very distinctive and consist of two regions. A first region of low antibiotic concentration is similar for both, NCPs and SCVs and pertain to slowly decaying fraction of recovering bacteria, $F_R(c)$. The second region, which we referred to us a **transition region** starts at a gentamicin concentration of 1 μg/ml and decays with increasing antibiotic concentration. In the case of NCPs, the transition region has a sharp decline and ends at 2 μg/ml, while for SCVs, it has a gentle, elongated slope reminding a **'tail'** reaching 32 μg/ml. The population of SCVs is more heterogeneous and tolerant to gentamicin than NCPs. scMIC was determined at the end of the tail when the antibiotic kills at least 95% of bacteria.

3.4.2. Impact of SCVs density on scMIC and heterogeneity profile

As we characterized the scMIC profiles for NCPs and SCVs, we wanted to investigate their impact on the scMIC distribution within pre-mixed populations of a known proportion. Selected on agar plates and resuspended in culture medium homogenous suspensions of NCPs and SCVs were combined into mixtures containing 12 and 50% of SCVs with 88 and 50% of NCPs, respectively (Figure 46a).

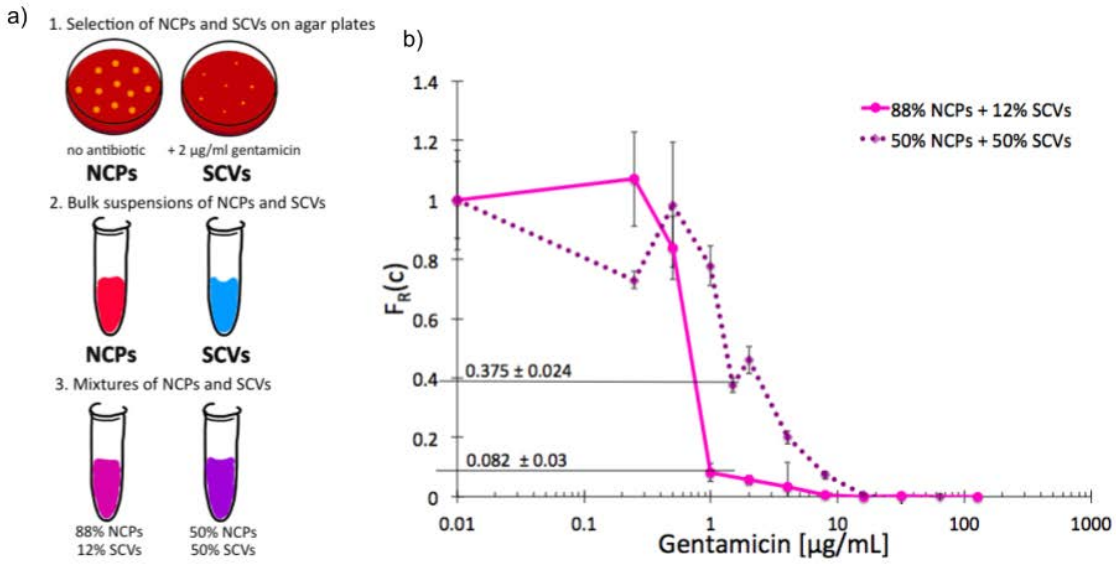

Figure 46. The method allows for heterogeneity profile determination of mixtures of phenotypic variants of *S. aureus*. a) schematic representation of sample preparation consisting of NCPs and SCVs homogenous bulk suspension formation and combination of both populations into mixtures of known proportions; b) scMIC curves for phenotypically heterogenic samples containing 12% (solid pink) and 50% (dotted purple) of small colony variants mixed with normal cells at 88 and 50%, respectively. The X-axis indicates gentamicin concentration, while Y-axis corresponds to a fraction of recovering bacteria.

We have found that the scMIC mixture profiles are the combinations of distributions presented in Fig. 45d,e. They consist of two characteristic regions (Figure 46b). For the

mixture of 12% SCVs, we observed a rapid decline of bacteria survivability at 1 mg/ml gentamicin and the tail between 1 and 8 mg/ml corresponding to SCVs content in the sample. When the concentration of SCVs increases, the breath of heteroresistance expands, and the scMIC value rises, which is visible in the 50% SCVs mix population (Figure 46b). These results suggest how to quantify tolerant to antibiotic subpopulations employing scMIC profile determination, analysis of curve transitions, and readout of the tail height. Our calculations led us to the following SCVs concentrations in both mixtures: 8.2 ± 3.0% and 37.5 ± 2.4%. The standard deviations presented in scMIC profiles are mainly related to the method of droplet recognition and estimation of positive droplet fraction in an ideal condition of stable droplets. However, we found another source of much higher standard deviation speculatively caused by aggregation of *S. aureus* SH1000 leading to droplet coalescence, which is described in the next chapter studying methods' precision.

3.4.3. Precision of an assay

We expected the error of the fraction of recovering bacteria to be inversely proportional to the square root of the number of non-empty droplets[175]:

$$\sigma_{F_R(c)} \approx \sqrt{F_R(c)/Nf_+(0)},$$

$F_R(c)$- fraction of recovering bacteria,
N- total number of droplets,
$f_+(0)$- fraction of non-empty droplets without antibiotic treatment of bacteria.

One thousand positive compartments typically used in our experiments would give $F_R(c)$ fluctuations below 3%. The scMIC profile would be a smooth and monotonically decreasing curve. However, we observed more significant fluctuations, and we decided to test the precision of SCVs quantification by our scMIC approach. We cultured *S. aureus* biofilm for 72 hours in the presence of gentamicin. Biofilm was dispersed and subjected to scMIC study in three replicates measured one by one. Figure 47 shows the heterogeneity profiles of all repetitions. We found the highest deviation from the mean 38% in the transition region for one gentamicin concentration of 0.5 mg/ml. The rest of the data points are affected by the deviation not higher than 7%. The samples without antibiotic or containing a low concentration of gentamicin are affected by more significant standard deviations. Most probably, it is related to decreasing droplet stability with an increasing number of bacteria cells. It is particularly noticeable in *S. aureus* SH1000 cells which tend to create clumps and aggregates. Our numerical analysis revealed the following SCVs concentrations in repetitions

no 1, 2 and 3: 17.9 ± 1.4%, 31.3 ± 2.9%, 29.8 ± 3.0%, respectively. The average size of SCVs subpopulation is 26% and the variability (standard deviation) in obtained results is 7.3%. The relative error ($7.3\%/26\% = 28\%$) explains some discrepancies between expected and obtained SCVs concentrations.

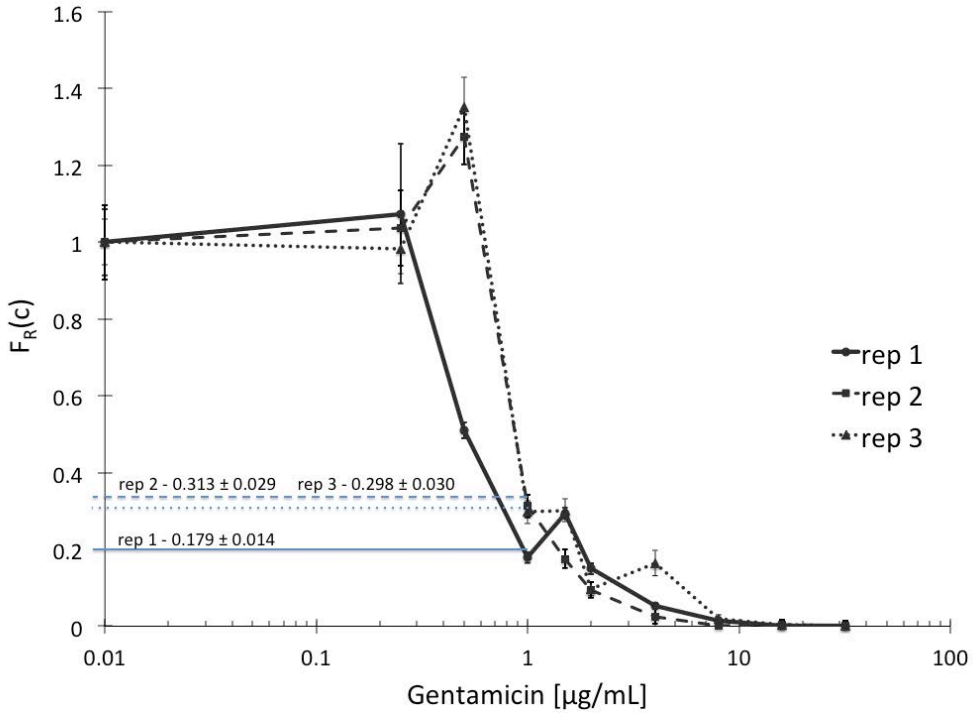

Figure 47. Precision of heterogeneity profile determination. The graph compares three scMIC curves resulting from the analysis of biofilm sample measured in three replicates. X-axis indicates gentamicin concentration, while Y-axis corresponds to fraction of recovering bacteria.

3.4.4. Heterogeneity profiles of biofilm samples

The recalcitrance of *S. aureus* biofilms is commonly associated with the emergence of a tolerant to antibiotic subpopulation, such as the SCVs. They can occur at low abundance and transiently, so they can avoid detection using standard antibiotic testing. We studied the scMIC profiles of biofilms with different contributions of SCVs and we investigated whether our label-free approach is suitable for quantification of antibiotic tolerant subpopulations in complex samples. We formed biofilms under various conditions to obtain samples containing different sizes of SCVs subpopulations (Figure 48a).

Firstly, we aimed to obtain unique scMIC profiles of homogenous NCPs and SCVs populations. They were isolated from biofilms cultured with and without gentamicin, selected on agar plates (Figure 48a) and subsequently subjected separately to scMIC studies. Figure 48b presents compared susceptibility distributions on the basis of which we estimated single-cell MIC values for NCPs and SCVs at 1.5 µg/ml and 32 µg/ml, respectively. They

correspond to those determined for either populations isolated from bulk suspensions (Figure 45c). Moreover, the distinctive shapes of the transition regions for either NCPs or SCVs were confirmed as sharp decline and gentle slope, respectively.

We subsequently wanted to use scMIC profiling for SCVs quantification in the biofilms cultured in vitro in the presence and absence of gentamicin (Figure 48a). Both biofilm samples were dispersed and subjected to scMIC studies. As shown in Figure 48c gentamicin treatment increases scMIC. We observed a sharp decline of recovering bacteria fraction at 1 μg/ml and the tail ending at 8 μg/ml. The height of the tail indicates the SCVs content at 6.8 ± 1.9% (Figure 48d), which highly correlates with the quantification conducted by plate counting (4.3 ± 1.3%). It demonstrates the role of sub-MIC concentrations of gentamicin in triggering heteroresistance within a biofilm culture.

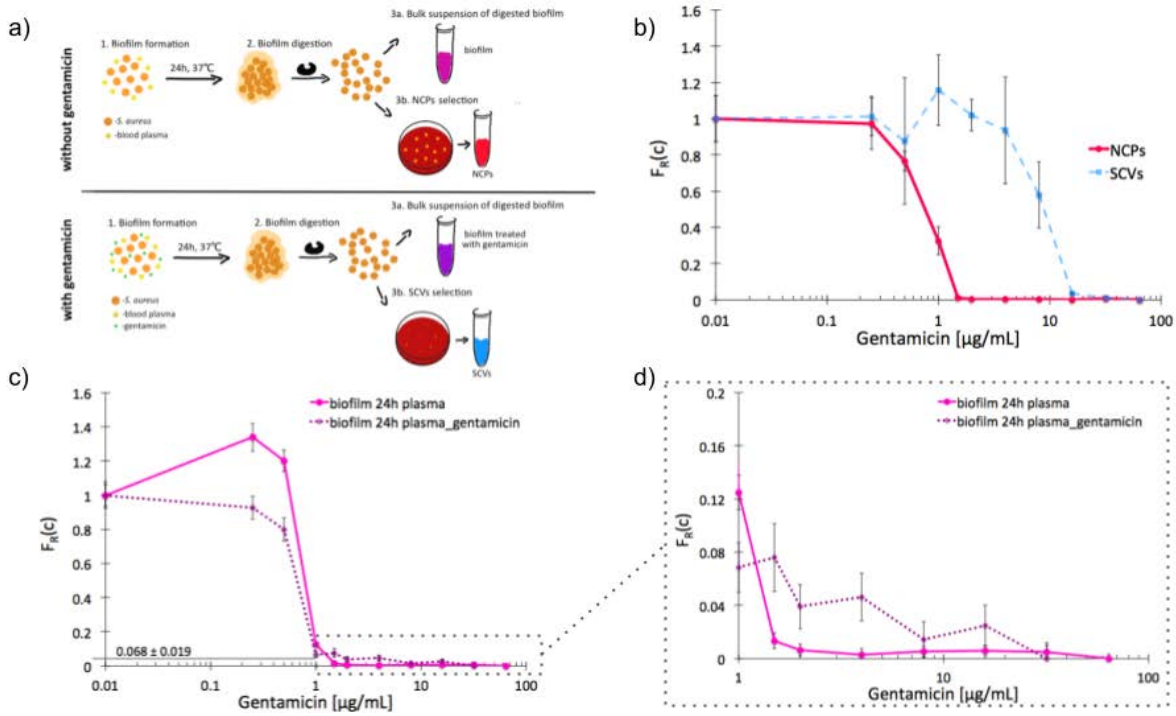

Figure 48. Phenotypic heterogeneity of *S. aureus* dispersed from biofilms. a) Schematic workflow of biofilm formation, enzyme digestion, preparation of bulk suspensions and NCPs (top), SCVs (bottom) isolation; b) heterogeneity profiles of NCPs (solid red) and SCVs (dotted blue) isolated from biofilm cultured over 24 hours with gentamicin; c) scMIC curves obtained for biofilms growing with blood plasma in the absence (solid pink) or in the presence (dotted purple) of gentamicin; d) the tails of scMIC profiles shown in c). X and Y axis correspond to gentamicin concentration and fraction of recovering bacteria, respectively (b-d).

3.4.5. Heterogeneity profile of polymicrobial samples

Some of the most common infectious diseases are caused by more than one pathogen, for example soft tissue infections, peritonitis, cystic fibrosis, urinary tract infections and endocarditis[194]. We investigated whether scMIC profiling can be applied to analyze the phenotypic heterogeneity of polymicrobial samples and quantify coexisting subpopulations. We prepared pre-mixed populations of *Staphylococcus aureus* MSSA476 and *Pseudomonas aeruginosa* PAO1 of known proportions and subjected them to scMIC studies using two different antibiotics. Both species are known as competitors of cystic fibrosis lung. Firstly, bacteria were encapsulated into 1 nl droplets at the single-cell level and incubated at 37^{o}C for 18 hours. Subsequently, we detected the scattered light and native fluorescence intensity in each compartment. We took advantage of inability of *S. aureus* growth detection based on autofluorescence signal. The droplets containing *P. aeruginosa* were recognized in both scattered and fluorescence channels, while the compartments with *S. aureus* were detected only by the high intensity of scattered light (Figure 49a).

The pre-mixed populations of *S. aureus* and *P. aeruginosa* were subjected to scMIC measurement using ciprofloxacin and tobramycin. The antibiotics were selected based on their widespread use in the infection treatment and their MIC values determined in bulk suspensions (Figure 49b). We aimed to choose various conditions where both species are differently susceptible to antibiotics.

The scMIC profiles for polymicrobial samples were determined directly based on the number of positive droplets ($\mathbf{f}_{+}$, fraction of positive droplets). We obtained the scMIC values at 1.5 mg/ml for ciprofloxacin and 4 mg/mL for tobramycin, corresponding to the breakpoint concentrations of more tolerant to antibiotic strains. The distribution obtained based on scattered light intensity provides information concerning both species and consists of two distinctive regions. The first region of low antibiotic concentration represents both species in a mixture, up to 0.25 μg/ml for ciprofloxacin and 0.5 μg/ml for tobramycin (Figure 49c-d). The second region was the susceptibility distribution only of *P. aeruginosa* (Figure 49c) or *S. aureus* (Figure 49d) when lower antibiotic concentration inhibited the growth of co-existing bacteria. The scMIC profile determined based on native fluorescence intensity represents the susceptibility distribution of only *P. aeruginosa*, which is indispensable for mixed culture with a significant predominance of one of the two species when the distinctive decline in the scattered-based scMIC profile is not observed (Figure 49d).

These results demonstrate that scMIC distribution is an effective tool for high-resolution (comparing to standard methods for analysis of bacterial heteroresistance) susceptibility testing and quantification of subpopulation sizes of complex bacterial populations. Mixed populations of similar proportions in co-existing pathogens can be analyzed using only scattered-based detection. Yet, in case of a significant disproportion in subpopulation sizes, autofluorescence measurement is essential.

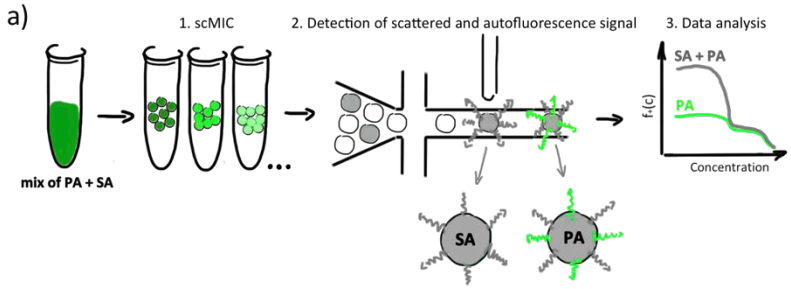

b)	ciprofloxacin [μg/mL]	tobramicin [μg/mL]
S. aureus MSSA476	0.5	8
P. aeruginosa PAO1	2	2

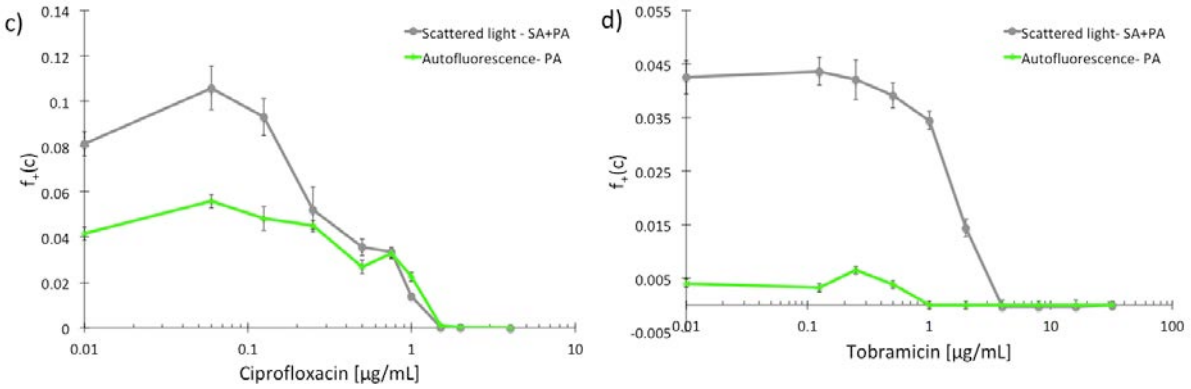

Figure 49. Our dual label-free detection allows for determination of scMIC profiles of binary polymicrobial samples. a) Schematic representation of an experimental workflow for label-free scMIC and phenotypic heterogeneity determination; b) MIC values determined by standard microdilution method for ciprofloxacin and tobramycin against investigated *S. aureus* MSSA476 and *P. aeruginosa* PAO1; c,d) graphs showing a number of positive droplets as a function of antibiotic concentration measured based on scattered light (grey line) and autofluorescence (green line) intensity. The scattered-based profile carries information regarding both species, while autofluorescence-based distribution informs about *P. aeruginosa* susceptibility.

4. Conclusions

This chapter describes general conclusions stemming from the presented projects in Chapter 3. The enhancements comparing to standard methods and summarized results are provided. Finally, the limitations and the possible solutions are indicated.

4.1. Droplet digital CFU (ddCFU) assay for precise quantification of bacteria over a broad dynamic range

Classical droplet digital quantification approach offers a convenient alternative for bacteria enumeration comparing to time- and labor-consuming plate counting. Unfortunately, it needs a vast number of compartments for highly concentrated samples and requires testing of multiple samples with presumed concentrations ranging over many orders of magnitude. The ddCFU technology is an alternative approach of droplet digital assays, which implements a rational design and drastically reduce the number of compartments needed for bacteria quantification over a wide dynamic range.

The results obtained by ddCFU technology highly correlate with data determined by gold-standard plate counting approach. Determination of bacteria concentration can be provided in a range of over 9log with precision of the assessment comparable to single-volume assays. The assay time can be around three times shortened comparing to the traditional plate counting (tested with *E. coli* and *E. aerogenes*) due to faster target accumulation in the small volume to detectable concentration. Our approach can be applied in time-kill assays or antibiotic susceptibility testing.

At the current stage, the system is not optimized for very low bacteria concentrations. For that purpose, the bacteria sample can be concentrated by centrifuging and dispersing the pellet in a smaller liquid volume. However, it is the additional inconvenient step extending the entire quantification process. Also, our approach is not suitable for non-fluorescent bacteria, which restricts its application and hinders the analysis of the most interesting strains.

4.2. Species specific, accurate and precise quantification and identification of bacteria in mixed samples

We demonstrated a direct droplet digital PCR (dddPCR) for simultaneous identification and quantification of bacteria in a bacterial mixture. The method was designed for three bacterial species, *Staphylococcus aureus, Staphylococcus epidermidis, and Staphylococcus capitis*. The digital format of our assay allows for calibration-free bacteria quantification, where in the traditional qPCR technique, the determination of the calibration curve is an essential step. Besides, we eliminate the errors and workload associated with the extraction and purification of bacterial DNA by direct encapsulation of cells into droplets.

The results of bacteria enumeration obtained by our approach highly correlates with data determined by standard plate counting. The TaqMan® hydrolysis probes provide high specificity of bacteria recognition, tested with real-time PCR and dddPCR. The relative standard deviations (%SD) of the count of target bacteria remain within a few percent, with the most extensive spread for *S. epidermidis*. We found that dddPCR is more tolerant to the presence of background bacteria than traditional qPCR. It makes our approach highly promising in analyzing polymicrobial clinical samples from infected patients or testing the effect of antimicrobial agents on the bacterial mixture's composition.

The limiting factor of our method is a requirement of primers and probes design for every bacterial species. However, since PCR reagents are correctly selected, the identification and quantification of target bacteria take just ~3.5 hours. DddPCR was optimized using Gram-positive species. Their cell wall is much harder to destroy compared to Gram-negative bacteria. It emphasizes the robustness of our approach for the direct analysis of bacteria.

4.3. High-throughput label-free readout of bacteria density in nanoliter droplets

We have developed a method for detecting bacteria growth in nanoliter droplets without the requirement of chemical dyes addition (markers of metabolic or enzymatic activity) that may leak from the droplets or complicated genetic modification of the cells (fluorescent proteins expression).

Our label-free system detects bacteria proliferation in droplets based on the intensity of scattered or native fluorescence light. Comparing to the approaches already presented in the literature, our system outstands with at least five times higher frequency of droplet screening (1200 droplets/s). The determination of the number of positive droplets in the sample is conducted over a broad dynamic range, and obtained results are in high correlation with data determined by the standard fluorescence-based approach. We found that the measurement of bacteria density based on scattered light intensity works with almost any bacterial species. The method based on native fluorescence intensity detection is more constricted. It does not come in useful for the *Staphylococcus* genus. Both approaches can be used for monitoring of bacteria proliferation and were used for single-cell MIC determination and analysis of bacterial population heterogeneity.

The limitations of using our system are detecting bacteria challenging to culture in droplets (slow growers, filamentous phenotype) and strong dependence of the measurement on the laser beam position. The possible solution would be introducing laser light by optical fiber directly to the microfluidic chip. Despite these constraints, the proposed label-free detection method is still a powerful technique bringing innovation in the analysis of most clinically interesting bacterial species. It increases the prevalence of droplet microfluidics use in analytical microbiology.

4.4. Droplet-based assay for quantitative characterization of bacterial populations

We have developed an assay for the accurate characterization of bacterial population response to antibiotics. We can precisely determine single-cell MIC for any antibiotic, obtain heterogeneity profiles, the size of phenotypically distinct and coexisting bacteria subpopulations. We optimized the method with *Staphylococcus aureus* SH1000, *Staphylococcus aureus* MSSA476, and *Pseudomonas aeruginosa* PAO1 using scattered- or/and autofluorescence-based bacteria growth detection in droplets.

Our approach is based on the scMIC profile determination, which differs for normal colony phenotypes (NCPs) and small colony variants (SCVs). The distinctive heterogeneity distributions allow for quantification of both populations in pre-mixed cultures and biofilm samples. The population of SCVs creates a distinct ‘tail’ in scMIC distribution, making the quantification of SCVs very convenient and low-maintenance. Besides, the scMIC profile can inform the composition of polymicrobial samples by simultaneous measurements of droplet’s scattered and native fluorescence light intensities. We tested *S. aureus* and *P. aeruginosa* cultures. Their differentiation was possible due to no detectable in our system natural emission of light of any *Staphylococcus spp.* isolates. The method’s precision was obtained by triple quantification of SCVs subpopulation in biofilm sample formed in the presence of gentamicin.

We found that the droplets containing *S. aureus* SH1000 and none or low antibiotic concentration are much more unstable. Consequently, the measurement of the number of positive droplets is disturbed and affected by a much higher standard deviation. We speculate that it stems from the clump-forming nature of *S. aureus* SH1000. The possible solution

would be a new surfactant highly stabilizing the droplets. However, currently, there is no commercially accessible product to employ. Under that reasoning, some species of bacteria can not be cultured in droplets, and it corresponds to slow growers and filamentous phenotype species. Besides, despite high-throughput droplet generation and detection techniques, our system does not allow high-throughput experiments because each sample is split into droplets and then screened separately and manually. The desirable denouement would be an automation of both processes. The samples could be delivered on a 96-well plate, automatically split into droplets, collected again on the plate, incubated, and then transferred to the detection mode, where all the samples could be automatically screened one by one. In spite of all, we hope that our model can be used and paves the way for better characterization of antibiotic susceptibility in complex heterogeneous and/or polymicrobial samples.

4.5. General conclusions

The dissertation presents four projects for bacteria counting, identification, and susceptibility testing. Due to the compartmentalization of bacteria in tiny volume droplets, our methods and systems allow for precise bacteria counting over a broad dynamic range, simultaneous bacteria identification and quantification without genetic material extraction, and calibration curve preparation. Additionally, the dddPCR method is characterized by the reduced influence of background inhibitors on amplification. Our label-free detection approaches (based on scattered and native fluorescence intensities) allow for high-throughput analysis of various clinically critical bacterial species, which further significantly facilitated the analysis of complex bacterial samples, including polymicrobial samples and quantification of heteroresistant subpopulations in biofilms. We believe that our innovations bring new research possibilities in microbiology.

5. References

(1) Srivastava, S.; Srivastava, P. S.; Srivastava, S.; Srivastava, P. S. Cell Structure and Organization. In *Understanding Bacteria*; Springer Netherlands, 2003; pp 61–95. https://doi.org/10.1007/978-94-017-0129-7_4.

(2) Abbott, A. Scientists Bust Myth That Our Bodies Have More Bacteria than Human Cells. *Nature* **2016**. https://doi.org/10.1038/NATURE.2016.19136.

(3) Relman, D. A. Microbiology: Learning about Who We Are. *Nature*. Nature Publishing Group June 14, 2012, pp 194–195. https://doi.org/10.1038/486194a.

(4) Fleischmann, C.; Scherag, A.; Adhikari, N. K. J.; Hartog, C. S.; Tsaganos, T.; Schlattmann, P.; Angus, D. C.; Reinhart, K. Assessment of Global Incidence and Mortality of Hospital-Treated Sepsis Current Estimates and Limitations. *Am. J. Respir. Crit. Care Med.* **2016**, *193* (3), 259–272. https://doi.org/10.1164/rccm.201504-0781OC.

(5) Wen, Z.; Zhang, J. R. Bacterial Capsules. In *Molecular Medical Microbiology: Second Edition*; Elsevier Ltd, 2014; Vol. 1–3, pp 33–53. https://doi.org/10.1016/B978-0-12-397169-2.00003-2.

(6) Bruslind, L. General Microbiology. Oregon State University.

(7) Ferris, F. G.; Beveridge, T. J. Functions of Bacterial Cell Surface Structures. *Bioscience* **1985**, *35* (3), 172–177. https://doi.org/10.2307/1309867.

(8) Kapoor, G.; Saigal, S.; Elongavan, A. Action and Resistance Mechanisms of Antibiotics: A Guide for Clinicians. *Journal of Anaesthesiology Clinical Pharmacology*. Medknow Publications July 1, 2017, pp 300–305. https://doi.org/10.4103/joacp.JOACP_349_15.

(9) Laxminarayan, R.; Duse, A.; Wattal, C.; Zaidi, A. K. M.; Wertheim, H. F. L.; Sumpradit, N.; Vlieghe, E.; Hara, G. L.; Gould, I. M.; Goossens, H.; Greko, C.; So, A. D.; Bigdeli, M.; Tomson, G.; Woodhouse, W.; Ombaka, E.; Peralta, A. Q.; Qamar, F. N.; Mir, F.; Kariuki, S.; Bhutta, Z. A.; Coates, A.; Bergstrom, R.; Wright, G. D.; Brown, E. D.; Cars, O. Antibiotic Resistance-the Need for Global Solutions. *The Lancet Infectious Diseases*. Elsevier December 1, 2013, pp 1057–1098. https://doi.org/10.1016/S1473-3099(13)70318-9.

(10) Wright, G. D. Molecular Mechanisms of Antibiotic Resistance. *Chem. Commun.* **2011**, *47* (14), 4055–4061. https://doi.org/10.1039/c0cc05111j.

(11) Blair, J. M. A.; Webber, M. A.; Baylay, A. J.; Ogbolu, D. O.; Piddock, L. J. V.

Molecular Mechanisms of Antibiotic Resistance. *Nature Reviews Microbiology*. Nature Publishing Group January 11, 2015, pp 42–51. https://doi.org/10.1038/nrmicro3380.

(12) Munita, J. M.; Arias, C. A. Mechanisms of Antibiotic Resistance. *Microbiol. Spectr.* **2016**, *4* (2), 10.1128/microbiolspec.VMBF-0016–2015. https://doi.org/10.1128/microbiolspec.VMBF-0016-2015.

(13) Andrews, J. M. Determination of Minimum Inhibitory Concentrations. *J. Antimicrob. Chemother*. **2001**, *48* (SUPPL. 1), 5–16. https://doi.org/10.1093/jac/48.suppl_1.5.

(14) Wiegand, I.; Hilpert, K.; Hancock, R. E. W. Agar and Broth Dilution Methods to Determine the Minimal Inhibitory Concentration (MIC) of Antimicrobial Substances. *Nat. Protoc.* **2008**, *3* (2), 163–175. https://doi.org/10.1038/nprot.2007.521.

(15) van Belkum, A.; Burnham, C. A. D.; Rossen, J. W. A.; Mallard, F.; Rochas, O.; Dunne, W. M. Innovative and Rapid Antimicrobial Susceptibility Testing Systems. *Nature Reviews Microbiology*. Nature Research May 1, 2020, pp 299–311. https://doi.org/10.1038/s41579-020-0327-x.

(16) Andersson, D. I.; Nicoloff, H.; Hjort, K. Mechanisms and Clinical Relevance of Bacterial Heteroresistance. *Nat. Rev. Microbiol. 2019 178* **2019**, *17* (8), 479–496. https://doi.org/10.1038/s41579-019-0218-1.

(17) Dewachter, L.; Fauvart, M.; Michiels, J. Bacterial Heterogeneity and Antibiotic Survival: Understanding and Combatting Persistence and Heteroresistance. *Mol. Cell* **2019**, *76* (2), 255–267. https://doi.org/10.1016/j.molcel.2019.09.028.

(18) OM, E.-H.; MA, V. Antimicrobial Heteroresistance: An Emerging Field in Need of Clarity. *Clin. Microbiol. Rev.* **2015**, *28* (1), 191–207. https://doi.org/10.1128/CMR.00058-14.

(19) VI, B.; EK, C.; BA, N.; CM, H.; GK, T.; K, V.; J, P.; TD, R.; SE, B.; MS, T.; EM, B.; DS, W. Antibiotic Failure Mediated by a Resistant Subpopulation in Enterobacter Cloacae. *Nat. Microbiol.* **2016**, *1* (6). https://doi.org/10.1038/NMICROBIOL.2016.53.

(20) VI, B.; SW, S.; EM, B.; MM, F.; JT, J.; DS, W. Carbapenem-Resistant Klebsiella Pneumoniae Exhibiting Clinically Undetected Colistin Heteroresistance Leads to Treatment Failure in a Murine Model of Infection. *MBio* **2018**, *9* (2). https://doi.org/10.1128/MBIO.02448-17.

(21) K, H.; H, N.; DI, A. Unstable Tandem Gene Amplification Generates Heteroresistance (Variation in Resistance within a Population) to Colistin in Salmonella Enterica. *Mol. Microbiol.* **2016**, *102* (2), 274–289. https://doi.org/10.1111/MMI.13459.

(22) McGann, P.; Courvalin, P.; Snesrud, E.; Clifford, R. J.; Yoon, E. J.; Onmus-Leone, F.;

Ong, A. C.; Kwak, Y. I.; Grillot-Courvalin, C.; Lesho, E.; Waterman, P. E. Amplification of Aminoglycoside Resistance Gene AphA1 in Acinetobacter Baumannii Results in Tobramycin Therapy Failure. *MBio* **2014**, *5* (2). https://doi.org/10.1128/MBIO.00915-14.

(23) Nicoloff, H.; Hjort, K.; Levin, B. R.; Andersson, D. I. The High Prevalence of Antibiotic Heteroresistance in Pathogenic Bacteria Is Mainly Caused by Gene Amplification. *Nat. Microbiol.* **2019**, *4* (3), 504–514. https://doi.org/10.1038/s41564-018-0342-0.

(24) Wong, S. S. Y.; Ho, P. L.; Woo, P. C. Y.; Yuen, K. Y. Bacteremia Caused by Staphylococci with Inducible Vancomycin Heteroresistance. *Clin. Infect. Dis.* **1999**, *29* (4), 760–767. https://doi.org/10.1086/520429.

(25) Claeys, K. C.; Lagnf, A. M.; Hallesy, J. A.; Compton, M. T.; Gravelin, A. L.; Davis, S. L.; Rybaka, M. J. Pneumonia Caused by Methicillin-Resistant Staphylococcus Aureus: Does Vancomycin Heteroresistance Matter? *Antimicrob. Agents Chemother.* **2016**, *60* (3), 1708–1716. https://doi.org/10.1128/AAC.02388-15.

(26) Maor, Y.; Hagin, M.; Belausov, N.; Keller, N.; Ben-David, D.; Rahav, G. Clinical Features of Heteroresistant Vancomycin-Intermediate Staphylococcus Aureus Bacteremia versus Those of Methicillin-Resistant S. Aureus Bacteremia. *J. Infect. Dis.* **2009**, *199* (5), 619–624. https://doi.org/10.1086/596629.

(27) Zhang, S.; Sun, X.; Chang, W.; Dai, Y.; Ma, X. Systematic Review and Meta-Analysis of the Epidemiology of Vancomycin-Intermediate and Heterogeneous Vancomycin-Intermediate Staphylococcus Aureus Isolates. *PLoS One* **2015**, *10* (8), e0136082. https://doi.org/10.1371/JOURNAL.PONE.0136082.

(28) Yau, W.; Owen, R. J.; Poudyal, A.; Bell, J. M.; Turnidge, J. D.; Yu, H. H.; Nation, R. L.; Li, J. Colistin Hetero-Resistance in Multidrug-Resistant Acinetobacter Baumannii Clinical Isolates from the Western Pacific Region in the SENTRY Antimicrobial Surveillance Programme. *J. Infect.* **2009**, *58* (2), 138–144. https://doi.org/10.1016/j.jinf.2008.11.002.

(29) Hermes, D. M.; Pitt, C. P.; Lutz, L.; Teixeira, A. B.; Ribeiro, V. B.; Netto, B.; Martins, A. F.; Zavascki, A. P.; Barth, A. L. Evaluation of Heteroresistance to Polymyxin B among Carbapenem-Susceptible and -Resistant Pseudomonas Aeruginosa. *J. Med. Microbiol.* **2013**, *62* (8), 1184–1189. https://doi.org/10.1099/JMM.0.059220-0.

(30) Sun, J. D.; Huang, S. F.; Yang, S. S.; Pu, S. L.; Zhang, C. M.; Zhang, L. P. Impact of Carbapenem Heteroresistance among Clinical Isolates of Invasive Escherichia Coli in

Chongqing, Southwestern China. *Clin. Microbiol. Infect.* **2015**, *21* (5), 469.e1-469.e10. https://doi.org/10.1016/j.cmi.2014.12.013.

(31) Silva, A. E. B. da; Martins, A. F.; Nodari, C. S.; Magagnin, C. M.; Barth, A. L. Carbapenem-Heteroresistance among Isolates of the Enterobacter Cloacae Complex: Is It a Real Concern? *Eur. J. Clin. Microbiol. Infect. Dis. 2017 371* **2017**, *37* (1), 185–186. https://doi.org/10.1007/S10096-017-3138-X.

(32) Peláez, T.; Cercenado, E.; Alcalá, L.; Marín, M.; Martín-López, A.; Martínez-Alarcón, J.; Catalán, P.; Sánchez-Somolinos, M.; Bouza, E. Metronidazole Resistance in Clostridium Difficile Is Heterogeneous. *J. Clin. Microbiol.* **2008**, *46* (9), 3028–3032. https://doi.org/10.1128/JCM.00524-08.

(33) Edwards, A. M. Phenotype Switching Is a Natural Consequence of Staphylococcus Aureus Replication. *J. Bacteriol.* **2012**, *194* (19), 5404–5412. https://doi.org/10.1128/JB.00948-12.

(34) Bigger, J. TREATMENT OF STAPHYLOCOCCAL INFECTIONS WITH PENICILLIN BY INTERMITTENT STERILISATION. *Lancet* **1944**, *244* (6320), 497–500. https://doi.org/10.1016/S0140-6736(00)74210-3.

(35) Vulin, C.; Leimer, N.; Huemer, M.; Ackermann, M.; Zinkernagel, A. S. Prolonged Bacterial Lag Time Results in Small Colony Variants That Represent a Sub-Population of Persisters. *Nat. Commun.* **2018**, *9* (1). https://doi.org/10.1038/s41467-018-06527-0.

(36) Conlon, B. P.; Rowe, S. E.; Gandt, A. B.; Nuxoll, A. S.; Donegan, N. P.; Zalis, E. A.; Clair, G.; Adkins, J. N.; Cheung, A. L.; Lewis, K. Persister Formation in Staphylococcus Aureus Is Associated with ATP Depletion. *Nat. Microbiol.* **2016**, *1* (5). https://doi.org/10.1038/nmicrobiol.2016.51.

(37) Zalis, E. A.; Nuxoll, A. S.; Manuse, S.; Clair, G.; Radlinski, L. C.; Conlon, B. P.; Adkins, J.; Lewis, K. Stochastic Variation in Expression of the Tricarboxylic Acid Cycle Produces Persister Cells. *MBio* **2019**, *10* (5). https://doi.org/10.1128/mBio.01930-19.

(38) Opota, O.; Jaton, K.; Greub, G. Microbial Diagnosis of Bloodstream Infection: Towards Molecular Diagnosis Directly from Blood. *Clinical Microbiology and Infection*. Elsevier April 1, 2015, pp 323–331. https://doi.org/10.1016/j.cmi.2015.02.005.

(39) A O, O.; J J, M.; S M, A.; M N, K.; Ouma, D. A Longitudinal Study of Milk Somatic Cell Counts and Bacterial Culture from Cows on Smallholder Dairy Farms in Kiambu District, Kenya. **1996**.

(40) Schmidt, H.; Eickhorst, T. Detection and Quantification of Native Microbial Populations on Soil-Grown Rice Roots by Catalyzed Reporter Deposition-Fluorescence in Situ Hybridization. https://doi.org/10.1111/1574-6941.12232.

(41) Campbell, J. High-Throughput Assessment of Bacterial Growth Inhibition by Optical Density Measurements. *Curr. Protoc. Chem. Biol.* **2010**, *2* (4), 195–208. https://doi.org/10.1002/9780470559277.ch100115.

(42) Shapiro, H. M. *Practical Flow Cytometry*; Wiley, 2003. https://doi.org/10.1002/0471722731.

(43) CLARKE, P. H.; COWAN, S. T. Biochemical Methods for Bacteriology. *J. Gen. Microbiol.* **1952**, *6* (1–2), 187–197. https://doi.org/10.1099/00221287-6-1-2-187.

(44) Schreckenberger, P. C.; Blazevic, D. J. Rapid Methods for Biochemical Testing of Anaerobic Bacteria. *Appl. Microbiol.* **1974**, *28* (5), 759–762. https://doi.org/10.1128/aem.28.5.759-762.1974.

(45) Sauget, M.; Valot, B.; Bertrand, X.; Hocquet, D. Can MALDI-TOF Mass Spectrometry Reasonably Type Bacteria? *Trends in Microbiology*. Elsevier Ltd June 1, 2017, pp 447–455. https://doi.org/10.1016/j.tim.2016.12.006.

(46) O, S.; B, G.; A, K. Nucleic Acid Detection Technologies and Marker Molecules in Bacterial Diagnostics. *Expert Rev. Mol. Diagn.* **2014**, *14* (4), 489–500. https://doi.org/10.1586/14737159.2014.908710.

(47) Sandle, T. Microbial Identification. In *Pharmaceutical Microbiology*; Elsevier, 2016; pp 103–113. https://doi.org/10.1016/b978-0-08-100022-9.00009-8.

(48) Váradi, L.; Luo, J. L.; Hibbs, D. E.; Perry, J. D.; Anderson, R. J.; Orenga, S.; Groundwater, P. W. Methods for the Detection and Identification of Pathogenic Bacteria: Past, Present, and Future. *Chemical Society Reviews*. Royal Society of Chemistry August 21, 2017, pp 4818–4832. https://doi.org/10.1039/c6cs00693k.

(49) Li, J.; Shi, X.; Yin, W.; Wang, Y.; Shen, Z.; Ding, S.; Wang, S. A Multiplex SYBR Green Real-Time PCR Assay for the Detection of Three Colistin Resistance Genes from Cultured Bacteria, Feces, and Environment Samples. *Front. Microbiol.* **2017**, *8* (OCT), 2078. https://doi.org/10.3389/fmicb.2017.02078.

(50) Chen, X.; Lu, L.; Xiong, X.; Xiong, X.; Liu, Y. Development of a Real-Time PCR Assay for the Identification and Quantification of Bovine Ingredient in Processed Meat Products. *Sci. Rep.* **2020**, *10* (1), 1–10. https://doi.org/10.1038/s41598-020-59010-6.

(51) Laxminarayan, R.; Duse, A.; Wattal, C.; Zaidi, A. K. M.; Wertheim, H. F. L.; Sumpradit, N.; Vlieghe, E.; Hara, G. L.; Gould, I. M.; Goossens, H.; Greko, C.; So, A.

D.; Bigdeli, M.; Tomson, G.; Woodhouse, W.; Ombaka, E.; Peralta, A. Q.; Qamar, F. N.; Mir, F.; Kariuki, S.; Bhutta, Z. A.; Coates, A.; Bergstrom, R.; Wright, G. D.; Brown, E. D.; Cars, O. Antibiotic Resistance-the Need for Global Solutions. *The Lancet Infectious Diseases*. December 2013, pp 1057–1098. https://doi.org/10.1016/S1473-3099(13)70318-9.

(52) Barenfanger, J.; Drake, C.; Kacich, G. Clinical and Financial Benefits of Rapid Bacterial Identification and Antimicrobial Susceptibility Testing. *J. Clin. Microbiol.* **1999**, *37* (5), 1415–1418. https://doi.org/10.1128/jcm.37.5.1415-1418.1999.

(53) Reller, L. B.; Weinstein, M.; Jorgensen, J. H.; Ferraro, M. J. Antimicrobial Susceptibility Testing: A Review of General Principles and Contemporary Practices. *Clin. Infect. Dis.* **2009**, *49* (11), 1749–1755. https://doi.org/10.1086/647952.

(54) Stalons, D. R.; Thornsberry, C. *Broth-Dilution Method for Determining the Antibiotic Susceptibility of Anaerobic Bacteria*; 1975; Vol. 7.

(55) Fiebelkorn, K. R.; Crawford, S. A.; Mcelmeel, M. L.; Jorgensen, J. H. Practical Disk Diffusion Method for Detection of Inducible Clindamycin Resistance in Staphylococcus Aureus and Coagulase-Negative Staphylococci Downloaded From. *J. Clin. Microbiol.* **2003**, *41* (10), 4740–4744. https://doi.org/10.1128/JCM.41.10.4740-4744.2003.

(56) Balouiri, M.; Sadiki, M.; Ibnsouda, S. K. Methods for in Vitro Evaluating Antimicrobial Activity: A Review. *J. Pharm. Anal.* **2016**. https://doi.org/10.1016/j.jpha.2015.11.005.

(57) Jorgensen, J. H.; Ferraro, M. J. Antimicrobial Susceptibility Testing: A Review of General Principles and Contemporary Practices. *Clin. Infect. Dis.* **2009**. https://doi.org/10.1086/647952.

(58) Livermore, D. M.; Brown, D. F. J. Detection of β-Lactamase-Mediated Resistance. *J. Antimicrob. Chemother.* **2001**, *48* (SUPPL. 1), 59–64. https://doi.org/10.1093/jac/48.suppl_1.59.

(59) Jorgensen, J. H.; Barry, A. L.; Traczewski, M. M.; Sahm, D. F.; McElmeel, M. L.; Crawford, S. A. Rapid Automated Antimicrobial Susceptibility Testing of Streptococcus Pneumoniae by Use of the BioMerieux VITEK 2. *J. Clin. Microbiol.* **2000**, *38* (8), 2814–2818. https://doi.org/10.1128/jcm.38.8.2814-2818.2000.

(60) Alexander, H. E.; Leidy, G. MODE OF ACTION OF STREPTOMYCIN ON TYPE b H. INFLUENZAE I. ORIGIN OF RESISTANT ORGANISMS. *J. Exp. Med.* **1947**, *85* (4), 329–338. https://doi.org/10.1084/JEM.85.4.329.

(61) KI, U.; N, P.; P, A.; F, B.; BR, L. Functional Relationship between Bacterial Cell Density and the Efficacy of Antibiotics. *J. Antimicrob. Chemother.* **2009**, *63* (4), 745–757. https://doi.org/10.1093/JAC/DKN554.

(62) Tuchscherr, L.; Bischoff, M.; Lattar, S. M.; Noto Llana, M.; Pförtner, H.; Niemann, S.; Geraci, J.; Van de Vyver, H.; Fraunholz, M. J.; Cheung, A. L.; Herrmann, M.; Völker, U.; Sordelli, D. O.; Peters, G.; Löffler, B. Sigma Factor SigB Is Crucial to Mediate Staphylococcus Aureus Adaptation during Chronic Infections. *PLoS Pathog.* **2015**, *11* (4). https://doi.org/10.1371/journal.ppat.1004870.

(63) Davis, K. M.; Isberg, R. R. Defining Heterogeneity within Bacterial Populations via Single Cell Approaches. *BioEssays* **2016**, *38* (8), 782–790. https://doi.org/10.1002/bies.201500121.

(64) Hassan, M. M.; Butler, M. S.; Ranzoni, A.; Cooper, M. A. Detection and Quantification of the Heterogeneity of S. Aureus Bacterial Populations to Identify Antibiotic-Induced Persistence 2. https://doi.org/10.1101/320093.

(65) Manina, G.; Dhar, N.; McKinney, J. D. Stress and Host Immunity Amplify Mycobacterium Tuberculosis Phenotypic Heterogeneity and Induce Nongrowing Metabolically Active Forms. *Cell Host Microbe* **2015**, *17* (1), 32–46. https://doi.org/10.1016/j.chom.2014.11.016.

(66) Roostalu, J.; Jõers, A.; Luidalepp, H.; Kaldalu, N.; Tenson, T. Cell Division in Escherichia Coli Cultures Monitored at Single Cell Resolution. **2008**. https://doi.org/10.1186/1471-2180-8-68.

(67) Helaine, S.; Thompson, J. A.; Watson, K. G.; Liu, M.; Boyle, C.; Holden, D. W. Dynamics of Intracellular Bacterial Replication at the Single Cell Level. *Proc. Natl. Acad. Sci. U. S. A.* **2010**, *107* (8), 3746–3751. https://doi.org/10.1073/pnas.1000041107.

(68) Terskikh, A.; Fradkov, A.; Ermakova, G.; Zaraisky, A.; Tan, P.; Kajava, A. V.; Zhao, X.; Lukyanov, S.; Matz, M.; Kim, S.; Weissman, I.; Siebert, P. "Fluorescent Timer": Protein That Changes Color with Time. *Science (80-.).* **2000**, *290* (5496), 1585–1588. https://doi.org/10.1126/science.290.5496.1585.

(69) Verkhusha, V. V.; Otsuna, H.; Awasaki, T.; Oda, H.; Tsukita, S.; Ito, K. An Enhanced Mutant of Red Fluorescent Protein DsRed for Double Labeling and Developmental Timer of Neural Fiber Bundle Formation. *J. Biol. Chem.* **2001**, *276* (32), 29621–29624. https://doi.org/10.1074/jbc.C100200200.

(70) Claudi, B.; Spröte, P.; Chirkova, A.; Personnic, N.; Zankl, J.; Schürmann, N.; Schmidt,

A.; Bumann, D. Phenotypic Variation of Salmonella in Host Tissues Delays Eradication by Antimicrobial Chemotherapy. *Cell* **2014**, *158* (4), 722–733. https://doi.org/10.1016/j.cell.2014.06.045.

(71) Abou-Hassan, A.; Sandre, O.; Cabuil, V. Microfluidics in Inorganic Chemistry. *Angewandte Chemie - International Edition*. John Wiley & Sons, Ltd August 23, 2010, pp 6268–6286. https://doi.org/10.1002/anie.200904285.

(72) Sackmann, E. K.; Fulton, A. L.; Beebe, D. J. The Present and Future Role of Microfluidics in Biomedical Research. *Nature*. Nature Publishing Group March 12, 2014, pp 181–189. https://doi.org/10.1038/nature13118.

(73) Schneider, T.; Kreutz, J.; Chiu, D. T. The Potential Impact of Droplet Microfluidics in Biology. *Analytical Chemistry*. American Chemical Society April 2, 2013, pp 3476–3482. https://doi.org/10.1021/ac400257c.

(74) Manz, A.; Graber, N.; Widmer, H. M. Miniaturized Total Chemical Analysis Systems: A Novel Concept for Chemical Sensing. *Sensors Actuators B. Chem.* **1990**, *1* (1–6), 244–248. https://doi.org/10.1016/0925-4005(90)80209-I.

(75) Reyes, D. R.; Iossifidis, D.; Auroux, P. A.; Manz, A. Micro Total Analysis Systems. 1. Introduction, Theory, and Technology. *Analytical Chemistry*. American Chemical Society June 15, 2002, pp 2623–2636. https://doi.org/10.1021/ac0202435.

(76) Anna, S. L.; Bontoux, N.; Stone, H. A. Formation of Dispersions Using “Flow Focusing” in Microchannels. *Appl. Phys. Lett.* **2003**, *82* (3), 364–366. https://doi.org/10.1063/1.1537519.

(77) Walker, G. M.; Beebe, D. J. A Passive Pumping Method for Microfluidic Devices. *Lab Chip* **2002**, *2* (3), 131–134. https://doi.org/10.1039/b204381e.

(78) Berry, S. M.; MacCoux, L. J.; Beebe, D. J. Streamlining Immunoassays with Immiscible Filtrations Assisted by Surface Tension. *Anal. Chem.* **2012**, *84* (13), 5518–5523. https://doi.org/10.1021/ac300085m.

(79) Lee, S. H.; Helnz, A. J.; Shln, S.; Jung, Y. G.; Chol, S. E.; Park, W.; Roe, J. H.; Kwon, S. Capillary Based Patterning of Cellular Communities in Laterally Open Channels. *Anal. Chem.* **2010**, *82* (7), 2900–2906. https://doi.org/10.1021/ac902903q.

(80) Zhang, C.; Xing, D.; Li, Y. Micropumps, Microvalves, and Micromixers within PCR Microfluidic Chips: Advances and Trends. **2007**. https://doi.org/10.1016/j.biotechadv.2007.05.003.

(81) Harrison, D. J.; Fluri, K.; Seiler, K.; Fan, Z.; Effenhauser, C. S.; Manz, A. Micromachining a Miniaturized Capillary Electrophoresis-Based Chemical Analysis

System on a Chip. *Science (80-.).* **1993**, *261* (5123), 895–897. https://doi.org/10.1126/science.261.5123.895.

(82) Persat, A.; Suss, M. E.; Santiago, J. G. Basic Principles of Electrolyte Chemistry for Microfluidic Electrokinetics. Part II: Coupling between Ion Mobility, Electrolysis, and Acid-Base Equilibria. *Lab on a Chip*. Royal Society of Chemistry September 7, 2009, pp 2454–2469. https://doi.org/10.1039/b906468k.

(83) Persat, A.; Chambers, R. D.; Santiago, J. G. Basic Principles of Electrolyte Chemistry for Microfluidic Electrokinetics. Part I: Acid-Base Equilibria and PH Buffers. *Lab on a Chip*. Royal Society of Chemistry September 7, 2009, pp 2437–2453. https://doi.org/10.1039/b906465f.

(84) Wang, H.; Liu, Z.; Shin, D. M.; Chen, Z. G.; Cho, Y.; Kim, Y. J.; Han, A. A Continuous-Flow Acoustofluidic Cytometer for Single-Cell Mechanotyping. *Lab Chip* **2019**, *19* (3), 387–393. https://doi.org/10.1039/c8lc00711j.

(85) Ottesen, E. A.; Jong, W. H.; Quake, S. R.; Leadbetter, J. R. Microfluidic Digital PCR Enables Multigene Analysis of Individual Environmental Bacteria. *Science (80-.).* **2006**, *314* (5804), 1464–1467. https://doi.org/10.1126/science.1131370.

(86) Obeid, P. J.; Christopoulos, T. K. Continuous-Flow DNA and RNA Amplification Chip Combined with Laser-Induced Fluorescence Detection. *Anal. Chim. Acta* **2003**, *494* (1–2), 1–9. https://doi.org/10.1016/S0003-2670(03)00898-5.

(87) Dalerba, P.; Kalisky, T.; Sahoo, D.; Rajendran, P. S.; Rothenberg, M. E.; Leyrat, A. A.; Sim, S.; Okamoto, J.; Johnston, D. M.; Qian, D.; Zabala, M.; Bueno, J.; Neff, N. F.; Wang, J.; Shelton, A. A.; Visser, B.; Hisamori, S.; Shimono, Y.; Van De Wetering, M.; Clevers, H.; Clarke, M. F.; Quake, S. R. Single-Cell Dissection of Transcriptional Heterogeneity in Human Colon Tumors. *Nat. Biotechnol.* **2011**, *29* (12), 1120–1127. https://doi.org/10.1038/nbt.2038.

(88) Jammes, F. C.; Maerkl, S. J. How Single-Cell Immunology Is Benefiting from Microfluidic Technologies. *Microsystems and Nanoengineering*. Springer Nature December 1, 2020, pp 1–14. https://doi.org/10.1038/s41378-020-0140-8.

(89) Zenobi, R. Single-Cell Metabolomics: Analytical and Biological Perspectives. *Science*. December 6, 2013, pp 1243259–1243259. https://doi.org/10.1126/science.1243259.

(90) Hansen, C. L.; Skordalakest, E.; Berger, J. M.; Quake, S. R. A Robust and Scalable Microfluidic Metering Method That Allows Protein Crystal Growth by Free Interface Diffusion. *Proc. Natl. Acad. Sci. U. S. A.* **2002**, *99* (26), 16531–16536. https://doi.org/10.1073/pnas.262485199.

(91) Hansen, C.; Quake, S. R. Microfluidics in Structural Biology: Smaller, Faster... Better. *Current Opinion in Structural Biology*. Elsevier Ltd October 1, 2003, pp 538–544. https://doi.org/10.1016/j.sbi.2003.09.010.

(92) Mo, Y.; Lu, Z.; Rughoobur, G.; Patil, P.; Gershenfeld, N.; Akinwande, A. I.; Buchwald, S. L.; Jensen, K. F. Microfluidic Electrochemistry for Single-Electron Transfer Redox-Neutral Reactions. *Science (80-.).* **2020**, *368* (6497), 1352–1357. https://doi.org/10.1126/science.aba3823.

(93) Mulholland, T.; McAllister, M.; Patek, S.; Flint, D.; Underwood, M.; Sim, A.; Edwards, J.; Zagnoni, M. Drug Screening of Biopsy-Derived Spheroids Using a Self-Generated Microfluidic Concentration Gradient. *Sci. Rep.* **2018**, *8* (1), 14672. https://doi.org/10.1038/s41598-018-33055-0.

(94) Toh, Y. C.; Lim, T. C.; Tai, D.; Xiao, G.; Van Noort, D.; Yu, H. A Microfluidic 3D Hepatocyte Chip for Drug Toxicity Testing. *Lab Chip* **2009**, *9* (14), 2026–2035. https://doi.org/10.1039/b900912d.

(95) Squires, T. M.; Quake, S. R. Microfluidics: Fluid Physics at the Nanoliter Scale. *Rev. Mod. Phys.* **2005**, *77* (3), 977–1026. https://doi.org/10.1103/RevModPhys.77.977.

(96) Teh, S. Y.; Lin, R.; Hung, L. H.; Lee, A. P. Droplet Microfluidics. *Lab on a Chip*. Royal Society of Chemistry January 29, 2008, pp 198–220. https://doi.org/10.1039/b715524g.

(97) Baroud, C. N.; Gallaire, F.; Dangla, R. Dynamics of Microfluidic Droplets. *Lab on a Chip*. Royal Society of Chemistry August 21, 2010, pp 2032–2045. https://doi.org/10.1039/c001191f.

(98) Mashaghi, S.; Abbaspourrad, A.; Weitz, D. A.; van Oijen, A. M. Droplet Microfluidics: A Tool for Biology, Chemistry and Nanotechnology. *TrAC - Trends in Analytical Chemistry*. Elsevier B.V. September 1, 2016, pp 118–125. https://doi.org/10.1016/j.trac.2016.05.019.

(99) Zec, H.; Shin, D. J.; Wang, T. H. Novel Droplet Platforms for the Detection of Disease Biomarkers. *Expert Rev. Mol. Diagn.* **2014**, *14* (7), 787–801. https://doi.org/10.1586/14737159.2014.945437.

(100) Hung, L. Y.; Wang, C. H.; Fu, C. Y.; Gopinathan, P.; Lee, G. Bin. Microfluidics in the Selection of Affinity Reagents for the Detection of Cancer: Paving a Way towards Future Diagnostics. *Lab on a Chip*. Royal Society of Chemistry July 19, 2016, pp 2759–2774. https://doi.org/10.1039/c6lc00662k.

(101) Shembekar, N.; Chaipan, C.; Utharala, R.; Merten, C. A. Droplet-Based Microfluidics

in Drug Discovery, Transcriptomics and High-Throughput Molecular Genetics. *Lab on a Chip*. Royal Society of Chemistry April 21, 2016, pp 1314–1331. https://doi.org/10.1039/c6lc00249h.

(102) Neužil, P.; Giselbrecht, S.; Länge, K.; Huang, T. J.; Manz, A. Revisiting Lab-on-a-Chip Technology for Drug Discovery. *Nature Reviews Drug Discovery*. Nature Publishing Group August 1, 2012, pp 620–632. https://doi.org/10.1038/nrd3799.

(103) Basova, E. Y. u.; Foret, F. Droplet Microfluidics in (Bio)Chemical Analysis. *The Analyst*. Royal Society of Chemistry January 7, 2015, pp 22–38. https://doi.org/10.1039/c4an01209g.

(104) Song, H.; Chen, D. L.; Ismagilov, R. F. Reactions in Droplets in Microfluidic Channels. *Angewandte Chemie - International Edition*. Angew Chem Int Ed Engl November 13, 2006, pp 7336–7356. https://doi.org/10.1002/anie.200601554.

(105) Theberge, A. B.; Courtois, F.; Schaerli, Y.; Fischlechner, M.; Abell, C.; Hollfelder, F.; Huck, W. T. S. Microdroplets in Microfluidics: An Evolving Platform for Discoveries in Chemistry and Biology. *Angewandte Chemie - International Edition*. John Wiley & Sons, Ltd August 9, 2010, pp 5846–5868. https://doi.org/10.1002/anie.200906653.

(106) Zhu, P.; Wang, L. Passive and Active Droplet Generation with Microfluidics: A Review. *Lab Chip* **2017**, *17* (1), 34–75. https://doi.org/10.1039/C6LC01018K.

(107) Shang, L.; Cheng, Y.; Zhao, Y. Emerging Droplet Microfluidics. *Chemical Reviews*. American Chemical Society June 28, 2017, pp 7964–8040. https://doi.org/10.1021/acs.chemrev.6b00848.

(108) Amstad, E.; Chemama, M.; Eggersdorfer, M.; Arriaga, L. R.; Brenner, M. P.; Weitz, D. A. Robust Scalable High Throughput Production of Monodisperse Drops. *Lab Chip* **2016**, *16* (21), 4163–4172. https://doi.org/10.1039/c6lc01075j.

(109) Conchouso, D.; Castro, D.; Khan, S. A.; Foulds, I. G. Three-Dimensional Parallelization of Microfluidic Droplet Generators for a Litre per Hour Volume Production of Single Emulsions. *Lab Chip* **2014**, *14* (16), 3011–3020. https://doi.org/10.1039/c4lc00379a.

(110) Nisisako, T.; Torii, T. Microfluidic Large-Scale Integration on a Chip for Mass Production of Monodisperse Droplets and Particles. *Lab Chip* **2008**, *8* (2), 287–293. https://doi.org/10.1039/b713141k.

(111) Yadavali, S.; Jeong, H. H.; Lee, D.; Issadore, D. Silicon and Glass Very Large Scale Microfluidic Droplet Integration for Terascale Generation of Polymer Microparticles. *Nat. Commun.* **2018**, *9* (1), 1–9. https://doi.org/10.1038/s41467-018-03515-2.

(112) Thorsen, T.; Roberts, R. W.; Arnold, F. H.; Quake, S. R. Dynamic Pattern Formation in a Vesicle-Generating Microfluidic Device. *Phys. Rev. Lett.* **2001**, *86* (18), 4163–4166. https://doi.org/10.1103/PhysRevLett.86.4163.

(113) Cramer, C.; Fischer, P.; Windhab, E. J. Drop Formation in a Co-Flowing Ambient Fluid. *Chem. Eng. Sci.* **2004**, *59* (15), 3045–3058. https://doi.org/10.1016/j.ces.2004.04.006.

(114) Nisisako, T.; Torii, T.; Higuchi, T. Droplet Formation in a Microchannel Network. In *Lab on a Chip*; Royal Society of Chemistry, 2002; Vol. 2, pp 24–26. https://doi.org/10.1039/b108740c.

(115) Christopher, G. F.; Noharuddin, N. N.; Taylor, J. A.; Anna, S. L. Experimental Observations of the Squeezing-to-Dripping Transition in T-Shaped Microfluidic Junctions. *Phys. Rev. E - Stat. Nonlinear, Soft Matter Phys.* **2008**, *78* (3), 036317. https://doi.org/10.1103/PhysRevE.78.036317.

(116) Garstecki, P.; Fuerstman, M. J.; Stone, H. A.; Whitesides, G. M. Formation of Droplets and Bubbles in a Microfluidic T-Junction - Scaling and Mechanism of Break-Up. *Lab Chip* **2006**, *6* (3), 437–446. https://doi.org/10.1039/b510841a.

(117) Dollet, B.; Van Hoeve, W.; Raven, J. P.; Marmottant, P.; Versluis, M. Role of the Channel Geometry on the Bubble Pinch-off in Flow-Focusing Devices. *Phys. Rev. Lett.* **2008**, *100* (3), 034504. https://doi.org/10.1103/PhysRevLett.100.034504.

(118) Nie, Z.; Seo, M. S.; Xu, S.; Lewis, P. C.; Mok, M.; Kumacheva, E.; Whitesides, G. M.; Garstecki, P.; Stone, H. A. Emulsification in a Microfluidic Flow-Focusing Device: Effect of the Viscosities of the Liquids. *Microfluid. Nanofluidics* **2008**, *5* (5), 585–594. https://doi.org/10.1007/s10404-008-0271-y.

(119) Collins, D. J.; Neild, A.; deMello, A.; Liu, A. Q.; Ai, Y. The Poisson Distribution and beyond: Methods for Microfluidic Droplet Production and Single Cell Encapsulation. *Lab on a Chip*. Royal Society of Chemistry July 21, 2015, pp 3439–3459. https://doi.org/10.1039/c5lc00614g.

(120) Zhou, J.; Ellis, A. V.; Voelcker, N. H. Recent Developments in PDMS Surface Modification for Microfluidic Devices. *Electrophoresis*. John Wiley & Sons, Ltd January 1, 2010, pp 2–16. https://doi.org/10.1002/elps.200900475.

(121) Commons, S.; Mongersun, A.; Smeenk, I.; Pratx, G.; Asuri, P.; Abbyad, P. Droplet Microfluidic Platform for the Determination of Single-Cell Lactate Release Recommended Citation. **2016**. https://doi.org/10.1021/acs.analchem.5b04681.

(122) Pan, C. W.; Horvath, D. G.; Braza, S.; Moore, T.; Lynch, A.; Feit, C.; Abbyad, P. Lab

on a Chip Lab on a Chip Sorting by Interfacial Tension (SIFT): Label-Free Selection of Live Cells Based on Single-Cell Metabolism †. *Lab Chip* **2019**, *19*, 1344. https://doi.org/10.1039/c8lc01328d.

(123) Bibette, ’ ’, J.; Morse, D. C.; Witten, T. A.; Weitz ’, D. A. *Stability Criteria for Emulsions*; 1992; Vol. 69.

(124) Dai, B.; Leal, L. G. The Mechanism of Surfactant Effects on Drop Coalescence. In *Physics of Fluids*; American Institute of Physics Inc., 2008; Vol. 20, p 040802. https://doi.org/10.1063/1.2911700.

(125) Agresti, J. J.; Antipov, E.; Abate, A. R.; Ahn, K.; Rowat, A. C.; Baret, J. C.; Marquez, M.; Klibanov, A. M.; Griffiths, A. D.; Weitz, D. A. Ultrahigh-Throughput Screening in Drop-Based Microfluidics for Directed Evolution. *Proc. Natl. Acad. Sci. U. S. A.* **2010**, *107* (9), 4004–4009. https://doi.org/10.1073/pnas.0910781107.

(126) Baret, J. C.; Beck, Y.; Billas-Massobrio, I.; Moras, D.; Griffiths, A. D. Quantitative Cell-Based Reporter Gene Assays Using Droplet-Based Microfluidics. *Chem. Biol.* **2010**, *17* (5), 528–536. https://doi.org/10.1016/j.chembiol.2010.04.010.

(127) Pekin, D.; Skhiri, Y.; Baret, J. C.; Le Corre, D.; Mazutis, L.; Ben Salem, C.; Millot, F.; El Harrak, A.; Hutchison, J. B.; Larson, J. W.; Link, D. R.; Laurent-Puig, P.; Griffiths, A. D.; Taly, V. Quantitative and Sensitive Detection of Rare Mutations Using Droplet-Based Microfluidics. *Lab Chip* **2011**, *11* (13), 2156–2166. https://doi.org/10.1039/c1lc20128j.

(128) Marcoux, P. R.; Dupoy, M.; Mathey, R.; Novelli-Rousseau, A.; Heran, V.; Morales, S.; Rivera, F.; Joly, P. L.; Moy, J. P.; Mallard, F. Micro-Confinement of Bacteria into w/o Emulsion Droplets for Rapid Detection and Enumeration. *Colloids Surfaces A Physicochem. Eng. Asp.* **2011**, *377* (1–3), 54–62. https://doi.org/10.1016/j.colsurfa.2010.12.013.

(129) Baret, J. C. Surfactants in Droplet-Based Microfluidics. *Lab on a Chip*. Royal Society of Chemistry February 7, 2012, pp 422–433. https://doi.org/10.1039/c1lc20582j.

(130) Bibette, J.; Calderon, F. L.; Poulin, P. *Emulsions: Basic Principles*; 1999; Vol. 62.

(131) Taylor, P. Ostwald Ripening in Emulsions. *Colloids Surfaces A Physicochem. Eng. Asp.* **1995**, *99* (2–3), 175–185. https://doi.org/10.1016/0927-7757(95)03161-6.

(132) Kaminski, T. S.; Scheler, O.; Garstecki, P. Droplet Microfluidics for Microbiology: Techniques, Applications and Challenges. *Lab Chip* **2016**, *16* (12), 2168–2187. https://doi.org/10.1039/c6lc00367b.

(133) Jiang, L.; Boitard, L.; Broyer, P.; Chareire, A. C.; Bourne-Branchu, P.; Mahé, P.;

Tournoud, M.; Franceschi, C.; Zambardi, G.; Baudry, J.; Bibette, J. Digital Antimicrobial Susceptibility Testing Using the MilliDrop Technology. *Eur. J. Clin. Microbiol. Infect. Dis.* **2016**. https://doi.org/10.1007/s10096-015-2554-z.

(134) Damodaran, S. P.; Eberhard, S.; Boitard, L.; Rodriguez, J. G.; Wang, Y.; Bremond, N.; Baudry, J.; Bibette, J.; Wollman, F.-A. A Millifluidic Study of Cell-to-Cell Heterogeneity in Growth-Rate and Cell-Division Capability in Populations of Isogenic Cells of Chlamydomonas Reinhardtii. *PLoS One* **2015**, *10* (3), e0118987. https://doi.org/10.1371/journal.pone.0118987.

(135) Jakiela, S.; Kaminski, T. S.; Cybulski, O.; Weibel, D. B.; Garstecki, P. Bacterial Growth and Adaptation in Microdroplet Chemostats. *Angew. Chemie* **2013**, *125* (34), 9076–9079. https://doi.org/10.1002/ange.201301524.

(136) Kehe, J.; Kulesa, A.; Ortiz, A.; Ackerman, C. M.; Thakku, S. G.; Sellers, D.; Kuehn, S.; Gore, J.; Friedman, J.; Blainey, P. C. Massively Parallel Screening of Synthetic Microbial Communities. *Proc. Natl. Acad. Sci. U. S. A.* **2019**, *116* (26), 12804–12809. https://doi.org/10.1073/pnas.1900102116.

(137) Terekhov, S. S.; Smirnov, I. V.; Stepanova, A. V.; Bobik, T. V.; Mokrushina, Y. A.; Ponomarenko, N. A.; Belogurov, A. A.; Rubtsova, M. P.; Kartseva, O. V.; Gomzikova, M. O.; Moskovtsev, A. A.; Bukatin, A. S.; Dubina, M. V.; Kostryukova, E. S.; Babenko, V. V.; Vakhitova, M. T.; Manolov, A. I.; Malakhova, M. V.; Kornienko, M. A.; Tyakht, A. V.; Vanyushkina, A. A.; Ilina, E. N.; Masson, P.; Gabibov, A. G.; Altman, S. Microfluidic Droplet Platform for Ultrahigh-Throughput Single-Cell Screening of Biodiversity. *Proc. Natl. Acad. Sci. U. S. A.* **2017**, *114* (10), 2550–2555. https://doi.org/10.1073/pnas.1621226114.

(138) Boedicker, J. Q.; Li, L.; Kline, T. R.; Ismagilov, R. F. Detecting Bacteria and Determining Their Susceptibility to Antibiotics by Stochastic Confinement in Nanoliter Droplets Using Plug-Based Microfluidics. *Lab Chip* **2008**. https://doi.org/10.1039/b804911d.

(139) Scheler, O.; Kaminski, T. S.; Ruszczak, A.; Garstecki, P. Dodecylresorufin (C12R) Outperforms Resorufin in Microdroplet Bacterial Assays. *ACS Appl. Mater. Interfaces* **2016**, *8* (18), 11318–11325. https://doi.org/10.1021/acsami.6b02360.

(140) Courtois, F.; Olguin, L. F.; Whyte, G.; Theberge, A. B.; Huck, W. T. S.; Hollfelder, F.; Abell, C. Controlling the Retention of Small Molecules in Emulsion Microdroplets for Use in Cell-Based Assays. *Anal. Chem.* **2009**, *81* (8), 3008–3016. https://doi.org/10.1021/ac802658n.

(141) Chen, Y.; Wijaya Gani, A.; Tang, S. K. Y. Characterization of Sensitivity and Specificity in Leaky Droplet-Based Assays. *Lab Chip* **2012**, *12* (23), 5093–5103. https://doi.org/10.1039/c2lc40624a.

(142) Stapleton, J. A.; Swartz, J. R. Development of an In Vitro Compartmentalization Screen for High-Throughput Directed Evolution of [FeFe] Hydrogenases. *PLoS One* **2010**, *5* (12), e15275. https://doi.org/10.1371/journal.pone.0015275.

(143) Baret, J. C.; Miller, O. J.; Taly, V.; Ryckelynck, M.; El-Harrak, A.; Frenz, L.; Rick, C.; Samuels, M. L.; Hutchison, J. B.; Agresti, J. J.; Link, D. R.; Weitz, D. A.; Griffiths, A. D. Fluorescence-Activated Droplet Sorting (FADS): Efficient Microfluidic Cell Sorting Based on Enzymatic Activity. *Lab Chip* **2009**, *9* (13), 1850–1858. https://doi.org/10.1039/b902504a.

(144) Najah, M.; Griffiths, A. D.; Ryckelynck, M. Teaching Single-Cell Digital Analysis Using Droplet-Based Microfluidics. *Anal. Chem.* **2012**, *84* (3), 1202–1209. https://doi.org/10.1021/ac202645m.

(145) Scheler, O.; Pacocha, N.; Debski, P. R.; Ruszczak, A.; Kaminski, T. S.; Garstecki, P. Lab on a Chip Optimized Droplet Digital CFU Assay (DdCFU) Provides Precise Quantification of Bacteria over a Dynamic Range of 6 Logs and beyond †. **2017**, *17*. https://doi.org/10.1039/c7lc00206h.

(146) Martin, K.; Henkel, T.; Baier, V.; Grodrian, A.; Schön, T.; Roth, M.; Köhler, J. M.; Metze, J. Generation of Larger Numbers of Separated Microbial Populations by Cultivation in Segmented-Flow Microdevices. *Lab Chip* **2003**, *3* (3), 202–207. https://doi.org/10.1039/b301258c.

(147) Huebner, A.; Srisa-Art, M.; Holt, D.; Abell, C.; Hollfelder, F.; DeMello, A. J.; Edel, J. B. Quantitative Detection of Protein Expression in Single Cells Using Droplet Microfluidics. *Chem. Commun.* **2007**, *2* (12), 1218–1220. https://doi.org/10.1039/b618570c.

(148) Pacocha, N.; Bogusławski, J.; Horka, M.; Makuch, K.; Liżewski, K.; Wojtkowski, M.; Garstecki, P. High-Throughput Monitoring of Bacterial Cell Density in Nanoliter Droplets: Label-Free Detection of Unmodified Gram-Positive and Gram-Negative Bacteria. *Anal. Chem.* **2020**, acs.analchem.0c03408. https://doi.org/10.1021/acs.analchem.0c03408.

(149) Horka, M.; Sun, S.; Ruszczak, A.; Garstecki, P.; Mayr, T. Lifetime of Phosphorescence from Nanoparticles Yields Accurate Measurement of Concentration of Oxygen in Microdroplets, Allowing One to Monitor the Metabolism of Bacteria. *Anal. Chem.*

2016, *88* (24), 12006–12012. https://doi.org/10.1021/acs.analchem.6b03758.

(150) Boitard, L.; Cottinet, D.; Kleinschmitt, C.; Bremond, N.; Baudry, J.; Yvert, G.; Bibette, J. Monitoring Single-Cell Bioenergetics via the Coarsening of Emulsion Droplets. *Proc. Natl. Acad. Sci.* **2012**, *109* (19), 7181–7186. https://doi.org/10.1073/pnas.1200894109.

(151) Liao, D. S.; Raveendran, J.; Golchi, S.; Docoslis, A. Fast and Sensitive Detection of Bacteria from a Water Droplet by Means of Electric Field Effects and Micro-Raman Spectroscopy. *Sens. Bio-Sensing Res.* **2015**, *6*, 59–66. https://doi.org/10.1016/j.sbsr.2015.09.005.

(152) Zang, E.; Brandes, S.; Tovar, M.; Martin, K.; Mech, F.; Horbert, P.; Henkel, T.; Figge, M. T.; Roth, M. Real-Time Image Processing for Label-Free Enrichment of Actinobacteria Cultivated in Picolitre Droplets. *Lab Chip* **2013**, *13* (18), 3707–3713. https://doi.org/10.1039/c3lc50572c.

(153) Liu, X.; Painter, R. E.; Enesa, K.; Holmes, D.; Whyte, G.; Garlisi, C. G.; Monsma, F. J.; Rehak, M.; Craig, F. F.; Smith, C. A. High-Throughput Screening of Antibiotic-Resistant Bacteria in Picodroplets. *Lab Chip* **2016**. https://doi.org/10.1039/c6lc00180g.

(154) Hengoju, S.; Wohlfeil, S.; Munser, A. S.; Boehme, S.; Beckert, E.; Shvydkiv, O.; Tovar, M.; Roth, M.; Rosenbaum, M. A. Optofluidic Detection Setup for Multi-Parametric Analysis of Microbiological Samples in Droplets. *Biomicrofluidics* **2020**, *14* (2), 024109. https://doi.org/10.1063/1.5139603.

(155) Hindson, B. J.; Ness, K. D.; Masquelier, D. A.; Belgrader, P.; Heredia, N. J.; Makarewicz, A. J.; Bright, I. J.; Lucero, M. Y.; Hiddessen, A. L.; Legler, T. C.; Kitano, T. K.; Hodel, M. R.; Petersen, J. F.; Wyatt, P. W.; Steenblock, E. R.; Shah, P. H.; Bousse, L. J.; Troup, C. B.; Mellen, J. C.; Wittmann, D. K.; Erndt, N. G.; Cauley, T. H.; Koehler, R. T.; So, A. P.; Dube, S.; Rose, K. A.; Montesclaros, L.; Wang, S.; Stumbo, D. P.; Hodges, S. P.; Romine, S.; Milanovich, F. P.; White, H. E.; Regan, J. F.; Karlin-Neumann, G. A.; Hindson, C. M.; Saxonov, S.; Colston, B. W. High-Throughput Droplet Digital PCR System for Absolute Quantitation of DNA Copy Number. *Anal. Chem.* **2011**. https://doi.org/10.1021/ac202028g.

(156) Pinheiro, L. B.; Coleman, V. A.; Hindson, C. M.; Herrmann, J.; Hindson, B. J.; Bhat, S.; Emslie, K. R. Evaluation of a Droplet Digital Polymerase Chain Reaction Format for DNA Copy Number Quantification. *Anal. Chem.* **2012**, *84* (2), 1003–1011. https://doi.org/10.1021/ac202578x.

(157) Kiss, M. M.; Ortoleva-Donnelly, L.; Reginald Beer, N.; Warner, J.; Bailey, C. G.;

Colston, B. W.; Rothberg, J. M.; Link, D. R.; Leamon, J. H. High-Throughput Quantitative Polymerase Chain Reaction in Picoliter Droplets. *Anal. Chem.* **2008**, *80* (23), 8975–8981. https://doi.org/10.1021/ac801276c.

(158) Pekin, D.; Skhiri, Y.; Baret, J. C.; Le Corre, D.; Mazutis, L.; Ben Salem, C.; Millot, F.; El Harrak, A.; Hutchison, J. B.; Larson, J. W.; Link, D. R.; Laurent-Puig, P.; Griffiths, A. D.; Taly, V. Quantitative and Sensitive Detection of Rare Mutations Using Droplet-Based Microfluidics. *Lab Chip* **2011**, *11* (13), 2156–2166. https://doi.org/10.1039/c1lc20128j.

(159) Lim, S. W.; Tran, T. M.; Abate, A. R. PCR-Activated Cell Sorting for Cultivation-Free Enrichment and Sequencing of Rare Microbes. *PLoS One* **2015**, *10* (1), e0113549. https://doi.org/10.1371/journal.pone.0113549.

(160) Ziegler, I.; Lindström, S.; Källgren, M.; Strålin, K.; Mölling, P. 16S RDNA Droplet Digital PCR for Monitoring Bacterial DNAemia in Bloodstream Infections. *PLoS One* **2019**, *14* (11), e0224656. https://doi.org/10.1371/journal.pone.0224656.

(161) Kang, D. K.; Ali, M. M.; Zhang, K.; Huang, S. S.; Peterson, E.; Digman, M. A.; Gratton, E.; Zhao, W. Rapid Detection of Single Bacteria in Unprocessed Blood Using Integrated Comprehensive Droplet Digital Detection. *Nat. Commun.* **2014**, *5*. https://doi.org/10.1038/ncomms6427.

(162) Avesar, J.; Rosenfeld, D.; Truman-Rosentsvit, M.; Ben-Arye, T.; Geffen, Y.; Bercovici, M.; Levenberg, S. Rapid Phenotypic Antimicrobial Susceptibility Testing Using Nanoliter Arrays. *Proc. Natl. Acad. Sci.* **2017**, *114* (29), E5787–E5795. https://doi.org/10.1073/PNAS.1703736114.

(163) Baltekin, Ö.; Boucharin, A.; Tano, E.; Andersson, D. I.; Elf, J. Antibiotic Susceptibility Testing in Less than 30 Min Using Direct Single-Cell Imaging. *Proc. Natl. Acad. Sci.* **2017**, 201708558. https://doi.org/10.1073/pnas.1708558114.

(164) Bamford, R. A.; Smith, A.; Metz, J.; Glover, G.; Titball, R. W.; Pagliara, S. Investigating the Physiology of Viable but Non-Culturable Bacteria by Microfluidics and Time-Lapse Microscopy. *BMC Biol.* **2017**, *15* (1), 121. https://doi.org/10.1186/s12915-017-0465-4.

(165) Wang, P.; Robert, L.; Pelletier, J.; Dang, W. L.; Taddei, F.; Wright, A.; Jun, S. Robust Growth of Escherichia Coli. *Curr Biol* **2010**, *20* (12), 1099–1103. https://doi.org/10.1016/j.cub.2010.04.045.

(166) Balaban, N. Q.; Merrin, J.; Chait, R.; Kowalik, L.; Leibler, S. Bacterial Persistence as a Phenotypic Switch. *Science (80-.).* **2004**, *305* (5690), 1622–1625.

https://doi.org/10.1126/science.1099390.

(167) Kulesa, A.; Kehe, J.; Hurtado, J. E.; Tawde, P.; Blainey, P. C. Combinatorial Drug Discovery in Nanoliter Droplets. *Proc. Natl. Acad. Sci. U. S. A.* **2018**, *115* (26). https://doi.org/10.1073/pnas.1802233115.

(168) Amselem, G.; Guermonprez, C.; Drogue, B.; Michelin, S.; Baroud, C. N. Universal Microfluidic Platform for Bioassays in Anchored Droplets. *Lab Chip* **2016**, *16* (21), 4200–4211. https://doi.org/10.1039/c6lc00968a.

(169) Sabhachandani, P.; Sarkar, S.; Zucchi, P. C.; Whitfield, B. A.; Kirby, J. E.; Hirsch, E. B.; Konry, T. Integrated Microfluidic Platform for Rapid Antimicrobial Susceptibility Testing and Bacterial Growth Analysis Using Bead-Based Biosensor via Fluorescence Imaging. *Microchim. Acta* **2017**, *184* (12), 4619–4628. https://doi.org/10.1007/S00604-017-2492-9.

(170) Churski, K.; Kaminski, T. S.; Jakiela, S.; Kamysz, W.; Baranska-Rybak, W.; Weibel, D. B.; Garstecki, P. Rapid Screening of Antibiotic Toxicity in an Automated Microdroplet System. *Lab Chip* **2012**. https://doi.org/10.1039/c2lc21284f.

(171) Postek, W.; Gargulinski, P.; Scheler, O.; Kaminski, T. S.; Garstecki, P. Microfluidic Screening of Antibiotic Susceptibility at a Single-Cell Level Shows the Inoculum Effect of Cefotaxime on: E. Coli. *Lab Chip* **2018**, *18* (23), 3668–3677. https://doi.org/10.1039/c8lc00916c.

(172) Schoepp, N. G.; Schlappi, T. S.; Curtis, M. S.; Butkovich, S. S.; Miller, S.; Humphries, R. M.; Ismagilov, R. F. Rapid Pathogen-Specific Phenotypic Antibiotic Susceptibility Testing Using Digital LAMP Quantification in Clinical Samples. *Sci. Transl. Med.* **2017**, *9* (410), 1–13. https://doi.org/10.1126/scitranslmed.aal3693.

(173) Athamanolap, P.; Hsieh, K.; Chen, L.; Yang, S.; Wang, T.-H. Integrated Bacterial Identification and Antimicrobial Susceptibility Testing Using PCR and High-Resolution Melt. *Anal. Chem* **2017**, *89*, 24. https://doi.org/10.1021/acs.analchem.7b02809.

(174) Kaushik, A. M.; Hsieh, K.; Chen, L.; Shin, D. J.; Liao, J. C.; Wang, T. H. Accelerating Bacterial Growth Detection and Antimicrobial Susceptibility Assessment in Integrated Picoliter Droplet Platform. *Biosens. Bioelectron.* **2017**, *97* (June), 260–266. https://doi.org/10.1016/j.bios.2017.06.006.

(175) Scheler, O.; Makuch, K.; Debski, P. R.; Horka, M.; Ruszczak, A.; Pacocha, N.; Sozański, K.; Smolander, O.-P.; Postek, W.; Garstecki, P. Droplet-Based Digital Antibiotic Susceptibility Screen Reveals Single-Cell Clonal Heteroresistance in an

Isogenic Bacterial Population. *Sci. Rep.* **2020**, *10* (1), 3282. https://doi.org/10.1038/s41598-020-60381-z.

(176) Artemova, T.; Gerardin, Y.; Dudley, C.; Vega, N. M.; Gore, J. Isolated Cell Behavior Drives the Evolution of Antibiotic Resistance. *Mol. Syst. Biol.* **2015**, *11* (7), 822. https://doi.org/10.15252/msb.20145888.

(177) Eun, Y. J.; Utada, A. S.; Copeland, M. F.; Takeuchi, S.; Weibel, D. B. Encapsulating Bacteria in Agarose Microparticles Using Microfluidics for High-Throughput Cell Analysis and Isolation. *ACS Chem. Biol.* **2011**, *6* (3), 260–266. https://doi.org/10.1021/cb100336p.

(178) Sun, L.; Talarico, S.; Yao, L.; He, L.; Self, S.; You, Y.; Zhang, H.; Zhang, Y.; Guo, Y.; Liu, G.; Salama, N. R.; Zhang, J. Droplet Digital PCR-Based Detection of Clarithromycin Resistance in Helicobacter Pylori Isolates Reveals Frequent Heteroresistance. *J. Clin. Microbiol.* **2018**, *56* (9). https://doi.org/10.1128/JCM.00019-18.

(179) Lyu, F.; Pan, M.; Patil, S.; Wang, J.-H.; Matin, A. C.; Andrews, J. R.; Tang, S. K. Y. Phenotyping Antibiotic Resistance with Single-Cell Resolution for the Detection of Heteroresistance. *Sensors Actuators B Chem.* **2018**, *270*, 396–404. https://doi.org/10.1016/J.SNB.2018.05.047.

(180) Davies, J. Origins and Evolution of Antibiotic Resistance. *Microbiología (Madrid, Spain)*. American Society for Microbiology September 1, 1996, pp 9–16. https://doi.org/10.1128/mmbr.00016-10.

(181) Palmer, A. C.; Kishony, R. Understanding, Predicting and Manipulating the Genotypic Evolution of Antibiotic Resistance. *Nat. Rev. Genet.* **2013**, *14* (4), 243–248. https://doi.org/10.1038/nrg3351.

(182) Ackermann, M. A Functional Perspective on Phenotypic Heterogeneity in Microorganisms. *Nature Reviews Microbiology*. Nature Publishing Group July 16, 2015, pp 497–508. https://doi.org/10.1038/nrmicro3491.

(183) Elowitz, M. B.; Levine, A. J.; Siggia, E. D.; Swain, P. S. Stochastic Gene Expression in a Single Cell. *Science (80-.).* **2002**, *297* (5584), 1183–1186. https://doi.org/10.1126/science.1070919.

(184) Raj, A.; van Oudenaarden, A. Nature, Nurture, or Chance: Stochastic Gene Expression and Its Consequences. *Cell*. Elsevier October 17, 2008, pp 216–226. https://doi.org/10.1016/j.cell.2008.09.050.

(185) Debski, P. R.; Gewartowski, K.; Sulima, M.; Kaminski, T. S.; Garstecki, P. Rational

Design of Digital Assays. *Anal. Chem.* **2015**, *87* (16), 8203–8209. https://doi.org/10.1021/acs.analchem.5b00942.

(186) Cho, S.; Kang, D. K.; Sim, S.; Geier, F.; Kim, J. Y.; Niu, X.; Edel, J. B.; Chang, S. I.; Wootton, R. C. R.; Elvira, K. S.; Demello, A. J. Droplet-Based Microfluidic Platform for High-Throughput, Multi-Parameter Screening of Photosensitizer Activity. *Anal. Chem.* **2013**, *85* (18), 8866–8872. https://doi.org/10.1021/ac4022067.

(187) Albur, M.; Noel, A.; Bowker, K.; MacGowan, A. Bactericidal Activity of Multiple Combinations of Tigecycline and Colistin against NDM-1-Producing Enterobacteriaceae. *Antimicrob. Agents Chemother.* **2012**, *56* (6), 3441–3443. https://doi.org/10.1128/AAC.05682-11.

(188) Collin, F.; Karkare, S.; Maxwell, A. Exploiting Bacterial DNA Gyrase as a Drug Target: Current State and Perspectives. *Applied Microbiology and Biotechnology*. Springer November 9, 2011, pp 479–497. https://doi.org/10.1007/s00253-011-3557-z.

(189) Pacocha, N.; Scheler, O.; Nowak, M. M.; Derzsi, L.; Cichy, J.; Garstecki, P. Direct Droplet Digital PCR (DddPCR) for Species Specific, Accurate and Precise Quantification of Bacteria in Mixed Samples. *Anal. Methods* **2019**, *11* (44), 5730–5735. https://doi.org/10.1039/c9ay01874c.

(190) Van Tongeren, S. P.; Degener, J. E.; Harmsen, H. J. M. Comparison of Three Rapid and Easy Bacterial DNA Extraction Methods for Use with Quantitative Real-Time PCR. *Eur. J. Clin. Microbiol. Infect. Dis.* **2011**, *30* (9), 1053–1061. https://doi.org/10.1007/s10096-011-1191-4.

(191) Witte, A. K.; Mester, P.; Fister, S.; Witte, M.; Schoder, D.; Rossmanith, P. A Systematic Investigation of Parameters Influencing Droplet Rain in the Listeria Monocytogenes PrfA Assay - Reduction of Ambiguous Results in DdPCR. *PLoS One* **2016**, *11* (12), e0168179. https://doi.org/10.1371/journal.pone.0168179.

(192) Rosenfeld, L.; Fan, L.; Chen, Y.; Swoboda, R.; Tang, S. K. Y. Break-up of Droplets in a Concentrated Emulsion Flowing through a Narrow Constriction. *Soft Matter* **2014**, *10* (3), 421–430. https://doi.org/10.1039/c3sm51843d.

(193) Liu, X.; Painter, R. E.; Enesa, K.; Holmes, D.; Whyte, G.; Garlisi, C. G.; Monsma, F. J.; Rehak, M.; Craig, F. F.; Smith, C. A. High-Throughput Screening of Antibiotic-Resistant Bacteria in Picodroplets. *Lab Chip* **2016**, *16* (9), 1636–1643. https://doi.org/10.1039/c6lc00180g.

(194) Brogden, K. A.; Guthmiller, J. M.; Taylor, C. E. Human Polymicrobial Infections. *Lancet* **2005**, *365* (9455), 253–255. https://doi.org/10.1016/s0140-6736(05)17745-9.